Aus der Klinik für kleine Haustiere
des Fachbereiches Veterinärmedizin
der Freien Universität Berlin

Purification and Partial Characterization of Canine Glutathione Transferase Alpha and the Development of an Immunoassay for the Measurement of Canine Glutathione Transferase Alpha Concentration in Serum

Inaugural-Dissertation
zur Erlangung des Grades eines
Doktors der Veterinärmedizin
an der
Freien Universität Berlin

vorgelegt von
Madeline Mischel
Tierärztin aus Berlin

Berlin 2016
Journal-Nr.: 3905

Gedruckt mit Genehmigung des Fachbereichs Veterinärmedizin

der Freien Universität Berlin

Dekan:	Univ.-Prof. Dr. J. Zentek
Erster Gutachter:	Univ.-Prof. Dr. B. Kohn
Zweiter Gutachter:	Univ.-Prof. Dr. J. M. Steiner
Dritter Gutachter:	Univ.-Prof. Dr. S. Amasheh

Deskriptoren (nach CAB-Thesaurus):
Dogs; glutathione transferase; liver diseases; immunoassay; evaluation; blood serum; markers

Tag der Promotion: 23.06.2016

Bibliografische Information der *Deutschen Nationalbibliothek*
Die Deutsche Nationalbibliothek verzeichnet diese Publikation in der Deutschen Nationalbibliografie; detaillierte bibliografische Daten sind im Internet über <http://dnb.ddb.de> abrufbar.

ISBN: 978-3-86387-756-9
Zugl.: Berlin, Freie Univ., Diss., 2016
Dissertation, Freie Universität Berlin
D 188

Choriner Str. 85 - 10119 Berlin
verlag@menschundbuch.de – www.menschundbuch.de

Dedicated to my parents,

Maja & Martin Mischel

TABLE OF CONTENT

LIST OF ABBREVIATIONS

%CV	coefficient of variation; %CV = (SD/mean)*100
^{125}I	iodine-125
ALP	alkaline phosphatase
ALT	alanine aminotransferase
AST	aspartate aminotransferase
ATP	adenosine triphosphate
BSA	bovine serum albumin
CDNB	1-Chloro-2,4-dinitrobenzene
cGST	canine glutathione transferase
CPM	counts per minute
Da	dalton
DCNB	1,2-dichloro-4-nitrobenzene
DEAE	diethylaminoethanol
EDTA	Ethylenediaminetetraacetic acid
GGT	gamma-glutamyl transferase
GS	glutathionyl
GSH	glutathione
GST	glutathione (S-) transferase
GSTA	glutathione transferase alpha
GSTM1	glutathione transferase mu-1
GSTO	glutathione transferase omega
GSTP1	glutathione transferase pi-1
GSTT1	glutathione transferase theta-1
h	hour
H_2O_2	hydrogen peroxide
hGST	human glutathione transferase
HPLC	high performance liquid chromatography
IEF	isoelectric focusing
IPG	immobilized pH gradient

kDa	kilo Dalton
LC/MS/MS	liquid chromatography – mass spectrometry – mass spectrometry
µg	microgram
µl	microliter
MALDI – TOF	matrix-assisted laser desorption/ionization – time of flight mass spectrometry
MAP3K5	mitogen-activated protein kinase kinase kinase 5
MAPEK	membrane-associated proteins in eicosanoid and glutathione metabolism
mg	milligram
min	minutes
ml	milliliter
MOPS	3-(N-morpholino)propanesulfonic acid
MRP	multidrug resistance protein
m/z	mass to charge ratio
NB	nonspecific binding
nm	nanometer
PBS	phosphate-buffered saline
pI	isoelectric point
PPT	precipitation solution
CPSS	congenital portosystemic shunt
RIA	radioimmunoassay
ROS	reactive oxygen species
rp-HPLC	reverse phase – high performance liquid chromatography
SD	standard deviation
SDS-PAGE	sodium dodecyl sulfate polyacrylamide gel electrophoresis
SNP	single nucleotide polymorphism
TC	total count
TRIS	tris(hydroxymethyl)aminomethane
V	volt

I. INTRODUCTION

Hepatic disease is a major cause of morbidity and mortality in dogs. However, a definitive diagnosis of hepatic disease can often be challenging. The clinical signs of hepatic disease can be extremely variable and in some cases the animal is asymptomatic (Poldervaart et al. 2009). This is due to the liver's functional reserve capacity and ability to regenerate. Indeed up to 90% of functional liver tissue must be destroyed before clinically apparent hepatic failure ensues (Heidelbaugh et al. 2006). Currently, the gold standard for diagnosing and assessing the severity of many hepatic diseases is through histological evaluation of a liver biopsy specimen. This procedure is invasive and costly, poses some risk to the patient, and ultimately the results are still subjective. Non-invasive diagnostic tests of liver disease are also commonly used and include measurement of liver enzyme activities in serum. However, the hepatic enzyme markers currently used in dogs are not consistently accurate indicators of hepatocellular damage or of the prognosis of hepatic disease (Mannes et al. 1982, Valentine et al. 1990).

Glutathione transferases (GST) are a very diverse family of isoenzymes involved in the detoxification of a range of xenobiotic compounds by conjugation to glutathione (Kilty et al. 1998). High concentrations of the isoenzyme GST alpha can be found in the cytoplasm of both periportal and centrilobular hepatocytes (Abei et al. 1989). In humans, GST alpha has been shown to be an early, more specific, and more sensitive indicator of hepatocellular injury than the commonly used aminotransferases, regardless of the cause of liver injury (Beckett et al. 1989, Trull et al. 1994, Bailey et al. 2012). Therefore, it is possible that GST alpha could also be a useful biomarker of hepatocellular injury in dogs.

1. Hypothesis and objectives

The hypothesis of this study was that serum concentration of GST alpha is a useful marker of hepatocellular injury in dogs. Therefore, the aim of this initial study was to evaluate serum GST alpha concentrations in dogs with hepatobiliary disease and compare them to those of healthy dogs.

In order to prove or disprove this hypothesis, the specific objectives of this study were: 1) to purify GST alpha from canine hepatic tissue; 2) to develop and validate an immunoassay for the measurement of canine GST alpha in serum; and 3) to compare serum concentrations of GST alpha in healthy dogs and dogs with liver disease.

II. LITERATURE REVIEW

1. Glutathione transferase (GST)

Glutathione transferases were first identified in 1961 as enzymes found in cytosolic liver extracts from rats, that catalyze the addition of glutathione to 1,2-dichloro-4-nitrobenzene (DCNB) (Booth et al. 1961). Since then, they have been recognized to have several important functions and to be biomarkers of hepatic disease. GSTs are probably the single most important family of enzymes involved in the metabolism and detoxification of xenobiotics and also have a number of functions in the metabolism of endogenous substances (Armstrong 1997).

Glutathione transferases are widely distributed in nature and can be found in bacteria, fungi, plants, parasites, fish, and mammals (Hayes et al. 1995). In mammals, they have been detected in most organs, however, high inter-individual variation in the relative abundance of isoforms has been demonstrated (Ommen 1990). In the liver, GSTs of the alpha class are most abundant and are located in high concentrations in the cytoplasm of hepatocytes (Abei et al. 1989). In humans GSTA1 is the major isoenzyme in the liver representing about 2% of the total cytosolic proteins (van Ommen et al. 1990). Due to GSTA1's high cytosolic concentration, specific localization and short serum half-life, it has been studied as a novel marker of hepatocellular injury in humans (Beckett et al. 1985, Kilty et al. 1998, Sidlova et al. 2003)

1.1.Nomenclature

Glutathione S-transferases (GSTs) are classified under the Enzyme Commission number 2.5.1.18, which is associated with the recommended name "glutathione transferase" due to the fact that the sulfur atom is not transferred per se, but rather the glutathionyl group. However, the abbreviation GST can still be used, if the "S" stands for glutathionyl (GS-) transferase (Mannervik et al. 2005). They are transferase enzymes that catalyze the transfer of a glutathione, from a donor to an acceptor.

Glutathione transferases are extremely diverse in their amino acid sequences (Atkinson et al. 2009). Three superfamilies of GSTs are recognized: cytosolic, mitochondrial, and microsomal (MAPEG) proteins, which share similar protein sequences and structures (Sheehan et al. 2001).

Cytosolic and mitochondrial GSTs are soluble enzymes that share similarities in their 3-dimensional structure and seem to have diverged from a common thioredoxin progenitor (Ladner et al. 2004). Cytosolic GSTs are the largest superfamily and are divided into 13 classes designated by Greek letters based upon their primary structure similarities: alpha, beta, delta, epsilon, zeta, theta, mu, nu, pi, sigma, tau, phi, and omega, with members of the same class possessing at least 50% amino acid sequence homology, but with some possessing over 90% homology (Mannervik et al. 1988, Mannervik et al. 1992, Mannervik et al. 2005, Oakley 2011). They also have been classified depending on their isoelectric point (pI), with alpha being considered basic (pI > 8), mu neutral (pI 7-8), and pi acidic (pI < 7) (Boyer 1989). Mitochondrial GSTs make up the kappa class and have a deep evolutionary relationship with cytosolic GSTs. The microsomal superfamily, now labeled membrane-associated proteins in eicosanoid and glutathione metabolism (MAPEG), consists of subgroups I-IV, sharing less than 20% sequence homology (Oakley 2011).

The standardized GST nomenclature identifies the species to which the GST belongs to with a lowercase letter, preceding the abbreviation GST (e.g., "c" for canine - cGST). The different classes of cytosolic GSTs include different isozymes, which are identified with an uppercase letter (e.g., "A" for alpha), followed by an Arabic numeral representing the subunit. Mitochondrial and cytosolic GSTs exist as dimers, and can form heterodimers between members of the same class. Therefore, two Arabic numbers can follow for each subunit denoted with a hyphen (e.g. cGSTA1-1) (Mannervik et al. 1982, Mannervik et al. 1985, Mannervik et al. 1992, Hayes et al. 1995, Mannervik et al. 2005).

1.2.Structure

Mitochondrial and cytosolic GSTs are dimeric proteins (Bass et al. 1977, Tars et al. 2010). The quaternary structure of alpha, mu, and pi enzymes derives from hydrophobic intersubunit interactions between the C-terminal domain of one subunit and the N-terminal domain of the other (Armstrong 1997), whereas sigma GSTs form hydrophilic interactions (Stevens et al. 1998). Catalytically active monomers have not been observed and studies with the porcine pi GST class suggest that the dimeric structure stabilizes the tertiary structure of the subunits and possibly the two domains of the subunit (Erhardt et al. 1995).

The subunits of cytosolic GSTs have a molecular mass/weight of approximately 25 kDa (Sinning et al. 1993, Josephy 2010), and can form homodimers, as well as heterodimers between members of the same class (Bass et al. 1977, Mannervik et al. 1982). Each subunit contains a larger C-terminal domain composed of alpha-helixes and a smaller N-terminal thioredoxin-like domain composed of β-sheets sandwiched between α-helices. The N-terminal domain makes up the hydrophilic binding site for GSH (G-site) and is highly conserved between all GSTs, because of its high specificity for glutathione (GSH). Both domains, but mainly the alpha-helical domain, form the hydrophobic H-site (Figure 1). The H-site shows greater variability between different GSTs and binds structurally diverse electrophilic acceptor substrates bearing numerous functional groups (Reinemer et al. 1991, Reinemer et al. 1992, Ji et al. 1994, Tars et al. 2010, Oakley 2011).

Interestingly, individual genes for each human GST class are clustered together on the same chromosome, with different classes being located on different chromosomes. The GST alpha class genes are localized on a small region of chromosome 6p12 (Board et al. 1987) and consist of 5 genes. Of these genes, the hGSTA4 gene shows the least homology with the other alpha GST genes (Morel et al. 2002). In comparison, the canine GST alpha class genes are located on chromosome 12 (NCBI Reference Sequence: NP_001301024). Human and canine alpha GSTs consist of about 222 amino acids and are extremely similar in their primary structure (Ahmad et al. 1993) (Figure 2). Hence, the human GST A1-1 and GST A2-2 have 95% sequence homology (Sinning et al. 1993) and human GST A2-2 and A3-3 are 89% identical (Tars et al. 2010). Different isoenzymes of canine GSTA also have a high level of sequence similarity as seen in figure 3.

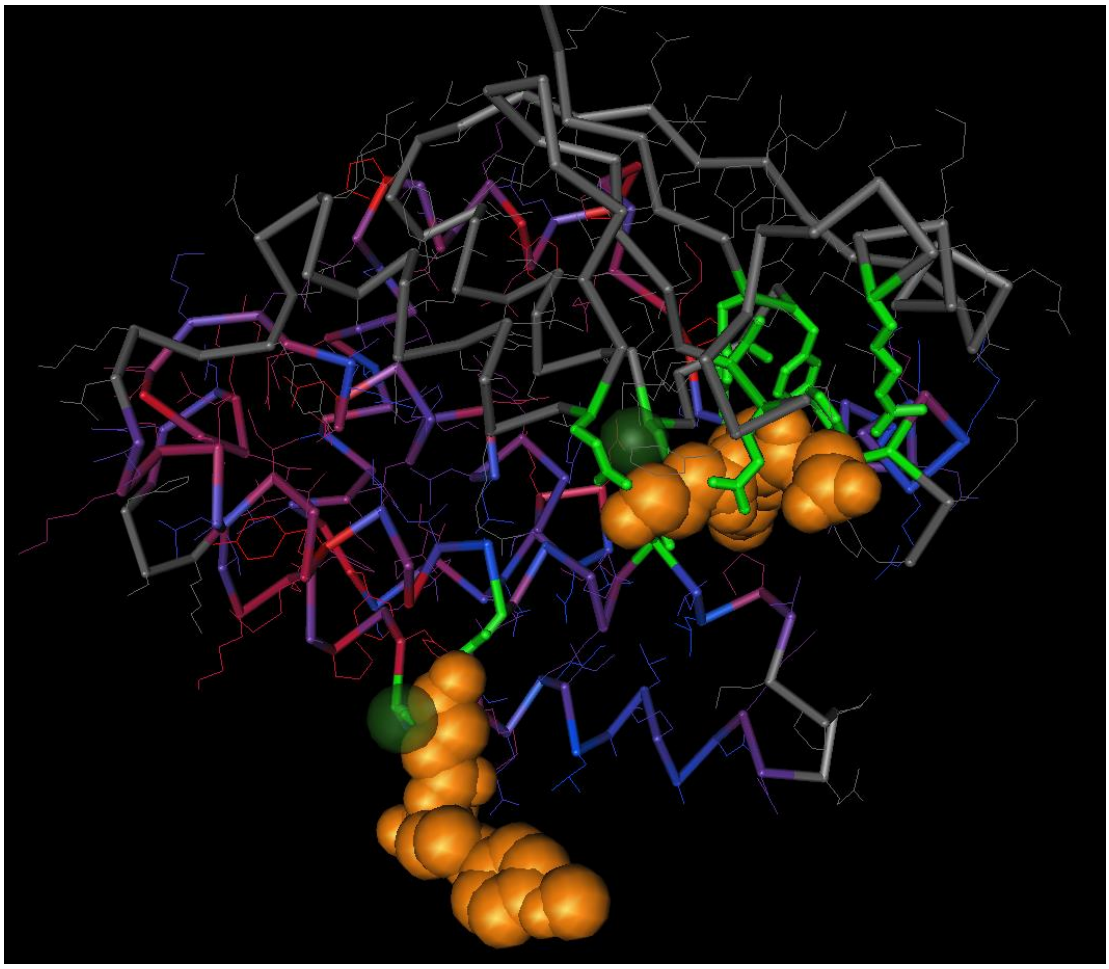

Figure 1: 3D structure of hGSTA isoforms

This image shows a human GSTA1-1 dimer with two molecules of bound substrate (Marchler-Bauer et al. 2015). The GST active site is composed of a specific GSH binding site (G-site), formed by residues from the N-terminal domain and common to all GSTs, as well as of a nonspecific substrate binding site (H-site). The H-site varies between different classes and isoforms and is mainly comprised of residues from the C-terminal alpha helical domain with multiple overlapping hydrophobic subsites. A single substrate may occupy multiple positions and orientations within a single H-site.

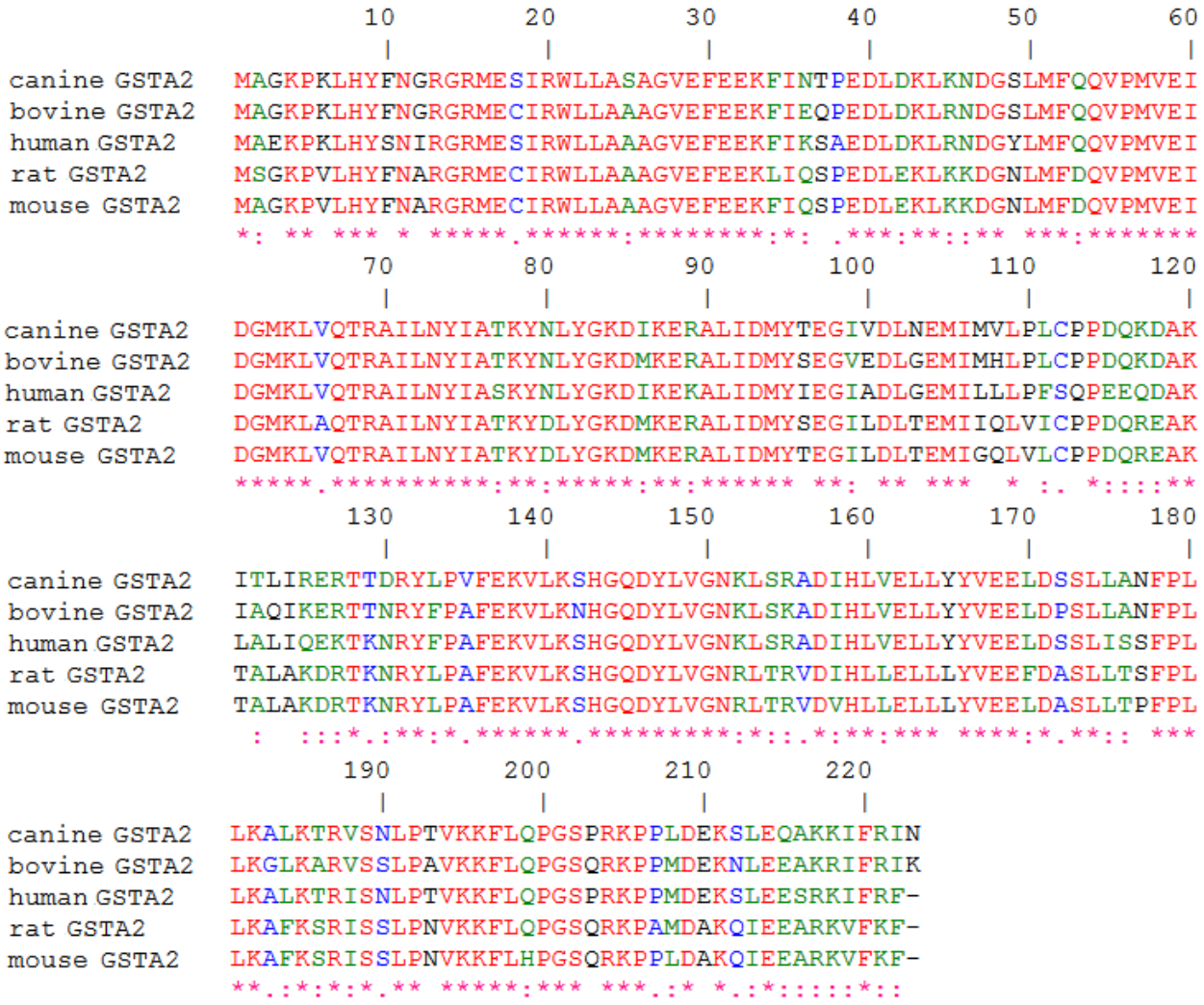

Figure 2: Amino acid sequence alignment of GSTA2 from different species

The amino acid sequence alignment of canine GSTA2 compared to bovine, human, rat, and mouse GSTA2 was performed with Clustal Omega sequence alignment program (Combet et al. 2000) and shows a high degree of homology of this isoenzyme between species. Canine GSTA1 has not been sequenced yet or the sequence is not available in the NCBI database. Therefore, the predicted sequence of cGSTA2, which is assumed to be the closest relative of cGSTA1, was chosen for comparison. The number above each column indicates the position of the amino acid marked. Consensus symbols underneath each column represent the degree of similarity between amino acids of the different species:

(***** (asterisk) fully conserved residue; **:** (colon) conservation with strongly similar properties; **.** (period) conservation with weakly similar properties).

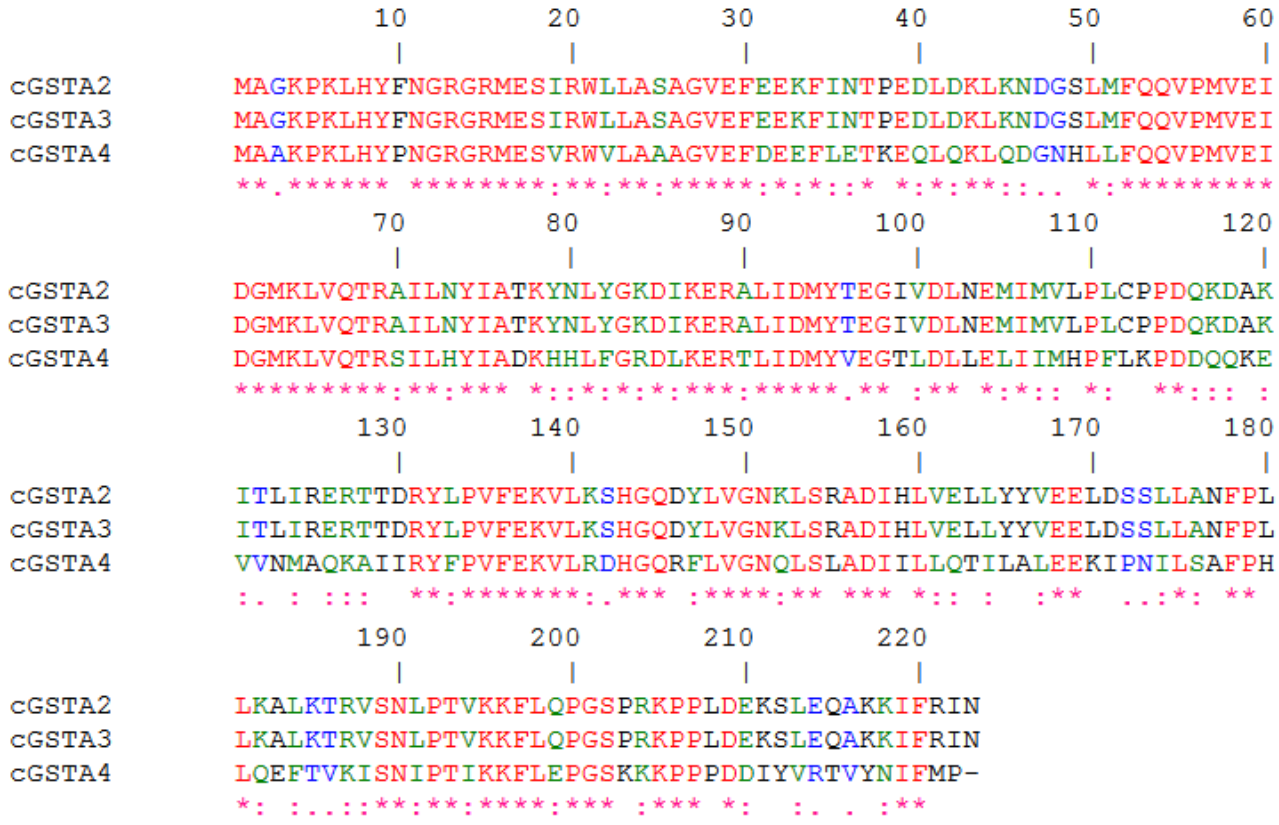

Figure 3: Amino acid sequence alignment of different canine GST alpha isoforms

The amino acid sequence alignment of canine GSTA2 compared to cGSTA3 and cGSTA4 was performed with Clustal Omega sequence alignment program (Combet et al. 2000) and shows high homology of the different isoenzymes in this species. Canine GSTA1 has not been sequenced yet or the sequence is not available in the NCBI database and could therefore not be included. The number above each column indicates the position of the amino acid marked. Consensus symbols underneath each column represent the degree of similarity between amino acids of the different species: (***** (asterisk) fully conserved residue; **:** (colon) conservation with strongly similar properties; **.** (period) conservation with weakly similar properties).

1.3.Genetic polymorphisms

Genetic polymorphisms of GST-encoding genes modify the expression of these enzymes and likely contribute to individual differences in response to xenobiotics. In humans, polymorphisms of GST classes influence susceptibility to various types of cancer, diabetes, atherosclerosis, allergies, and other inflammatory diseases (Palmer et al. 2003, Gilliland et al. 2004, Wang et al. 2006). For example, GST omega (GSTO) polymorphism has been associated with the development of leukemia in children (Pongstaporn et al. 2009), and polymorphism of the GSTP1 gene that leads to a lower enzyme activity was found to be associated with the development of Barrett's epithelium and esophageal adenocarcinoma (van Lieshout et al. 1999). Lacking GSTM1 or being homozygous nulled for a combination of both GSTM1 and GSTP1 genes was significantly associated with the development of lung cancer in humans (Zhong et al. 1991, Anttila et al. 1993, Ryberg 1997). It has also been suggested that the homozygous deletion of the GSTM1 gene may increase susceptibility to the development of irreversible liver damage after ethanol abuse (Savolainen et al. 1996). In fact, about 50% of the Caucasian population is homozygous for a deletion of the GSTM1 gene (null genotype), causing the enzyme to be inactive (van Ommen et al. 1990, Zhong et al. 1991), and in some populations up to 60% possess a GSTT1 null allele (Lien et al. 2002). Similar to non-Hodgkin lymphoma in humans, a GSTT1 polymorphism was associated with the development of lymphoma in dogs, possibly due to impaired detoxification of environmental chemicals (Ginn et al. 2014).

Furthermore, polymorphisms of several human GST classes, such as GSTP1 and GSTT1, seem to modify chemotherapy response and therefore influence survival times of patients receiving treatment (Lien et al. 2002, Stoehlmacher et al. 2002). Significant individual differences in the activity of GSTs of the liver and kidney were observed in dogs, with some dogs displaying low GST activity. However, GST protein concentrations were almost the same as in dogs with higher GST activity. Also, in these dogs with low GST activity substantially higher 1,2-dichloro-4-nitrobenzene (DCNB) concentrations in plasma were observed after a single dose of DCNB. These results suggested that there are individual differences in the expression of theta GST in the dog, and that dogs with low GST activity might have a higher susceptibility to toxins or other compounds metabolized by theta GST (Watanabe et al. 2004, Watanabe et al. 2006).

Polymorphisms of the human alpha class GSTs affect GSTA1/2/3/4 and are quite abundant in the population impacting the susceptibility to diseases and chemotherapy. Functional single

nucleotide polymorphisms (SNPs) of GSTA1, A2, or A3 can influence their activity and lead to a low hepatic expression (Morel et al. 2002, Ning et al. 2004, Tetlow et al. 2004). Of human GSTA1, two variants, A and B, have been named according to the linked SNP, and their frequencies of occurrence are similar in African, Caucasian, and Pacific Islanded populations (Coles et al. 2001, Ning et al. 2004). Coles et al. (2001) found that the expression of hGSTA1 in the liver of homozygous hGSTA1*A donors was 4 times higher than in those of homozygous hGSTA1*B donors. The gene encoding hGSTA2 has 3 validated SNPs in the coding region that result in 3 amino acid substitutions and 4 different proteins, found in Africans, Caucasians, and Chinese (Ning et al. 2004, Tetlow et al. 2004). There also seems to be a disequilibrium between hGSTA1 and A2 polymorphisms in Caucasians, with homozygous hGSTA1*A individuals having a higher GSTA1 expression than heterozygous and especially than homozygous hGSTA1*B individuals. However, their hepatic expression of GSTA2 is lower, whereas homozygous hGSTA1*B individuals show a much higher GSTA2 expression (Coles et al. 2001). GSTA3 polymorphism alters the specific activity of the protein towards different substrates, with exception of the steroid isomerase activity, and was found in 15% of the African population. Interestingly, knockout mice that lack the mGSTA4 gene show an altered sensitivity to xenobiotics, a lower litter size, and are more susceptible to bacterial infections (Engle et al. 2004).

Thus, these polymorphisms of the GST classes may influence the susceptibility to degenerative diseases, such as cancer, as well as the efficacy of certain chemotherapeutics and adverse drug reaction.

1.4.Localization

The different GST classes are found in a variety of mammalian organs, as well as in other eukaryotic species, prokaryotes, and plants. As previously mentioned, the different GST classes are also often involved in the pathogenesis of disease and exist in tumor cells. In the human lung, GSTP1, as well as varying concentrations of GSTA1/A2 and GSTM1/2/3, were located mostly in the airway epithelium, but GSTM was detected in lower quantities. GSTM3 concentrations varied extremely between individuals and were most abundant in the bronchial epithelium of smokers (Anttila et al. 1993).

The kidneys contain significant amounts of alpha GST, which in rats and humans was found only in the proximal tubule, as well as GST of the pi class, which was mostly found in the distal tubules (Sundberg et al. 1994, Branten et al. 2000, Raza et al. 2004). Also, microsomal GST was found with varying staining intensity in glomerula, interstitial endothelium, and collecting ducts in the medulla (Harrison et al. 1989). GST isoforms can be found in many other organs, such as the brain, where the classes mu and theta can be found (Beuckmann et al. 2000, Lien et al. 2002), or the esophagus, where GSTs of the pi class have important detoxification functions (van Lieshout et al. 1999).

Approximately 4% of the total amount of cytosolic protein in the human liver consists of GST. The GST alpha class makes up over 80% of the total GST in the liver, with more than half of it being GSTA1 (van Ommen et al. 1990, Mulder et al. 1999). Therefore, GSTA1 alone makes up about 2% of the total cytosolic protein content in the liver. GSTs of the pi and mu class have also been shown to exist in the liver. GST alpha and pi exhibit a unique region-specific distribution in the liver and kidney, with pi being found in biliary duct epithelium of the liver, whereas alpha is also located within hepatocytes (Abei et al. 1989, Campbell et al. 1991). Similarly to GST mu, GST alpha is heterogeneously distributed throughout the entire liver, with the hepatocytes near the central vein containing high enzyme amounts (Abei et al. 1989, Campbell et al. 1991, Raza et al. 2004).

In general, it can be said that GSTs of the pi class show a very wide distribution throughout many different tissues, but are especially found in ductular cells of the liver, pancreas, salivary glands, and kidney, and are also strongly expressed in tumor cells (Campbell et al. 1991, Sundberg et al. 1993). In contrast, the human alpha class shows a restricted distribution with most abundant expression in all hepatocytes and the proximal tubular cells of the kidney. GSTA was also found in the zona reticularis of the adrenal glands and Leydig cells of the testes, as well as to lesser intensities in the gastrointestinal epithelium, exocrine pancreas, and bile ducts (Sundberg et al. 1993, Raza et al. 2004). More specifically, hGSTA1 and hGSTA2 are expressed at high levels in the liver, as well as in the small intestine, kidneys, adrenal glands, and testes; hGSTA3 is expressed in steroidogenic tissues, lung, stomach, and trachea, whereas hGSTA4 is expressed in most tissues with a high degree of oxidative stress (Desmots et al. 2001, Morel et al. 2002). GSTA belongs to the cytosolic GST family, however, one isoform seems to be located in the cytoplasm as well as the nucleus of hepatocytes (Abei et al. 1989, Campbell et al. 1991). The

expression of the fifth isoenzyme of the human alpha GST class has not been documented, though the gene encoding for it has been confirmed to be a functional gene that can produce a mature mRNA and a catalytically active enzyme (Singh et al. 2010). This unique distribution of the GST isoforms explains their utility as biomarkers of organ injury.

1.5. Induction

GSTs can be synthesized by hepatocytes and changes in the GST subunit composition seem to be a reflection of de novo synthesis (Vandenberghe et al. 1990). Studies in rats provide evidence that GSTA expression can be induced by different drugs, such as phenobarbital or 3-methylcholanthrene, leading to a marked increase in enzyme activity in the liver (40 to 280%), but not in the kidney or small intestine. This increase in enzyme activity can best be explained by de novo synthesis in the liver (Fleischner et al. 1972, Mukhtar et al. 1976). Over 100 chemicals from drugs, but also from the diet, have been shown to induce hGSTA1 and A2 mRNA and protein (Morel et al. 1994, Hayes et al. 1995). GSTA4 may also be induced by oxidative stress (Desmots et al. 2001). Many of these inducers are themselves substrates for GST enzymes. In most cases, they effect the transcriptional activation of GST genes leading to the up-regulation of GST enzymes (Hayes et al. 1995).

1.6.Function

GSTs are phase II metabolic enzymes best known for their ability to catalyze the conjugation of the reduced form of the tripeptide glutathione to a variety of xenobiotic substrates for the purpose of detoxification (Hayes et al. 1999, Josephy 2010). The general catalytic reaction can be described as:

$$R\text{-}X + GSH \rightarrow HX + R\text{-}S\text{-}GSH$$

R-X is the electrophilic substrate, where R may be an aliphatic, aromatic, or heterocyclic group and X may be a sulfate, nitrile, or halide group. A nucleophilic attack of glutathione via a sulfhydryl group is initiated on the electrophilic center of hydrophobic substrate, thereby making it more water-soluble and decreasing its reactivity with cellular macromolecules (Keen et al. 1978, Armstrong 1997, Hayes et al. 1999).

To activate the sulfur for nucleophilic attack, the enzyme can lower the pKa of the sulfhydryl group of reduced glutathione from 9 to about 6.5, which leads to its deprotonation (Chen et al. 1988, Caccuri et al. 1997). For activation, GSH is bound at the hydrophilic G-site with the glutamyl residue pointing down towards the dimer interface in form of a large cavity and the sulfur pointing to the subunit to which it is bound. The glutamyl portion of the peptide is recognized by the most conserved ββα region of the G-site. Over a dozen electrostatic interactions, utilizing all of the hydrogen bonds of donor and acceptor sites on the peptide, anchor the GSH-molecule. Even though the orientation of the peptide in the active site is approximately the same for all of its isoenzymes, there are differences in the hydrogen-bonding interactions (Reinemer et al. 1991, Armstrong 1997). Variation in the binding of GSH results in a different mode of GSH-activation and separates subgroups of cytosolic GSTs. The eukaryotic classes alpha, mu, pi, and sigma use a tyrosine residue to activate glutathione, whereas the theta class, which is thought to be their evolutionary prototype, utilizes serine or cysteine residues instead (Liu et al. 1992, Board et al. 1995, Wilce et al. 1995, Atkinson et al. 2009). The substrate is bound at the hydrophobic H-site (Ji et al. 1994, Tars et al. 2010).

With this activity, GSTs detoxify reactive electrophiles, preventing them from damaging cellular components, such as proteins and nucleic acids. They therefore enable the inactivation and elimination of a diverse range of electrophilic xenobiotics, such as anticancer chemotherapeutics and other drugs (Lien et al. 2002). The resulting glutathione conjugates are more soluble and can be exported from the cell through ATP-dependent transporters, in particular MRP1 and MRP2 of the multidrug resistance-protein family (Ishikawa 1992, Keppler 1999, Cole et al. 2006). Subsequently, they are processed into mercapturic acids and excreted via the urine (Egner et al. 2008) or bile (Teichert et al. 2009).

GSTs have been shown to detoxify insecticides, herbicides, carcinogens, and by-products of oxidative stress (Abel et al. 2004, Abel et al. 2004). At least 100 chemicals have been identified to induce GST, and many of those occur naturally (Hayes et al. 1995). The environmental carcinogen aflatoxin B1-8,9-epoxide is formed from aflatoxin B_1 by cytochrome P450. Its conjugation with GSH by the GST is a major protective mechanism against mycotoxins in rodents (Hayes et al. 1999). Drugs that are metabolized to glutathione conjugates by GST include: acetaminophen, clozapine, and furosemide, as well as chemotherapeutic agents, such as adriamycin, 1,3-bis(2-chloroethyl)-1-nitrosourea, cisplatin, or mitoxantrone (Goto et al. 1999,

Awasthi et al. 2002, Lien et al. 2002). Studies implicated the overexpression of GST in mammalian tumor cells to cause acquired resistance to anticancer drugs and tumor chemical carcinogens (Hayes et al. 1995, Ban et al. 1996, Awasthi et al. 2002, Lien et al. 2002). GSTs are therefore of interest to pharmacologists and toxicologists to provide targets for antitumor drug therapies (Jakobsson et al. 1999, Ruscoe et al. 2001).

In addition, expression of GST was found to increase during cancer development (Hayes et al. 1995, Ali-Osman et al. 1997). Isoenzymes from several GST classes (e.g., mu, alpha, and pi) have been shown to associate with members of the mitogen-activated protein kinase (MAPK) pathways involved in modulating cell signaling pathways that control cell proliferation and cell death (Ruscoe et al. 2001). This non-enzymatic role is established by GST inhibiting mitogen-activated protein kinase kinase kinase 5 (MAP3K5), which is an enzyme that activates c-Jun N-terminal kinase and P38 signaling pathways, and is consequently critical for cytokine- and stress-induced apoptosis (Cho et al. 2001). Therefore, the inhibition of GSTs, in particular GSTP1-1, which seems to be the most ubiquitous non-hepatic isoenzyme, could be used as a potential therapeutic approach for the treatment of cancer and other diseases associated with aberrant cell proliferation (Laborde 2010).

Historically, GSTA was called ligandin, as it was found to be an abundant binding protein in the liver that binds both covalently and non-covalently to a wide spectrum of chemicals, such as carcinogen 3-methylcholanthrene, polycyclic aromatic hydrocarbons, azo-dyes, as well as bilirubin, bile acids, heme, glucuronic acid, fatty acids, steroids, thyroid hormones, and drugs, such as tetracycline and penicillin (Litwack et al. 1971, Habig et al. 1974, Hayes et al. 1991). GSTAs therefore contribute to intracellular transport and disposition of xenobiotics and hormones and reduce the susceptibility of the liver to carcinogenesis (Smith et al. 1977, Hayes et al. 1995).

In rats, GSTs of the alpha class form a high-affinity non-substrate binding site within the cleft between the two subunits, indicating that there are two distinct xenobiotic-binding sites in certain isoenzymes that form heterodimers (Vargo et al. 2001). Each subunit of a heterodimer may be able to bind its preferred substrate, thus increasing the amount of substrates bound and metabolized, which would provide an evolutionary reason why it is beneficial for members within the alpha and mu isoenzyme families to form heterodimers (Vargo et al. 2004).

Partially reduced oxygen can lead to the formation of superoxide ($\cdot O_2^-$), which is the precursor of most reactive oxygen species (ROS). The production of ROS is an unavoidable byproduct of aerobic respiration, but may cause significant damage to cellular structures, in particular DNA, membrane lipids, amino acids of proteins, or carbohydrates. This is known as oxidative stress and can be increased during times of environmental stress (Marnett et al. 2003, Pohanka 2013). Superoxide dismutase, as well as aldehyde and alcohol dehydrogenase, aldo-keto reductase, glutathione peroxidase, and the GST are some of the enzyme groups that are important for antioxidant defense, especially of radical induced lipid peroxidation of polyunsaturated fatty acids in cell membranes (Ketterer et al. 1989, Marnett et al. 2003). Microsomal GST of the alpha class, with high degree of homology to cytosolic GST A1 and A3, was found to have activity for lipid and phosphatidylcholine hydroperoxides in the liver (Prabhu et al. 2004). In addition to microsomal and cytosolic alpha GST, GSTs of the mu and theta class have since been shown to catalyze the detoxification of hydroperoxides, including both endogenous and exogenous compounds (Hurst et al. 1998, Leaver et al. 1998). In rats and mice, GSTs of the alpha class account for more than half of the glutathione peroxidase activity toward lipid hydroperoxides within membranes of the liver (Yang et al. 2002). These findings demonstrate that GSTs are essential for preventing oxidative damage to the phospholipid membranes and in the cellular antioxidant defense mechanism, indicating that their induction might be an evolutionarily conserved response of cells to oxidative stress.

Cytosolic GST and MAPEG also perform isomerization of various unsaturated compounds, which contributes significantly to hepatotoxicity after ingestion (Jakobsson et al. 1999, Khojasteh-Bakht et al. 1999). GSTs play an important role in the biosynthesis of eicosanoids produced from arachidonic acid and thus are involved in cell signaling. Cytosolic GST catalyzes the isomerization of prostaglandin H2 to prostaglandin D2 (Moyo et al. 2014), whereas the locally produced hormone prostaglandin E2 can be synthesized by MAPEG as well as cytosolic GST, such as GSTM (Beuckmann et al. 2000). Leukotrienes are another family of eicosanoids and important inflammatory mediators for regulation of the immune response, and their synthesis was also found to be catalyzed by MAPEGs. Here, they catalyze the conjugation of leukotriene A4 with glutathione, forming leukotriene C4 (Jakobsson et al. 1996). GSTs are even involved in the synthesis of the steroid hormones, testosterone and progesterone. GST A3-3 very efficiently catalyzes the isomerization of their precursors, delta(5)-androstene-3,17-dione and delta(5)-

pregnene-3,20-dione from 3β-hydroxy-5-pregnene-20-one (Benson et al. 1977). The catalytic rate of GST A3-3 is considerably higher than that of any other GST and even higher than the turnover rate of 3beta-hydroxysteroid dehydrogenase/isomerase, the enzyme generally considered to catalyze the double-bond isomerization (Johansson et al. 2001). This shows that the activity is not a characteristic of a particular class of GSTs. Instead, they display overlapping substrate specificities making it difficult to identify isoenzymes only based on their catalytic function (Lien et al. 2002).

2. Clinical relevance of glutathione transferases

GSTs are associated with a variety of diseases often due to the effects of their genetic polymorphisms. As previously mentioned, GSTs might play a role in the development and treatment of cancer by inhibition of apoptosis and drug detoxification and are therefore of great interest to the biomedical and pharmaceutical industries (Ruscoe et al. 2001, Lien et al. 2002). In the brain, GSTT1 appears to influence chemotherapy of tumors, whereas isoenzymes of the mu GST class may even play an important role in temperature regulation, nociception, and sleep-wake-regulation by producing prostaglandin E2 (Beuckmann et al. 2000, Lien et al. 2002). A polymorphism of the GSTP1 gene leads to lower GST enzyme activity levels in the esophagus of humans resulting in impaired detoxification and possibly the development of Barrett's epithelium and adenocarcinoma (van Lieshout et al. 1999).

Furthermore, studies show that there might be a connection between GSTT1 polymorphism and the development of diabetes mellitus (Wang et al. 2006). Insulin treatment seems to upregulate the antioxidant defenses of cells by increasing GST expression of the alpha- and pi-classes, whereas increased glucagon concentrations present during un-regulated diabetes decreased their expression in the liver of rats (Kim et al. 2003).

GSTs of the omega class have been associated with leukemia (Pongstaporn et al. 2009), neurological disease, as well as an increased risk for developing chronic obstructive pulmonary disease due to a polymorphism of the gene (Yanbaeva et al. 2009). Decreased GSTO gene expression may even result in a lower age of onset for Alzheimer's, Parkinson, and amyotrophic lateral sclerosis, most likely due to the role GSTO plays in the regulation of oxidative stress or in the activation of interleukin-1β (Board 2011).

2.1.GST as a marker of organ damage

Some GSTs show a high degree of region-specific distribution, which makes them useful as biomarkers for localizing and monitoring injury to defined cell types. For instance, GST alpha and pi function as markers of renal damage, when measured in the urine. In humans and rats, renal proximal tubular cells contain high concentrations of the basic alpha GST, while distal tubular cells contain high concentrations of the acidic pi GST (Harrison et al. 1989, Harpur et al. 2011). The enzyme can be measured in the urine, and its measurement appears to be superior to

that of blood urea nitrogen and serum creatinine for diagnosis of proximal tubular necrosis (Harpur et al. 2011). GST alpha and pi can therefore be used as a marker for the nephrotoxicity caused by certain drugs, such as cyclosporine and anesthetic agents (Sundberg et al. 1994, Eger et al. 1997), as well as to localize the site of renal tubular injury to the proximal or distal tubule, which can also give information about the progression of the disease (Branten et al. 2000).

Moreover, GST is significantly increased in the peripheral blood of humans with acute intestinal ischemia, a condition that is associated with high mortality rates, but lacks reliable noninvasive biological markers. The enzyme even shows isoform specificity in its distribution throughout the intestinal tract. Alpha GST is highly specific to and widely distributed in the small bowel and liver. Serum concentrations are especially high with postischemic reperfusion, whereas low alpha GST concentrations seem to exclude intestinal ischemia (Delaney et al. 1999, McMonagle et al. 2006). In rats, luminal GST alpha and mu increase in the peripheral blood with prolonged ischemia and worsening grades of intestinal injury (Khurana et al. 2002). Therefore, evaluation of GSTA may serve as a reliable and early marker to predict the presence or absence of acute intestinal ischemia.

GSTs can also be used as markers for the success of kidney transplantation, where acute tubular necrosis and renal transplant infarction result in a rapid elevation of both urine pi and alpha GST (Sundberg et al. 1994). In addition to post-transplant monitoring, GSTA also appears to be a very useful marker for the assessment of renal tissue injury in the perfusate of machine-preserved non-heart-beating (NHB) donor kidneys and thus a predictor of functional outcome of NHB donor grafts before transplantation (Daemen et al. 1997, Gok et al. 2003).

Likewise, GSTA has been shown to be a very sensitive biomarker of hepatocellular injury due to acute or chronic liver injury, following transplantation, drug or toxin exposure (Hughes et al. 1997, Abdel 2011, Bailey et al. 2012). GSTA is a useful marker for monitoring patients after organ transplantation in order to adequately adjust post-transplant recipient management. Its diffuse hepatic distribution, high cytosolic concentration, and short plasma half-life may make GSTA a better indicator for liver allograft rejection than transaminase enzyme activities. Unlike alanine aminotransferase (ALT), which is located mainly in centrilobular hepatocytes, GSTA is located in the centrilobular as well as peripheral hepatocytes. Due to their short plasma half-life, GSTAs return to baseline serum concentration following uncomplicated liver transplantation more quickly than other liver markers (Trull et al. 1994, Trull 2001). Additionally, serum GSTA

concentrations increase before alanine aminotransferase (ALT) after transplant rejection. Thus, monitoring GSTA leads to a greater survival rate, lower biopsy frequency, lower incidences of infections, less time spent in the hospital, less severe rejection, and halves the risk for graft loss (Hughes et al. 1997). The utility of GSTA as a marker of hepatocellular injury is discussed further below (2.3.).

2.2.Current enzymatic biomarkers of canine hepatocellular damage

Liver enzymes are relatively sensitive markers for canine hepatobiliary disease, but are not entirely specific. Liver enzyme markers can be categorized into those of hepatocellular injury and those of cholestasis. Markers of hepatocellular injury, such as alanine aminotransferase (ALT) and aspartate aminotransferase (AST), are released into circulation after hepatocyte necrosis or cell membrane damage. ALT is found in high concentrations in the cytoplasm of hepatocytes and is released into the blood within 12 hours after an increase in cell membrane permeability. Peak concentrations are reached after about 24 to 48 hours and the serum ALT activity usually returns back to the reference interval within 2-3 weeks of an acute liver injury. The enzyme half-life in dogs was found to be 59 hours in one study (Zinkl et al. 1971) and 149 hours in another (Dossin et al. 2005). Even though ALT is considered to be a liver specific marker in the dog, it is also found in skeletal muscle, cardiac muscle, erythrocytes, and renal tissue. Muscle disease can uncommonly lead to increases in canine serum ALT activities and should be correlated with serum creatinine kinase activities (Valentine et al. 1990, Chapman et al. 2015). Additionally, inflammatory or necrotizing disorders, as well as hepatic neoplasia, biliary tract disease, severe liver fibrosis or drugs, such as corticosteroids or phenobarbital, can lead to an increased serum ALT activity (Solter et al. 1994, Xu et al. 2012). Increases in serum ALT activities are for the most part proportional to the number of hepatocytes damaged, but it is possible for ALT activities to be within the reference interval in patients with liver disease, especially in those patients with hepatic failure (Kraft et al. 1983).

AST is located in the mitochondria and cytoplasm of canine hepatocytes. Again there is some disagreement concerning the half-life of AST between the studies, as Dossin et al. (2005) states it to be approximately 22 hours in dogs, whereas Zinkl et al. (1971) reported the half-life to be around 4.4 hours. Overall, AST is less liver-specific than ALT, as it is also localized in many

other tissues, such as the heart, skeletal muscle, erythrocytes, kidneys, and the brain. Therefore, serum AST activity can also be increased in dogs with hemolysis and myopathies. Thus, serum creatinine, ALT, and hematocrit should be determined together with AST activity.

The hepatobiliary enzymes alkaline phosphatase (ALP) and gamma-glutamyl-transferase (GGT) are considered to be markers of cholestasis and are associated with the cell membranes of hepatocytes and biliary epithelial cells. GGT is found in biliary epithelial cells, hepatocytes, as well as pancreatic, renal tubular, and mammary gland cells. Similarly to the ALP, GGT is elevated in patients with intra- or extrahepatic cholestasis, biliary tract disease, or hepatic necrosis (Center et al. 1992) and has a half-life of approximately 70 hours (Bengmark et al. 1974, Hoffmann et al. 1977). However, both enzymes can also be induced by drugs, such as corticosteroids, phenobarbital, phenytoin, or primidone. GGT usually has a low enzyme activity in dogs (Shull et al. 1979), but can be increased 2 to 3 times over the upper limit of the reference interval in young growing dogs. Even though GGT is more tissue specific, it is less sensitive in dogs than the ALP (Lum et al. 1972, Shull et al. 1979, Kraft et al. 1983, Center et al. 1992). ALP is located in the membranes of hepatocytes of the bile canaliculi and sinusoids and can indicate primary biliary tract or hepatic parenchymal disease. However, increased serum ALP activities can also be caused by various extrahepatic diseases. Extrahepatic sources of ALP include the kidney, pancreas, brain, bone marrow, spleen, testes, lymph nodes, placenta, as well as cardiac and skeletal muscle. Thus, ALP is not a liver specific biomarker (Center et al. 1992) and systemic diseases should be ruled out when working up a dog with increased serum ALP activity before making use of more invasive diagnostic tests, such as a liver biopsy.

Increased enzyme activities can occur in clinically normal animals. On the other hand, liver enzymes can be normal or just slightly increased in patients with end stage chronic hepatitis, so small variations in enzyme activities can be of clinical importance. Even dogs with severe liver disease don’t always show clinical signs. Consequently, further diagnostics should be considered in patients with continuously high liver enzymes. This is especially important for dogs with increased serum ALT activities because this enzyme is relatively liver specific.

2.3.GSTA as a marker of hepatocellular damage

Ideal attributes of a biomarker of hepatocellular damage would be high organ specificity, a strong correlation with histomorphologic changes, better diagnostic performance than serum ALT activity, accessibility by noninvasive procedures, as well as the ability to be measured with high throughput screening assays. Currently, ALT is the clinical chemistry reference standard, and even though it has great clinical utility and is highly sensitive, it occasionally gives false negative results with histopathological injury, as well as false positive results (Mannes et al. 1982, Valentine et al. 1990). On the other hand, glutathione transferase alpha has region-specific isoforms, with the GSTA1 being primarily located in the liver. In fact, it constitutes 50% of all GSTs in the human liver (van Ommen et al. 1990). This permits the identification of specific areas of damage, unaffected by hemolysis, muscle damage, or extrahepatic inflammation. In rats, GSTA was clearly shown to outperform ALT in terms of specificity against gastrointestinal and muscle injury in the absence of liver injury, but does increase in plasma due to kidney toxicity (Bailey et al. 2012).

Moreover, ALT is not able to detect certain hepatic injuries, such as biliary injury, or subtle hepatocellular lesions, as it is located mainly within the periportal areas of the liver, whereas GSTA is distributed evenly throughout the liver, in periportal as well as centrilobular hepatocytes (Abei et al. 1989, Campbell et al. 1991). GST alpha is the predominant GST class found in the liver, making up over 80% of GST, half of which is GSTA1 (van Ommen et al. 1990, Mulder et al. 1999). GSTA1's high cytosolic concentrations and very small molecular mass of about 26 kDa per subunit (about 50 kDa per dimer (Hoarau et al. 2002)) facilitate its quick release in high amounts into circulation with cell damage. For instance, hepatocellular damage due to paracetamol intoxication in humans primarily affects the centrilobular regions and can lead to abnormal GST concentrations within 4 hours of an overdose, whereas ALT increases much slower and can take 2 days to lead to abnormal enzyme activities (Beckett et al. 1985).

GSTA1 has a very short plasma half-life of approximately 1 hour in humans (Beckett et al. 1985), compared to ALT with a plasma half-life of approximately 48 hours, or GGT and ALP with a half-life of several days (Price et al. 1979, Dufour et al. 2000). Therefore, GSTA1 may give a more precise reflection of changes in the hepatocellular integrity and response to therapy, due to its fast clearance from circulation after resolution of liver damage (Sherman et al. 1983, Trull et al. 1994).

2.3.1. **GSTA as a marker of acute hepatocellular injury**

In humans, GSTA1 was found to be a specific and sensitive marker for acute liver disease, which responds rapidly to liver injury and recovery. Alpha GST outperforms ALT activity in terms of specificity in acute liver injury induced by several different toxins in rats (Bailey et al. 2012).
Following carbon tetrachloride hepatotoxicity in rats, alpha GST concentrations increase as early as 2 hours after exposure, whereas increases in AST concentration were not measurable at this point, nor was AST activity comparable in sensitivity to alpha GST several hours later. Alpha GST was also increased at five times lower doses as compared to AST (Clarke et al. 1997). Similar results can be obtained after paracetamol overdose, suggesting that alpha GST is a superior biomarker, especially of centrilobular hepatic injury, over the aminotransferases (Beckett et al. 1985, Beckett et al. 1989). This is supported by a study of GSTA1 as an early marker of liver damage after birth asphyxia, which occurs due to oxidative stress primarily in the centrilobular zones (Beckett et al. 1989).
GSTA may also be a more sensitive indicator of liver damage during the early stages of sepsis, as it increases before plasma lactate or the liver transaminases (Koo et al. 2000, Ramakers et al. 2009).

2.3.2. **GSTA as a marker of chronic hepatocellular injury**

Chronic hepatitis is the most common liver disease in the dog (Fuentealba et al. 1997, Poldervaart et al. 2009). The disease is histologically characterized by hepatocellular apoptosis and necrosis, an inflammatory cell infiltrate of primarily lymphocytes and plasma cells, as well as regeneration and fibrosis (Cullen 2009). Fibrosis can be severe and associated with hepatic failure. Therefore, early diagnosis and intervention are important for treatment success. Clinical signs are often nonspecific and may be subclinical early in the course chronic hepatitis (Poldervaart et al. 2009). Laboratory testing and diagnostic imaging are important diagnostic modalities in dogs with suspected chronic hepatitis, but histopathological evaluation of a liver biopsy is essential for establishing a definitive diagnosis.
In human patients with chronic hepatitis C, alpha GST seems to have a comparable sensitivity and specificity to ALT, but a higher sensitivity than that of other liver enzymes. In patients with normal ALT activities, alpha GST showed a higher sensitivity and specificity than

aminotransferases and seemed to detect patients with high viral loads that went undetected by aminotransferases, likely causing more severe liver damage (Giannini 2000, Abdel 2011).
In another study, all human patients with chronic hepatitis had increased serum concentrations of alpha class GST, which correlated significantly with the histologic severity of disease, whereas aminotransferase activities showed no such correlation (Sherman et al. 1983). In humans receiving immunosuppressive treatment for chronic autoimmune hepatitis, 65% showed increased serum GSTA1 concentrations, whereas only 23% showed increased serum AST activities, suggesting that GSTA1 may be superior for monitoring hepatic injury in these patients (Hayes et al. 1988). Furthermore, GSTA1 is useful for the detection of focal biliary cirrhosis with cystic fibrosis (Sidlova et al. 2003) and is generally increased in more than 50% of patients with cirrhosis (Sherman et al. 1983, Beckett et al. 1987). However, it seems to identify a different population than AST, possibly due to its more sensitive detection of alcohol induced centrilobular damage or its shorter half-life (Beckett et al. 1987).

2.4.GSTA as a marker of canine hepatocellular injury

The canine liver is known to possess high GST activity (Grover et al. 1964). Cytosolic GSTs make up approximately 3.5% of the total cytosolic protein in the canine liver (Wiener 1986), of which the alpha class appear to account for 3.1 % of the total soluble protein (Kilty et al. 1998). Early studies revealed the existence of three GST classes in the liver of dogs that cross-reacted with antibodies raised against the GST enzymes from other species, but not with members of different classes in the same species (Wiener 1986, Igarashi et al. 1991). They were determined to be of the alpha, mu, and pi class, as well as a GST of the theta class that showed no homology to any of the previously mentioned. Just as in humans, it was found that the N-terminus of the alpha GSTs in dogs is blocked for N-terminal sequencing (Igarashi 1991). In general, the GST distribution in animals is similar to those in humans; and thus, they may have utility as biomarkers of organ damage in other species. This was demonstrated in several animal species such as rats, where GST was shown to be a more sensitive liver marker than transaminases (van Wagensveld et al. 1997), and this was also suggested to be the case for dogs (Kilty et al. 1998). Kilty et al. (1998) purified GSTA by glutathione affinity chromatography from the liver of dogs and rats to develop an enzyme immunoassay. This assay was used to measure GST concentration

in the serum, following induced ischemic liver damage in adult Beagles. GST concentrations increased more quickly and with a greater initial peak than AST or ALT and then decreased to baseline sooner. These results suggest that GSTA may be a sensitive marker of hepatocellular injury early on in dogs and may have an advantage in the monitoring of recovery from liver injury. However, further studies are needed to compare the clinical performance of GSTA to that of existing markers of hepatocellular injury.

III. MATERIALS AND METHODS

1. Materials

1.1.Chemicals and Reagents

^{125}Iodine	Perkin Elmer, Waltham, MA, USA
Ampholytes (pH 3-10)	GE Healthcare, Uppsala, Sweden
Bovine serum albumin	Pierce Chemical CO, Rockford, IL, USA
Bovine serum albumin	EMD Millipore, Darmstadt, Germany
Chloramine T	Sigma Chemicals, St. Louis, MO, USA
Coomassie Brilliant Blue G-250	Pierce Chemical CO, Rockford, IL, USA
Glutathione S-Transferase assay kit	Sigma Aldrich, St. Louis, MO, USA
Glycerol	Mallinckrodt Pharmaceuticals, Dublin, Ireland
Guanidine hydrochloride	Sigma Aldrich, St. Louis, MO, USA
IEF standards	Bio-Rad Laboratories, Hercules, CA, USA
Imperial protein stain	Pierce Chemical CO, Rockford, IL, USA
L-glutathione reduced	Sigma Aldrich, St. Louis, MO, USA
Methanol	Fisher Scientific, Pittsburgh, PA, USA
Molecular mass markers – SeeBlue Plus2	Invitrogen, Carlsbad, CA, USA
NuPAGE 10% Bis-Tris gel	Invitrogen, Carlsbad, CA, USA
NuPAGE 12% Bis-Tris gel	Invitrogen, Carlsbad, CA, USA
NuPAGE LDS sample buffer	Invitrogen, Carlsbad, CA, USA
NuPAGE MOPS SDS running buffer	Invitrogen, Carlsbad, CA, USA
NuPAGE sample reducing agent	Invitrogen, Carlsbad, CA, USA
Phosphoric acid	Mallinckrodt Pharmaceuticals, Dublin, Ireland
Precipitating Solution (PPT)	MP Biomedicals, Santa Ana, CA, USA
Polyacrylamide	Bio-Rad Laboratories, Hercules, CA, USA
Potassium chloride	Sigma Aldrich, St. Louis, MO, USA
Potassium iodine	Sigma Aldrich, St. Louis, MO, USA
Potassium phosphate, monobasic	Sigma Aldrich, St. Louis, MO, USA
Rabbit carrier solution (RCS)	Sigma Chemicals, St. Louis, MO, USA

Silver stain kit	Pierce Chemical CO, Rockford, IL, USA
Sodium azide	Sigma Chemicals, St. Louis, MO, USA
Sodium chloride	EMD Millipore, Darmstadt, Germany
Sodium hydroxide	Mallinckrodt Pharmaceuticals, Dublin, Ireland
Sodium phosphate, dibasic	Sigma Chemicals, St. Louis, MO, USA
Sodium phosphate, monobasic	Sigma Chemicals, St. Louis, MO, USA
Trichloroacetic acid	Sigma Chemicals, St. Louis, MO, USA
TrizmaTM- HCl	Sigma Chemicals, St. Louis, MO, USA

1.2.Instruments

2470 Automatic Gamma Counter Wizard2™	Perkin Elmer, Waltham, MA, USA
AccuBlock™ Digital Dry Baths	Labnet International, Inc., Edison, NJ, USA
ÄKTA basic & fraction collector Frac-900	GE Healthcare, Uppsala, Sweden
Centrifuge 5810R	Eppendorf AG, Hamburg, Germany
Centrifuge Allegra® X-15R	Beckman Coulter, Brea, CA, USA
Centrifuge rotor F 34-6-38	Eppendorf AG, Hamburg, Germany
Centrifuge rotor A-4-81	Eppendorf AG, Hamburg, Germany
Centrifuge rotor SX4750A Aries™	Beckman Coulter, Brea, CA, USA
Desktop Personal Mini-Centrifuge	Clover Labs LCC, Whitehouse, OH, USA
Gel Doc™ XR+ System	Bio-Rad Laboratories, Hercules, CA, USA
GSTrap 4B affinity column	GE Healthcare, Uppsala, Sweden
Orbital Shaker	VWR, West Chester, PA, USA
pH-meter – Orion Star A211	Thermo Scientific, Rockford, IL, USA
Pipetman® (P-20, P-100, P-200, P-1000)	Rainin, Woburn, MA, USA
Pipette E4XLS Multichannel P-300	Rainin, Woburn, MA, USA
Pipettes E4XLS P-20, P-100, P-300, P-1000	Rainin, Woburn, MA, USA
Pipette P-5000	Eppendorf Research, Germany
Polytron homogenizer, PT-MR2100	Kinematica AG, Switzerland
Power Ease 500 (for electrophoresis)	Invitrogen life technologies, Carlsbad, CA, USA
Purelab Ultra (laboratory water purifier)	ELGA LLC, Woodbridge, NJ, USA
Resource™ S	GE Healthcare, Uppsala, Sweden
Sephadex™ G-25M (14.5×50 mm)	GE Healthcare Bio-Sciences AB, Uppsala, Sweden
Scaffold software package	Proteom Software Inc., Portland, OR, USA
Scale - Voyager Pro	Ohaus, Parsippany, NJ, USA
Scale – XS6002S	Mettler Toledo, Columbus, OH, USA
Shaker –Mircomix 5	DPC Cirrus Inc., Flanders, NJ, USA
Spectrophotometer, Nanodrop 1000	Thermo Scientific, Rockford, IL, USA
Spectrophotometer, Ultrospec 2000	GE Healthcare Bio-Sciences AB, Uppsala, Sweden

Standard Stirrer	VWR, West Chester, PA, USA
Statistical software package Prism 5.0	GraphPad Software Inc., San Diego, CA
Synergy 2 multi-mode plate reader	Biotek Instruments, Inc., Winooski, VT, USA
Vortex mixer	Fisher Scientific, Pittsburgh, PA, USA

1.3.Disposables

Blue Max™ Jr., polypropylene tube, 15 ml	Falcon, Franklin Lakes, NJ, USA
Centrifugal filter devices - Amicon Ultra – 4 ml & 15 ml; 10,000 MWCO	Millipore Corporation, Bedford, MA, USA
Centrifuge tubes (polypropylene, 50 ml)	VWR, West Chester, PA, USA
Culture tubes (polypropylene, 12 x 75 mm)	VWR, West Chester, PA, USA
Culture tubes (polystyrene, 12 x 75 mm)	VWR, West Chester, PA, USA
Disposable glass culture tubes (12 x 75 mm)	VWR, West Chester, PA, USA
Magnetic stir bar	VWR, West Chester, PA, USA
Membrane filters 0.2 µm – 10 µm	Pall Corporation, Port Washington, NY, USA
Microcentrifuge tube (1.5 ml)	USA Scientific, Orlando, FL, USA
Microcentrifuge tube seal-rite (2 ml & 0.5 ml)	USA Scientific, Orlando, FL, USA
Microplates, 96-well ELISA	Greiner Bio-One GmbH, Frickenhause, Germany
Nalgene® syringe filters, polyethersulfone, 25 mm (0.2 µm, 0.45 µm, 0.8 µm)	VWR, West Chester, PA, USA
Rainin® pipette tips (10, 250 & 1000 µl)	Rainin, Woburn, MA, USA
Tips GelWell 0.57mm 10 µL GT-10-6	Rainin, Woburn, MA, USA
Pleated dialysis tubing - Snakeskin 10k MW	Thermo Scientific, Rockford, IL, USA
Self-Standing centrifugal polypropylene tubes, 50 ml	Corning Incorporated, Corning, NJ, USA
Weighing paper	VWR, West Chester, PA, USA
Weight boats, small and medium	USA Scientific, Orlando, FL, USA

2. Methods

2.1.Purification of canine glutathione transferase alpha

2.1.1. Assay for enzymatic activity

A glutathione S-transferase activity assay kit was used to screen fractions obtained at different stages of the protein purification process for any GST activity. The assay was performed in 96-microwell plates. Briefly, 4 µl of test sample and a positive control were pipetted into wells in duplicates, 196 µl of master mix (Dulbecco's Phosphate Buffered Saline, 200 mM L-glutathione reduced, 100 mM 1-chloro-2,4-dinitrobenzene (CDNB)) were added to each well, and the plate was placed on a plate shaker for 10 seconds. It was then immediately placed in an automated plate reader and the increase in absorbance was measured over a period of 9 min at 340 nm.
The activity of GST was calculated using the formula:

$$\frac{(\Delta A_{340})/\text{min} \times V(\text{ml}) \times \text{dil}}{\varepsilon_{mM} \times V_{enz}\,(\text{ml})} = \mu\text{mol / ml / min}$$

dil = dilution factor of sample; $\varepsilon_{mM} = 5.3\ mM^{-1}$ (extinction coefficient for CDNB);
V = reaction volume; V_{enz} = volume of sample tested

2.1.2. Extraction of cGSTA

Liver was collected from healthy dogs euthanized for an unrelated research project, immediately frozen at -80°C, and stored until further use. For extraction, a portion of liver tissue was allowed to thaw at room temperature and cut into small pieces. Fractions of approximately 40 g each were homogenized with 160 ml of KCl buffer in a tissue grinder in order to lyse the liver cells. To avoid overheating of the solution and denaturation of the proteins, the sample was kept on ice during the entire process. The resulting suspension was collected in 50 ml polypropylene tubes. The tubes were placed in a fixed angle rotor centrifuge and spun at 10,000 x g at 4°C for 25 min to pellet cell debris. The supernatant was carefully transferred into new polypropylene tubes and the pellet was discarded. Subsequently, the supernatant was filtered under vacuum through a series of filter paper with decreasing pore size from 10 µm to 0.2 µm. The filtrate was either stored at -80°C or used immediately for purification. Prior to purification the buffer containing the liver filtrate was exchanged to PBS buffer, which was used as the binding buffer for GST

affinity chromatography (140 mM NaCl, 2.7 mM KCl, 10 mM Na_2HPO_4, 1.8 mM KH_2PO_4, pH 7.4). The buffer exchange was performed at 4°C over a total of 20 hours, with the dialysis buffer being exchanged after 5, 10, and 20 hours (Figure 4).

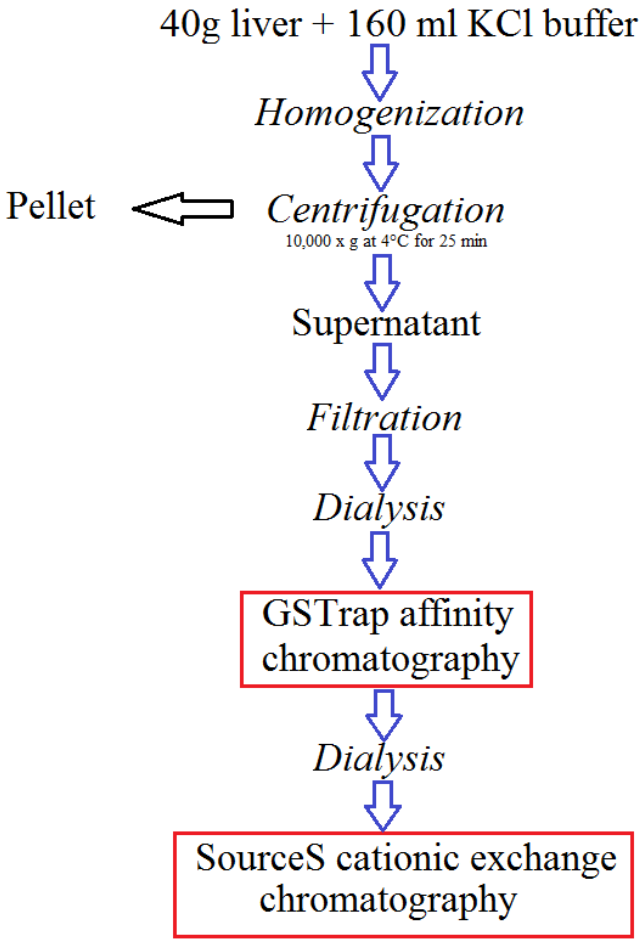

Figure 4: Overview of the purification of cGSTA from canine liver

This figure shows the major steps of the purification process of cGSTA from canine liver, starting with 40 g of liver tissue in 160 ml of KCl buffer.

2.1.3. **Purification of cGST by glutathione affinity chromatography**

The column used specifically binds GST's, such as the GST alpha. Its matrix consists of 4% agarose, which is coupled to the glutathione ligand via a 10-carbon linker. The column was equilibrated according to the manufacturer's instruction. Fresh running buffers were always prepared, as it was noticed that background absorbance was higher with buffers stored for a few days. Ten ml of the filtered and dialyzed protein solution were loaded onto the GSTrap^{TM} 4B column (5 ml) at a flow rate of 0.5 ml/min. The column was thereafter washed with 5 column volumes of binding buffer (10 mM Na_2HPO_4, 1.8 mM KH_2PO_4, 140 mM NaCl, 2.7 mM KCl, pH 7.4) at a flow rate of 1 ml/min in order to elute proteins that did not bind to the column. The bound GST proteins were eluted using an elution buffer containing reduced glutathione (50 mM Tris-HCl, 20 mM glutathione, pH 8). One ml fractions were collected and the fractions that showed high GST enzymatic activity were pooled.

2.1.4. **Purification of cGSTA by strong cation-exchange chromatography**

The pooled high GST activity fractions prepared from glutathione affinity chromatography underwent another buffer exchange to buffer A (20 mM Tris-HCl, pH 7) in order to prepare them for the next chromatography step. Dialysis tubing was used and dialysis was performed for a total of 20 hours at 4°C with three buffer exchanges at 5, 10, and 20 hours. Twenty ml of the dialyzed solution were loaded at a flow rate of 1 ml/min onto the Resource S 1 ml column that was previously equilibrated according to the manufacturer's instruction. The column matrix consisted of spherical rigid polymers with sulphonate functional groups.

The column was washed with about 10 column volumes of buffer A, so that proteins not bound to the column were washed out and the absorbance returned back to baseline. Thereafter, a linear salt gradient of 0 – 15% of buffer B (20 mM Tris-HCl buffer, 1 M NaCl, pH 7) over 5 column volumes at a flow rate of 1 ml/min was applied to elute the only weakly bound GSTA from the column. Fractions of 1 ml each were collected from the resulting peak and showed high enzymatic activity with CDNB. The fractions were pooled, then concentrated, and the buffer was exchanged to a PBS buffer using a 15 ml Millipore centrifugal filter device with a molecular mass cut off at 10,000 Da. The filtrate was centrifuged at 4°C four times at 5,000 x g for 25 min, each with PBS buffer, to achieve a buffer exchange and a protein concentration of approximately 1 mg/ml. The pure GSTA concentrate was stored at -80°C until further use.

2.1.5. **Sodium-dodecyl-sulfate gel electrophorese (SDS-PAGE)**

Sodium-dodecyl-sulfate-polyacrylamide gel electrophoresis (SDS-PAGE) was used to analyze the purity of the obtained protein under reducing conditions. In accordance with the manufacturer's instructions, precast 10% and 12% polyacrylamide vertical gels with a gel thickness of 1 mm were used. The gel cassette was tightly placed into the electrophoresis chamber and the inner and outer chambers were filled with MOPS SDS running buffer (5 mM 2-[N-morpholino] ethanesulfonic acid, 5 mM Tris base, 0.01% SDS, 0.1 mM EDTA, pH 7.7). The samples were prepared by adding 19.5 µl of sample to 3 µl NuPAGE® sample reducing agent (500 mM dithiothreitol) and 7.5 µl of NuPAGE® LDS sample buffer (106 mM Tris-HCl, 141 mM Tris base, 10% glycerol, 0.51 mM EDTA, 0.22 mM SERVA blue G250, 0.175 mM Phenol red, 2% lithium dodecyl sulfate, pH 8.4). The sample-buffer mixtures were incubated at 70°C for 10 min in order to denature the proteins. Usually, 10 µl of each sample-buffer mixture were loaded into the wells of the gel. In addition to the samples, 8 µl of a standard protein solution (SeeBlue® Plus2) were loaded into the first well. The standard protein solution contained 8 different proteins with a known molecular mass: myosin (191 kDa), phosphorylase B (97 kDa), bovine serum albumin (64 kDa), glutamic dehydrogenase (51 kDa), alcohol dehydrogenase (39 kDa), carbonic anhydrase (28 kDa), myoglobin-red (19 kDa), and lysozyme (14 kDa). The electrophoresis was run at a constant voltage of 200 V for 55 minutes. Immediately after completion the gel was removed from the cassette, washed in water for one minute, and stained with Imperial™ protein stain for one hour. Thereafter, the gel was destained in water over 12 hours and a digital image of the gel was taken with the Molecular Imager® Gel Doc™ XR using the Quantity One software.

2.2.Partial characterization of canine glutathione transferase alpha

2.2.1. **Protein identification and determination of purity**

The purity of the protein was established in three different ways.

Nano-spray liquid chromatography-tandem-mass spectrometry (LC/MS/MS) was performed to directly identify proteins in different fractions collected from cation exchange chromatography at the Protein Chemistry Laboratory, Department of Biochemistry and Biophysics at Texas A&M University. Briefly, for sample preparation purified protein was run on SDS-PAGE and stained under the conditions described in detail above (2.1.5). Thereafter, bands of the purified protein sample were cut out and submitted for LC/MS/MS. The protein was digested using trypsin and the resulting peptides were separated by capillary reverse phase-high performance liquid chromatography (rp-HPLC) prior to in-line analysis of their masses and fragmentation patterns. Finally, the measured mass spectra were used to search the NCBInr database of known protein sequences to match digestion patterns of the proteins.

In order to determine the purity of the final product an SDS-PAGE following the manufacturer's instructions as described in 2.1.5. was performed and stained with Imperial^{TM} Protein Stain. An amount of 1.94 µg of the purified sample was calculated to be loaded onto the gel in order to establish purity.

2.2.2. **Amino acid composition analysis**

Amino acid analysis of the purified protein was performed at the Protein Chemistry Laboratory, Department of Biochemistry and Biophysics at Texas A&M University in order to determine its purity and amino acid composition. Non-volatile amines, such as TRIS, were incompatible with the analysis and the TRIS-HCl buffer of the sample collected after cationic exchange chromatography thus needed to be exchanged to a PBS buffer using a disposable centrifugal filter device (see 2.1.4). The assay was run in duplicates with sample aliquots of 10 µl each that were mixed with 5 nmol of norvaline and sacosine used as the internal standard. The samples then underwent vapor phase hydrolysis by 6 M hydrochloric acid at 150°C for 1.5 hours. Samples were brought up in 0.4 N borate buffer for an optimal derivatization of the amino acids with o-phthalaldehyde (OPA) and 9-fluoromethyl-chloroformate (FMOC) at a pH of 10. The derivatized amino acids were separated by reverse phase HPLC and detected by fluorescence.

2.2.3. **Estimation of the molecular weight**

The apparent molecular weight of the purified canine glutathione transferase alpha was estimated by comparison to the standard protein solution SeeBlue® Plus2 on a gel. Therefore, SDS-PAGE was run following manufacturer's instruction as described in 2.1.5. and stained with Imperial™ Protein Stain. Finally, the image software BioNumerics 6.6 was used to estimate the molecular weight of canine GSTA by comparing it to the standard protein solution.

2.2.4. **Determination of the molecular mass**

The accurate molecular mass of canine GSTA was determined by Matrix Assisted Laser Desorption/Ionization-Time of Flight mass spectrometry (MALDI-TOF) performed at the Protein Chemistry Laboratory, Department of Biochemistry and Biophysics at Texas A&M University, College Station, Texas, USA. One µg of protein sample was mixed with the matrix compound α-cyanohydroxycinnamic acid on a predefined spot on the metal sample plate and allowed to air dry. The plate was then placed in a high vacuum source chamber in the mass spectrometer and analyzed. A mass-to-charge ratio (m/z) range of 100 to 30,000 was used.

2.2.5. **Estimation of isoelectric point**

For visualization and estimation of the isoelectric point, a polyacrylamide mini slab gel (8% polyacrylamide, and 2% ampholytes, pH range of 3 to 10) for gel electrophoresis was poured. A sample buffer consisting of 50% glycerol was prepared and mixed with sample in equal amounts. Seven mM phosphoric acid was prepared for the anode buffer and filled into the lower buffer chamber. The cathode buffer was prepared and consisted of 0.5 M sodium hydroxide and filled in the upper buffer chamber. A standard protein solution contained 9 different proteins, ranging from a pI of 9.6 (cytochrome C) to a pI 4.45 (phycocyanine), was used for comparison. The sample mixture and protein marker were loaded into the wells and run at a constant voltage of 100 V for 1 hour, followed by a constant voltage of 250 V for 1 hour, and finally at a constant voltage of 500 V for 30 minutes. The gel was then removed from the cassette and incubated for

10 minutes in a fixation solution consisting of 20% trichloroacetic acid. Finally, the gel was stained with a non-fixing silver stain method according to Blum et al. (1987).
Additionally, an immobilized pH gradient (IPG) strip (pH 3-10) was run at the Protein Chemistry Laboratory, Department of Biochemistry and Biophysics at Texas A&M University, College Station, Texas, USA to get another more accurate estimate of the pI of cGSTA.

2.2.6. **Determination of specific absorbance**

The specific absorbance of canine GSTA was determined based on the total amount of protein solution as estimated by the Bradford protein assay. The Bradford protein assay is a method to determine protein concentration by binding Coomassie Brilliant Blue G-250 dye to the proteins. When the dye binds to protein, it is converted to a stable unprotonated/anionic form, which can be detected at 595 nm. Thus, the amount of dye-protein complexes reflects the protein concentration of the solution.
The assay was performed using a 96-well microplate according to the manufacturer's instructions. Briefly, eight standards from bovine serum albumin (BSA) with concentrations ranging from 25 µg/ml to 2000 µg/ml (i.e., 25, 125, 250, 500, 750, 1000, and 2000 µg/ml) were prepared and loaded onto the plate. Purified canine GSTA was serially diluted in Millipore water, using dilutions from 1 in 2 to 1 in 16. Five microliters of each standard, sample dilution, and a blank were loaded into the wells of the microplate, followed by 250 µg of Coomassie Brilliant Blue G-250 dye. The plate was briefly placed on a shaker and then incubated at room temperature for 10 minutes. Finally, it was placed into an automated plate reader and the absorbance measured at 595 nm.
The absorbance of each standard and sample was corrected for non-specific binding (blank). A standard curve was established by plotting the average of the duplicates for each BSA standard against its concentration in µg/ml. The protein concentration of each unknown sample was interpolated from the standard curve.
To calculate the specific absorbance, the absorbance of the pure protein solution at 280 nm was measured with a spectrophotometer and then divided by the protein concentration, which was calculated with the Bradford protein assay and confirmed by amino acid analysis.

2.3. Production of anti-cGSTA antiserum

For the production of anti-cGSTA antiserum, two New Zealand White rabbits (*Oryctolagus cuniculus*) were injected with pure canine GSTA at Lampire Biological Laboratories, Pipersville, Pennsylvania, USA. Briefly, each rabbit was injected subcutaneously with 300 µg of canine GSTA protein in 0.5 ml of PBS, mixed with 0.5 ml complete Freund's adjuvant. Reinoculations with 300 µg of GSTA in 0.5 ml of PBS mixed with 0.5 ml of incomplete Freund's adjuvant were performed on days 21, 42, and 71 in order to boost the immune response to the antigen. Blood samples were collected by venipuncture of the ear vein 10, 8, and 14 days after each booster injection, respectively. After a total of 4 injections the animals were exsanguinated and the collected sera used for the development of a radioimmunoassay (RIA). Titers of anti-cGSTA antibodies in the serum of the rabbits were determined using pure GSTA radiolabeled with ^{125}I.

2.4. Production of tracer for the radioimmunoassay

Pure GSTA was radiolabeled with ^{125}I by the chloramine-T method (Hunter et al. 1962). Briefly, a miniature stir bar and 10 µl of a 0.25 M sodium phosphate buffer (pH 7.5) were placed in a 5 ml polystyrene tube above a stir plate. While stirring, 10 µl of ^{125}I (0.1 mCi/µl at the time of production) were added to the test tube using a Hamilton syringe, as well as 10 µl of purified GSTA in PBS (1 mg/ml) and 10 µl chloramine-T solution (2 mg/ml chloramine-T in 0.05 M sodium phosphate buffer). After 45 seconds, the following were added in rapid succession: 100 µl sodium metabisulfite solution (0.4 mg/ml $Na_2S_2O_5$ in 0.05 M sodium phosphate buffer, pH 7.5), and 860 µl potassium iodide solution (2 mg/ml KI in 0.05 M sodium phosphate buffer, pH 7.5). To measure the total radioactivity, 10 µl of this unfiltered mixture was pipetted into polystyrene tubes in duplicates and diluted with 990 µl of RIA buffer (0.05 M sodium phosphate solution, 0.2 g/L NaN_3, 5 g/L BSA, pH 7.5), leaving 980 µl for further processing. A disposable PD-10 desalting column (Sephadex^{TM} G-25M; 14.5×50 mm) was equilibrated with 3 column volumes of a concentrated BSA solution (50 mM monobasic sodium phosphate solution and 50 mM dibasic sodium phosphate solution mixed to achieve a pH of 7.5, with subsequent addition of 5 g/L BSA and 0.2 g of sodium azide) to prevent nonspecific protein binding to the dextran resin of the column. The remaining 980 µl of the solution were loaded onto the column in order to separate the iodinated protein from free ^{125}I by size-exclusion, and the eluent was collected in

a polystyrene tube. Subsequently, RIA buffer was used as the mobile phase and added in 1 ml aliquots. Resulting 1 ml fractions of eluent were collected in individual polystyrene tubes. This resulted in 14 fractions, numbered 2 to 15. Ten µl of each of these fractions were analyzed, along with 10 µl of the aliquot of the diluted unfiltered mixture previously described to determine the total radioactivity applied and the radioactivity of each fraction. The radioactivity was recorded in counts per minute (CPM). Plotting the CPM measured versus the fraction number, a curve with two peaks was established. The first peak included fractions 4 and 5 and the second peak included fractions 10 to 13, corresponding to the highest radioactivity. Since the iodinated protein has a higher molecular mass than free ^{125}I, it was expected to elute earlier and so the earlier fraction 4 was chosen for the production of the tracer. Fraction 4 was adjusted to approximately 40,000 CPM per 100 µl tracer by diluting with RIA buffer.

2.5. Determination of the antibody titer

An RIA was performed to estimate the antibody titer in the sera of the two rabbits, with all analyses performed in duplicate fashion. Two tubes received 100 µl of tracer in order to measure the total counts (TC) of the tracer, which was produced as described under 2.3.1. Two tubes were labeled NB (nonspecific binding) and contained a mix of 200 µl of RIA buffer and 100 µl of tracer. The following 10 tubes were used for a 2-fold serial dilution of the rabbit serum, starting with a 1 in 500 dilution and ending with a 1 in 256,000 dilution. For the initial dilution, 20 µl of serum was diluted with 180 µl of RIA buffer (0.5 M sodium phosphate solution, 0.2 g/L NaN_3, 5 g/L BSA, pH 7.5) to create a 1 in 10 dilution, and 20 µl of this solution was further diluted with 980 µl of RIA buffer to create the 1 in 500 dilution. Each level of dilution in the series was prepared for analysis in duplicates by combining 100 µl of the diluted solution, 100 µl of RIA buffer, and 100 µl of the previously produced tracer into two polypropylene tubes. The samples were vortexed and then incubated for 24 hours at room temperature. In the following, 100 µl of rabbit carrier solution (RCS), consisting of a 1 in 100 dilution of uninoculated rabbit serum in RIA buffer, was added. Next, 1 ml of a commercially available precipitation solution (PPT), which contains specific anti-rabbit-IgG antibodies, was added to each tube, except the TC tubes. The antibodies in the solution bind to the complexes of rabbit-derived antibodies and protein and precipitate it from the solution, forming a pellet in the bottom of the tube after centrifugation. All

tubes, except the tubes for measuring TC, were vortexed and then centrifuged at 3,800 RPM and 4°C for 30 min. The supernatants were carefully decanted and all tubes were counted for 1 min using an automated gamma counter. The unit for the measurement of radioactivity was counts per minute (CPM) and the results were expressed as a percentage of binding of the anti-GSTA antibodies to radiolabeled protein:

% binding = (mean of CPM – mean of NB)/(mean of TC – mean of NB)*100.

A titer curve was generated by plotting the results, with the x-axis showing the dilution of the serum and the y-axis showing the percent binding.

2.6. Establishment of a radioimmunoassay (RIA) for the measurement of cGSTA concentration in serum

For establishment of a standard curve, a dilutional series of canine GSTA in RIA buffer was performed. Canine GSTA standards with the following concentrations were prepared: 200 µg/L, 100 µg/L, 50 µg/L, 25 µg/L, 12.5 µg/L, 6.25 µg/L, and 3.125 µg/L. Polypropylene tubes were labeled in a duplicate fashion; and each tube received 100 µl tracer, 100 µl anti-GSTA antibody solution (diluted 1 in 20,000 in RIA buffer), as well as 100 µl of the GSTA standard dilutions (serial 2-fold dilutions from 200 µg/L to 3.125 µg/L). The total count (TC) tubes received only 100 µl of tracer each. Tubes for nonspecific binding (NB) contained 100 µl tracer and 200 µl RIA buffer. The zero standard (B_0 = negative control) contained 100 µl of tracer, 100 µl anti-GSTA antibody solution, and 100 µl RIA buffer.

For the antibody solution, approximately 1 mg/ml of purified polyspecific anti-GSTA antibody solution was used diluted 1 in 20,000 with RIA buffer and added to each tube, except for the TC. Tubes were vortexed for 20 seconds and incubated for 72 hours at room temperature. Then, 100 µl of RCS as well as 1,000 µl of a commercially available PPT were added to each duplicate, except for the TC. Again, all tubes were vortexed and then centrifuged at 4°C and 3,800 RPM for 30 min. Thereafter, all tubes were placed in a Styrofoam rack and the supernatant was decanted, with the exception of the TC tubes. All tubes including the TC tubes were then counted for 1 min with an automated gamma counter and the mean of the CPMs of the duplicates calculated. A standard curve was calculated using a 5-parameter curve fit ($y = d + [(a–d)/(1 + (x/c)b)e]$) with values on the x-axis representing the canine GSTA concentrations with a logarithmic scale and

values on the y-axis representing the CPM for each standard. All unknown samples as well as the standards were run in duplicate fashion and contained 100 µl tracer, 100 µl antibody solution and 100 µl sample each.
To determine the sample concentrations of canine GSTA in serum the CPM subtracted by the NB was plotted against the standard curve.

2.6.1. **Refinement of the RIA**

Optimal conditions for the assay were evaluated by testing standard curves with different antibody dilutions of 1:5,000, 1:10,000, 1:15,000, 1:20,000, 1:40:000, or 1:80,000. Different sample dilutions of 1:2, 1:4, 1:8, 1:16 as well as undiluted serum sample were tested. In addition, different incubation times (i.e. 2h, 24h, 48h, and 72h) were compared to each other, as well as adding an incubation step of several hours before adding the tracer.

2.6.2. **Analytical validation of the RIA**

For the analytical validation of the RIA its lower and upper limit of the working range, linearity, accuracy, precision, and reproducibility were determined.
The lower limit of detection of the RIA was determined by analyzing 10 duplicates of B0 in the same run, and calculating the mean and standard deviation (SD). The canine GSTA concentration that matched the mean CPM minus 3 times the SD plotted against the standard curve, was defined as the lower detection limit of the assay.
To determine the linearity, accuracy, precision, and reproducibility of the RIA, left over/ surplus samples from the Gastrointestinal Laboratory of Texas A&M University with low, moderate, and high canine GSTA concentrations were tested.
Assay linearity was evaluated by assessing dilutional parallelism for 4 different serum samples at serial twofold dilutions starting with an undiluted sample (i.e., undiluted, 1:2, 1:4, and 1:8).
The accuracy of the assay was assessed by spiking 4 different serum samples with an equal volume of solutions with known concentrations of canine GSTA (i.e., 1.56, 3.12, 6.25, 12.5, 25, 50, 100, and 200 µg/L). The percentage of standard antigen recovery was calculated as [observed value (µg/L)/expected value (µg/L)]x100.

To evaluate the precision of the RIA, 4 different serum samples from dogs were analyzed 10 times in duplicates within the same assay run. The intra-assay coefficient of variation (%CV = [SD/mean]x100) was then calculated.
Assay reproducibility was evaluated by assaying 4 different serum samples in 10 consecutive assay runs, followed by calculating the inter-assay %CVs. For both the intra- and inter-assay variability, sample 3 and 4 were spiked, by making a solution comprised of 80% serum sample and 20% of either a 200 ug/L or a 400 ug/L cGSTA solution.

2.7. Measurement of serum cGSTA concentrations in healthy dogs

In order to establish an initial reference interval for canine serum GSTA, serum samples from 49 healthy adult dogs were collected and analyzed. The dogs were owned by students or staff of Texas A&M University and underwent a physical examination before venipuncture. All interventions were approved by the Institutional Animal Care and Use Committee and informed client consent was obtained before the enrollment of the dogs. The health of the dogs was established based on the data from client questionnaires, physical examination findings, and the results of a complete blood count and a serum chemistry profile. The median (minimum to maximum) serum cGSTA concentrations for this group of dogs were calculated. The reference interval was calculated as the lower 95th percentile of serum cGSTA concentrations in these healthy dogs.

2.8. Measurement of serum cGSTA concentrations in dogs with hepatic disease

To characterize serum concentrations of GSTA in dogs with hepatobiliary disease, left over serum from 45 dogs undergoing liver biopsy that had been enrolled in another study were used. The dogs were cared for at Veterinary Medical Teaching Hospital at Texas A&M University and at Gulf Coast Veterinary Specialists. For each dog the diagnosis of hepatobiliary disease was based on laboratory findings, imaging findings, and histopathological assessment of the liver.
The dogs were assigned to 4 groups: group 1- congenital portosystemic shunt (CPSS), group 2- chronic hepatitis (including some dogs with copper associated chronic hepatitis), group 3-

hepatic neoplasia, and group 4- other hepatobiliary disease, such as gall bladder mucocoeles, acute hepatitis, toxic hepatitis, cholangiohepatitis and an acquired portosystemic shunt with portal vein hypoplasia.

Serum cGSTA concentrations were measured by the newly developed RIA in all 45 dogs. The data was tested for normality using visual inspection of frequency distribution plots and the Kolmogorov-Smirnov test. The Mann-Whitney U test was used to compare serum cGSTA concentrations between diseased and healthy The Kruskal-Wallis test followed by Dunn's post test as appropriate was used to compare serum cGSTA concentrations between more than 2 groups of dogs. Statistical significance was set as $p < 0.05$.

IV. RESULTS

1. Purification of canine glutathione transferase alpha (GSTA)

During the process of purification, the intracellular protein glutathione transferase was extracted from the hepatocytes. After homogenization and centrifugation a grey-red pellet had formed in the bottom of the tube, while the top layer was a red opaque solution, which was carefully collected. Following several filtration steps the solution became more clear and free of solid material. This filtrate showed high GST activity (Figure 6).

After dialysis, this protein-rich extract was further purified using a glutathione affinity column that binds glutathione transferases. Substantial purification of canine GSTA was obtained during this chromatography step and resulted in a solution that was clear with a hint of slight yellow. A typical chromatogram of the affinity chromatography is shown in Figure 5.

CDNB was used as a substrate in the activity assay to measure glutathione transferase activity. The increase in absorbance measured by an automated plate reader is shown in Figure 6.

SDS-PAGE was performed in order to monitor the purification of canine GSTA. Figure 7 shows a NuPAGE SDS gel of fractions from different stages of the separation of canine GST from cell debris and other liver proteins by glutathione affinity chromatography. Fractions of peak II showing high GST activity during the enzymatic assay, were buffer-exchanged and further separated by strong cation-exchange chromatography as seen in Figure 8. The collected fractions and their difference in color are depicted in Figure 9. Figure 10 shows a NuPAGE SDS gel of fractions from different stages of the cation exchange chromatography, which separates canine GSTA from different GST- isoforms and other residues. Figure 11 shows an SDS-PAGE, displaying the different purity stages of the protein solution during the purification of canine GSTA. Table 1 summarizes the major steps involved in the purification of canine GST from 5 g of liver. Percent of recovery and degree of purification are given for each step. Several different preparative runs gave essentially similar results to those shown in Table 1.

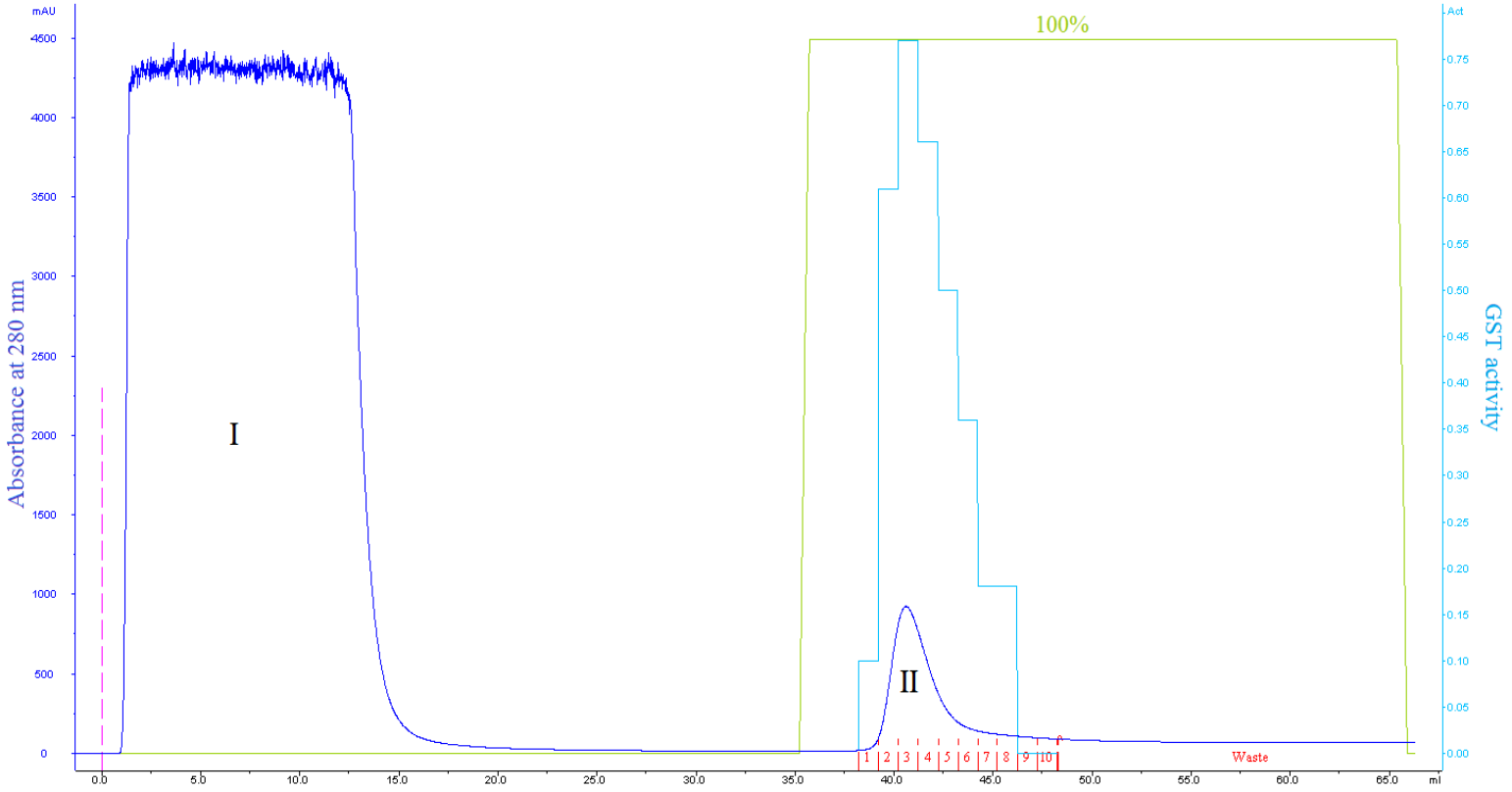

Figure 5: Chromatogram of glutathione affinity chromatography

In this figure, a typical chromatogram of an affinity chromatography of a canine liver extract is shown. The y-axis on the left displays the absorbance at 280 nm (blue), whereas the y-axis on the right shows the enzymatic activity of each fraction measured by the activity assay (light blue). The x-axis demonstrates the flow volume in milliliters. Two peaks can be viewed on the chromatogram (I-II). Peak I represents the majority of proteins that did not interact with the column matrix and were washed out immediately. Peak II represents proteins that bound and that were washed out with excess reduced glutathione in the elution buffer. The free glutathione competitively displaces the immobilized glutathione binding interaction with the GST, allowing it to emerge from the affinity column.

A)

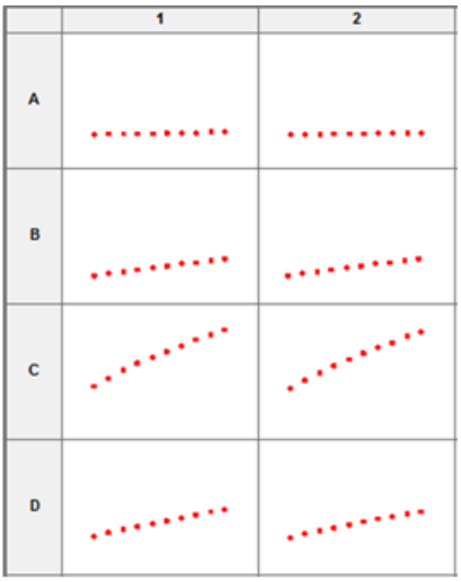

B)

	1	2
A	0.032	0.031
B	0.221	0.223
C	0.678	0.679
D	0.323	0.314

Figure 6: Measurement of GST activity

As described in section 2.1.1., the GST activity assay was performed in a 96-microwell format with CDNB as a substrate. The absorbance was measured over 9 minutes with one reading every minute at a wavelength of 340 nm using an automated plate reader. Samples were analyzed in duplicate fashion, as seen in column 1 and 2 of the panels. Panel A graphically displays the increase in absorbance over the 9 minutes, whereas Panel B shows the numerical values for the calculated change in absorbance of the same samples. In both panels row A represents a negative control (blank), barely showing any increase in absorbance and therefore indicating that no GST is present in these wells. Row B is a positive control and consists of 0.25 mg/ml GST and shows an increase in absorbance over time. Row C contains a fraction collected during peak II of the GST affinity chromatography, showing a marked increase in absorbance. Row D represents a fraction collected later in peak II and an increased absorbance can still be appreciated.

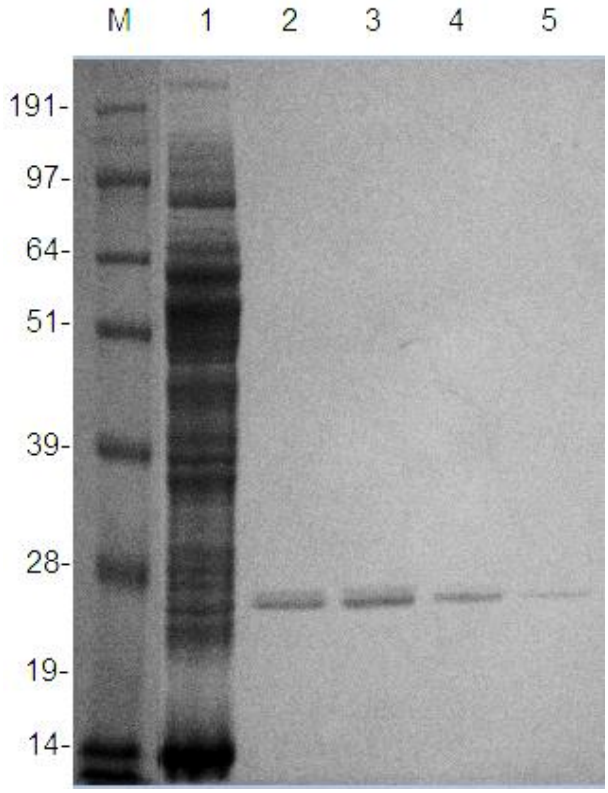

Figure 7: SDS-PAGE after affinity chromatography

SDS-PAGE was used to analyze the purity of the obtained protein under reducing conditions on a 10% Bis-Tris gel stained with Imperial™ Protein Stain. The first lane labeled "M" was loaded with 8µl of a standard protein solution (SeeBlue® Plus2) containing 8 different proteins with known molecular masses. The numbers on the left of the image represent the molecular mass of these standard proteins in kDa. Lanes 1 to 5 were loaded with 10 µl of sample. Lane 1 contains a variety of protein bands of different masses, displaying the flow through seen as peak I in the chromatogram. Lanes 2 to 5 contain two bands in close proximity of approximately 26 kDa, which represent GST. These lanes were loaded with fractions from peak II and showed high GST enzymatic activity. Lanes 4 and 5 contain less protein as these are fractions towards the end of the peak. The small differences in molecular mass can be explained by the minor size variations of the different isoforms of GST.

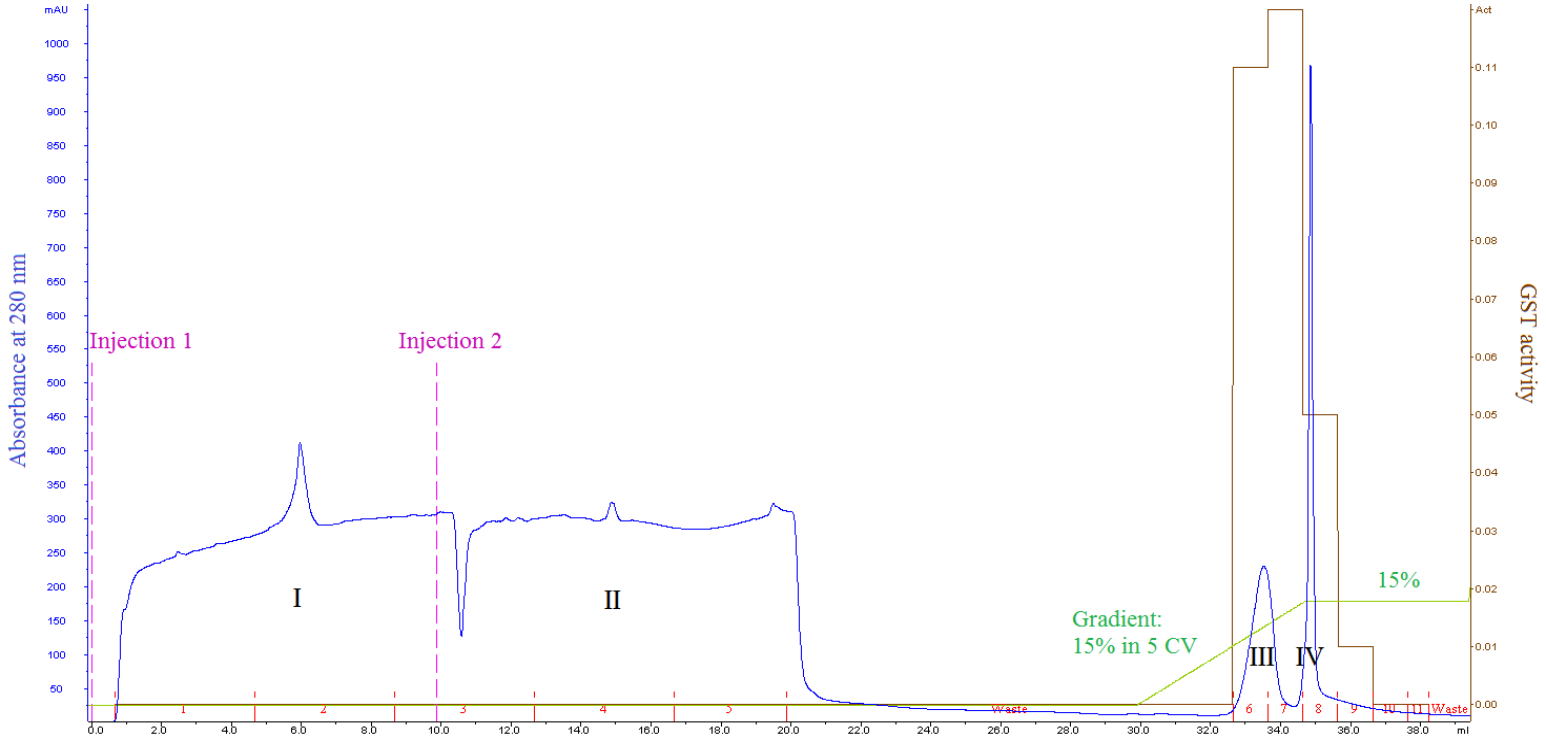

Figure 8: Chromatogram of strong cation-exchange chromatography

In this figure a typical chromatogram of a cation-exchange chromatography of high GST activity fractions, collected during GST-affinity chromatography, is shown. The y-axis on the left displays the absorbance at 280 nm (blue), whereas the y-axis on the right shows the enzymatic activity of each fraction measured by the activity assay (brown). The x-axis demonstrates the flow volume in milliliters. Four peaks can be viewed on the chromatogram (I-IV). Peak I and II represent the majority of proteins that did not interact with the column matrix and were washed out immediately. There are two peaks, because protein was injected twice, represented by the pink lines, using a volume of 10 ml each, as the volume capacity superloop^{TM} only held a volume of 10 ml. Peak III represents proteins that bound only weakly to the column matrix and were washed out with a low ionic strength buffer. This peak showed the highest GST activity and was eluted from the column with a salt concentration between 0.05 and 0.1 M NaCl. It was followed directly by a steep peak IV. The fractions of this peak showed lower enzymatic activity, but were of pale red color as seen in Figure 9. Therefore, this peak might include a substance of high absorbance with a lower molecular mass as seen in Figure 10.

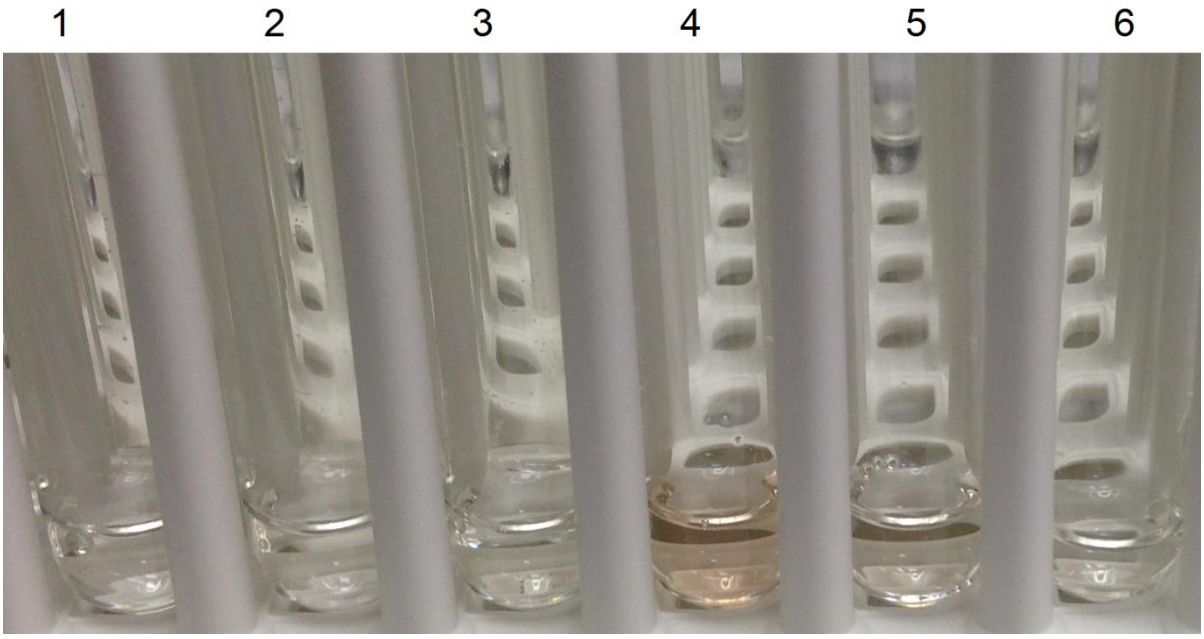

Figure 9: Fractions containing GST activity after strong cation exchange chromatography

This image depicts fractions collected during cation-exchange chromatography. The tubes labeled with 1 to 3 are high GST activity fractions collected during peak III of the chromatogram and are fairly clear in color. The fraction of tube 4 was eluted during peak IV and has a red tint, whereas the fractions in tubes 5 and 6 following peak IV are clear again.

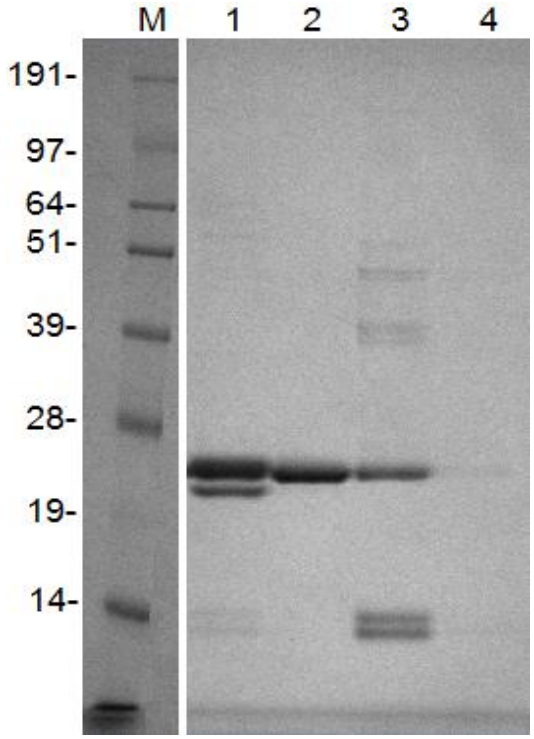

Figure 10: SDS-PAGE after strong cation exchange chromatography

SDS-PAGE was used to analyze the purity of the obtained protein under reducing conditions on a 12% Bis-Tris Gel stained with Imperial™ Protein Stain. The first lane labeled "M" was loaded with the standard protein solution (SeeBlue® Plus2) containing 8 different proteins with a known molecular mass. The numbers on the left of the image represent the molecular mass of these standard proteins in kDa. Several lanes in between the marker lane and the fraction lanes were removed, because they contained non relevant material. Two bands are visible in Lane 1, which are proteins that did not bind to the column and were eluted as peak I in the chromatogram. Lane 2 was loaded with high GST activity fractions of peak III in the chromatogram and contain only one band at approximately 26 kDa. This represents pure canine GSTA, as no contaminations with other proteins are visible. Several protein bands can be observed in lane 3, which contains fractions of peak VI with low enzymatic activity. There are two distinct bands in close proximity at approximately 19 kDa, which may cause the change in color. Lane 4 contains fractions collected directly following peak IV and do not contain any more protein.

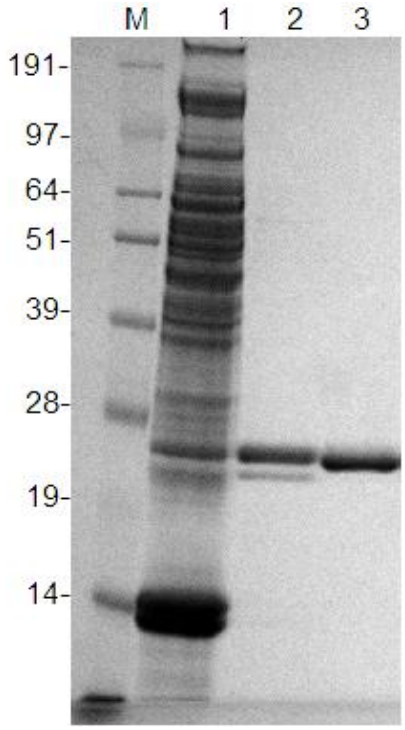

Figure 11: SDS-PAGE illustrating different stages of canine GSTA purification

This figure shows a typical SDS-PAGE on a 12% Bis-Tris Gel stained with Imperial™ Protein Stain. The first lane labeled "M" was loaded with the standard protein solution (SeeBlue® Plus2) containing 8 different proteins with a known molecular weight. The numbers on the left of the image represent the apparent molecular weight of these standard proteins in kDa. Lanes 1 to 3 were loaded with 3 µg of protein. Lane 1 contains the crude liver extract before chromatography. Lane 2 contains a pooled sample of high GST activity fractions after GST affinity chromatography. At least two bands can be observed. One band at approximately 26 kDa, representing GST and another band in close proximity with a slightly lower molecular weight, which might be another isoform of GST. Only one band can be observed in Lane 3, which contains the pure canine GSTA after strong cation-exchange chromatography.

Step	Purification Step	Total Protein	Total Activity	Specific Activity	Yield
		mg	Units	Units/mg	%
1	Liver extract	360	30.1	0.09	100.0
2	Post affinity chromatography	7.0	8.84	1.26	28.9
3	Post cationic exchange chromatography	0.25	0.34	1.36	1.11

Table 1: Recovery of purification of cGSTA from 5 g of canine liver

This table shows the total amount of protein in mg, the total GST activity, the specific GST activity, and the yield after each purification step starting with about 5 g of canine liver. Recovery is calculated based on the total activity.

2. Partial characterization of cGSTA

Nano-spray liquid chromatography-tandem-mass spectrometry (LC/MS/MS) was performed in order to identify whether canine GSTA was successfully purified from the liver and if the two protein bands in close proximity on SDS-PAGE represented the same protein. The results of the LC/MS/MS analysis are shown in Figure 12**Fehler! Verweisquelle konnte nicht gefunden werden.**.

N-terminal amino acid sequencing was not possible due to a blocked N-terminus of the alpha class of GSTs, instead amino acid content analysis was performed to determine the amino acid composition of the protein purified. This also was another method of establishing purity and verifying the concentration of the protein. It showed a pure protein sample with an amino acid composition very similar to that of canine GSTA3 (Table 2).

The apparent molecular weight of canine GSTA was estimated by SDS-PAGE analysis to be approximately 26,000 kDa (Figure 10 and 11).

The mass of the purified canine GSTA was determined using MALDI-TOF mass spectrometry. In Figure 13 two peaks of slightly different molecular mass can be seen, which both represent canine GSTA and confirm its molecular mass to be 25,651 Da.

An IPG dry strip showed that the pI for canine GSTA is approximately 8.9 (Figure 14).

The specific absorbance of canine GSTA was determined by spectrophotometry and the Bradford protein assay and was calculated to be 1.05 for a 1 mg/ml solution (Table 3).

Figure 12: LC/MS/MS analysis of purified protein

In this figure the results from the LC/MS/MS analysis of the purified protein sample as analyzed by Scaffold software are shown. The sample submitted underwent trypsin digestion and HPLC in order to break up the protein and do an inline analysis of the protein fragments. Their measured masses were used to search the NCBInr database of known protein sequences to match the digestion patterns of the proteins in the sample. The matched sequence is that of cGSTA2 and was identified with a probability of over 99.9%. The regions highlighted in yellow represent the peptide sequences detected by mass spectrometry sequencing. Eight unique peptides representing 41% coverage of the protein sequence were identified. The letters highlighted in green show amino acids with post-translational modifications.

A

Amino Acid	Amino acid mass	known number of residues	% Composition calculated from sequence	% Composition predicted by AAA
ASX	115.1	21	9.6%	10.5%
GLX	129.1	20	9.1%	11.1%
SER	87.1	18	8.2%	4.7%
HIS	137.2	4	1.8%	1.2%
GLY	57.1	13	5.9%	5.5%
THR	101.1	10	4.6%	4.2%
ALA	71.1	12	5.5%	5.1%
ARG	156.2	10	4.6%	5.5%
TYR	163.2	9	4.1%	4.5%
VAL	99.1	10	4.6%	5.6%
MET	131.2	7	3.2%	3.4%
IS(1)				
PHE	147.2	10	4.6%	3.6%
ILE	113.2	11	5.0%	5.5%
LEU	113.2	30	13.7%	13.9%
LYS	128.2	24	11.0%	10.0%
IS(2)				
PRO	97.1	10	4.6%	5.9%
	Sum:	**219**	**100%**	**100%**

B

Amino Acid	Replicate1 (nm)	Replicate2 (nm)	Average (nm)
ASX	13.68	14.15	13.92
GLX	14.59	15.02	14.80
SER	5.97	6.48	6.22
HIS	1.69	1.45	1.57
GLY	7.12	7.48	7.30
THR	5.54	5.65	5.60
ALA	6.74	6.88	6.81
ARG	7.30	7.30	7.30
TYR	6.13	5.85	5.99
VAL	7.32	7.47	7.39
MET	4.66	4.36	4.51
IS(1)	5.00	5.00	
PHE	4.82	4.84	4.83
ILE	7.22	7.37	7.30
LEU	18.38	18.47	18.43
LYS	12.99	13.54	13.26
IS(2)	5.00	5.00	
PRO	7.84	7.77	7.80
	131.99	**134.08**	**133.04**

Table 2: Amino acid composition analysis

This table shows the results for the amino acid composition analysis of the purified protein. Table A displays the amino acid composition of the purified protein as predicted by the amino acid analysis compared to the sequence of canine GST alpha 3 from the data base. Table B shows the amount of each amino acid of the purified protein in nanomoles (nm). The test was run in duplicates, so that the values for each replicate are shown in the center columns and the mean in the right column. The first column of each table gives the amino acid codes: ASX (asparagine/aspartic acid), GLX (glutamine/glutamic acid), SER (serine), HIS (histidine), GLY (glycine), THR (threonine), ALA (alanine), ARG (arginine), TYR (tyrosine), VAL (valine), MET (methionine), PHE (phenylalanine), ILE (isoleucine), LEU (leucine), LYS (lysine), PRO (proline) and the internal standards IS(1) (norvaline) and IS (2) (sarcosine).

This assay provided further evidence supporting the purity of the GSTA purified, as well as an accurate measurement for the amount of protein in the sample.

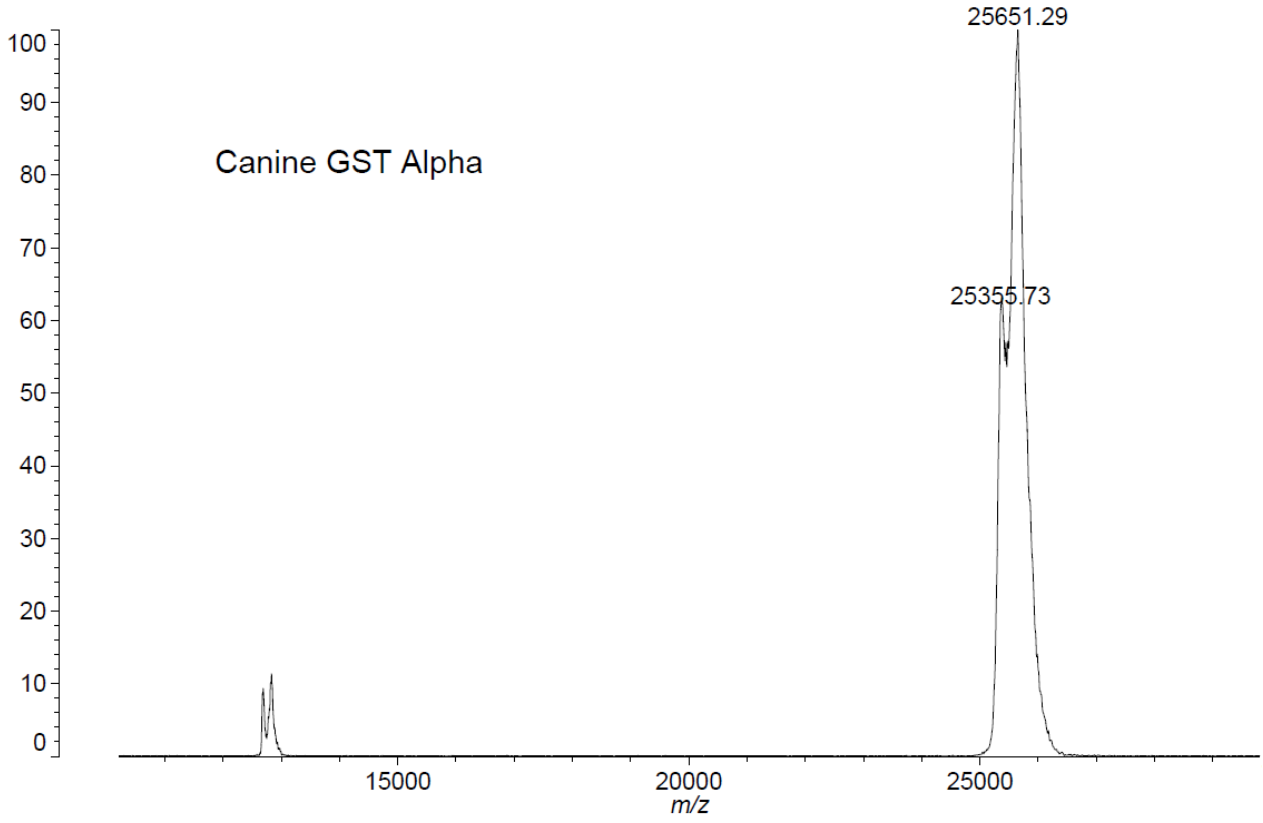

Figure 13: Mass analysis of cGSTA by MALDI-TOF mass spectrometry

This graph shows the mass of one sample of purified canine GSTA run on the MALDI-TOF mass spectrometer. The x-axis is labeled with mass to charge ratio (m/z), which was calculated as follows:

$$m/z = (\text{mass} + \text{charge}) / \text{charge}$$

On the y-axis the peak intensity can be assessed, but is reported without a unit. Two smaller peaks can be viewed at 12,678 Da and 12,826 Da, which represent the double charged molecular ions (M(Z=2)), whereas the following higher peaks represent the single charged molecular ions. Of these the higher peak was calculated to represent a protein of the size of 25651.29 Da. Attached to this peak is a smaller peak located at 25355.73 Da. This can be explained by the presence of a second protein in the sample. However, as previously demonstrated with LC/MS/MS, only canine GSTA was contained in the sample, so that both proteins represent GSTA. Therefore, it is more likely that it is a different isoform or a cleaved/altered form of canine GSTA.

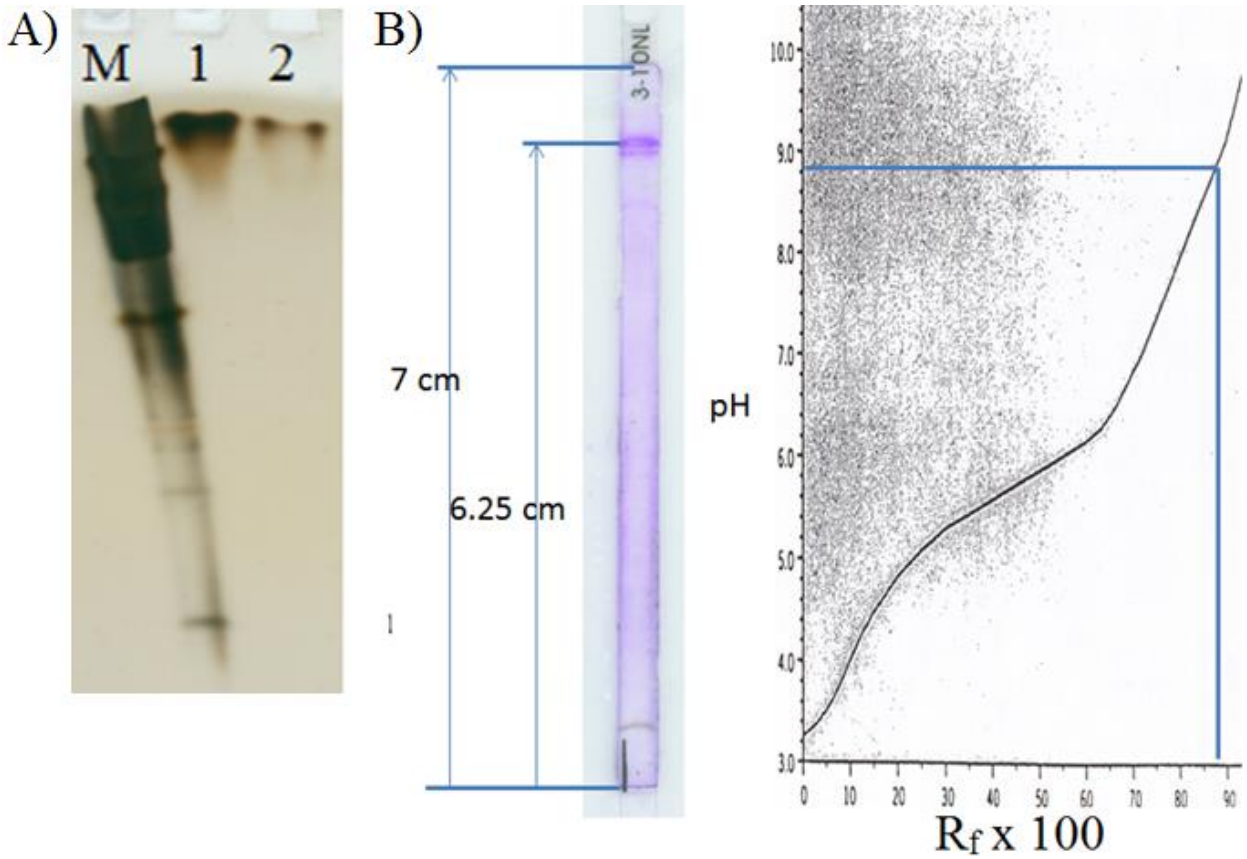

Figure 14: Isoelectric focusing of canine GSTA

Image A shows an IEF gel of the native protein lanes 1 and 2 show the band for GSTA. It displays a single band with a high pI of approximately 9-10, as compared to the marker bands of proteins with known isoelectric points in the first lane labeled “M”. However, as these markers could not clearly be identified, an IPG dry strip was run with the denatured protein. This is shown in image B and demonstrates a more distinct pI of approximately 8.9 for cGSTA, as compared to the predicted non-linear pH gradient of 3 to 10 displayed on the right. The pH gradient is shown on the y-axis, whereas the x-axis represents the relative mobility in percent, as compared to the IPG dry strip, where the protein still has 6.25 cm (89.3%) left to travel to the bottom of the strip.

Dilution factor	A280	Protein concentration (µg/ml)	Extinction coefficient
2	0.813	735	1.11
4	0.394	381	1.04
8	0.184	184	1.00
Mean			1.05

Table 3: Specific absorbance of cGSTA

This table shows the results of the Bradford protein assay for the concentration of GSTA, as well as the absorbance at 280 nm of pure canine GSTA in PBS, (pH 7.3). The absorption was measured with a spectrophotometer at a wavelength of 280 nm (A280). The mean of the calculated specific absorbance at 280 nm was calculated to be 1.05 or if calculated with the mass of 25.651 Da for cGSTA as determined by MALDI mass spectrometry the extinction coefficient is 26,642.8 $M^{-1}cm^{-1}$.

3. Production of anti-cGSTA antibodies

Canine GSTA was radiolabeled with ^{125}I. The produced tracer was used in an RIA to estimate the antibody titers of the sera of two New Zealand White rabbits that had been injected with canine GSTA (Figures 15 and 16). The pre-bleed sample was taken before the first antigen injection with purified canine GSTA and represents a baseline sample. The subsequent serum samples were collected 10 days after the second, 8 days after the third, and 14 days after the fourth antigen injection, respectively. No blood was collected after the first injection. After the second antigen injection a rapid increase in binding can be seen. The increase was lower after the third and fourth injection. However, the prozone phenomenon may have occurred meaning that the quality of the antibody produced increased over time leading to a higher affinity antibody preparation.

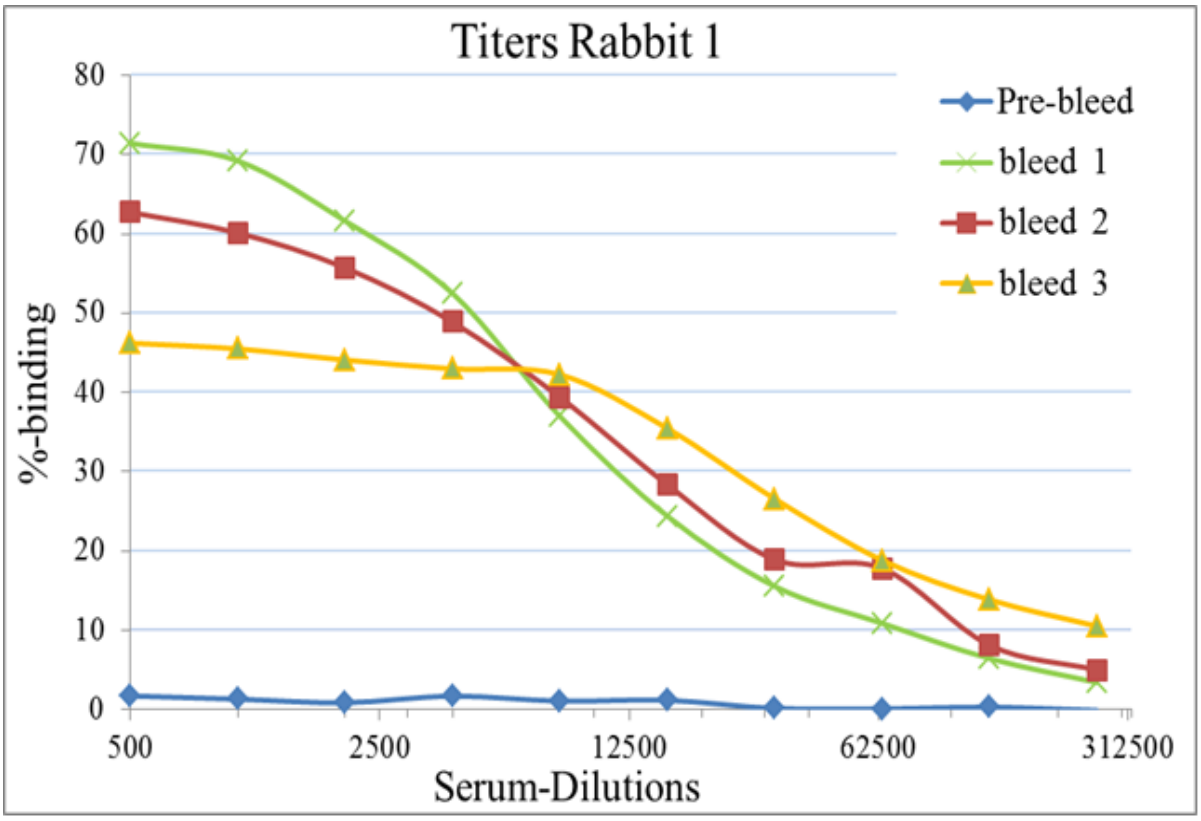

Figure 15: Titer curves for rabbit 1 after antigen injection

This figure shows the anti-cGSTA antibody titers for rabbit 1 before the start of the inoculation (pre-bleed) and at the first, second, and third bleed after each of the second, third, and fourth antigen injection, respectively. The x-axis shows the different serum/antibody dilutions measured by RIA with dilutions ranging from 1 in 500 to 1 in 256,000. The percentage of binding of the anti-cGSTA antibodies to cGSTA labeled with ^{125}I (tracer) was plotted on the y-axis.

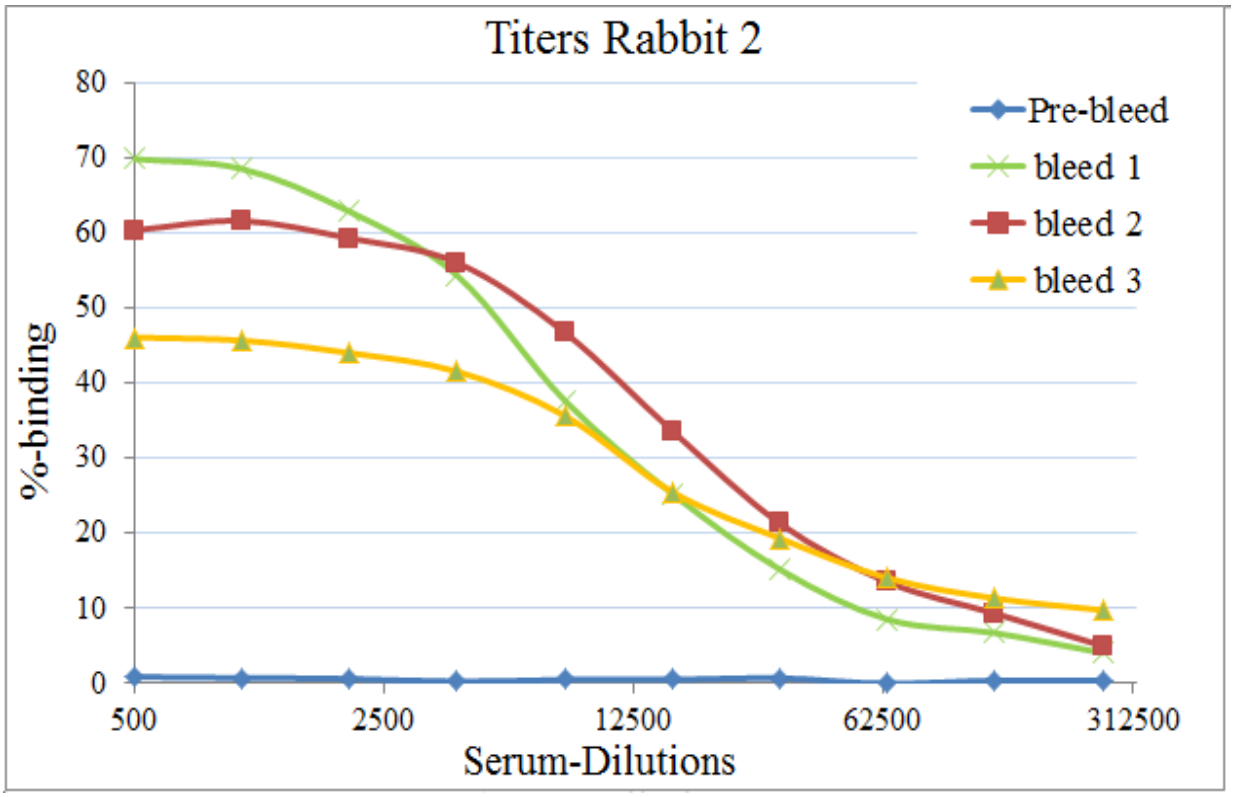

Figure 16: Titer curves for rabbit 2 after antigen injection

This figure shows the anti-cGSTA antibody titers for rabbit 2 before the start of the inoculation (pre-bleed) and at the first, second, and third bleed after each of the second, third, and fourth antigen injection, respectively. The x-axis shows the different serum/antibody dilutions measured by RIA with dilutions ranging from 1 in 500 to 1 in 256,000. The percentage of binding of the anti-cGSTA antibodies to cGSTA labeled with ^{125}I (tracer) was plotted on the y-axis.

4. Development and validation of an RIA for the measurement of cGSTA

A tracer with approximately 40,000 CPM per 100 µl was produced and different conditions for assay optimization were tested (Figure 17Figure 18). An antibody dilution of 1:20,000 was chosen for optimal assay performance. Also, standard and unknown samples were incubated for 6 hours before addition of the tracer and the assay was then incubated for 66 h, for a total incubation time of 72 h. These conditions appeared to optimize binding and resulted in reproducible standard curves with standards ranging from 3.125 to 200 µg/L (Figure 19).

The sensitivity or lower limit of detection (LLOD), defined by the formula LLOD = ((mean – 3 SD/B_0)/(1-(mean – 3 SD/B_0)), resulted in an assay lower detection limit of 1.03 µg/L.

The linearity of the assay was determined by the evaluation of dilutional parallelism of 4 different serum samples. The ratios of observed to expected values ranged between 60.8% and 199.6% with a mean of 99.3% and a SD of ± 45.4% (Table 4).

Accuracy was determined by evaluation the spiking recovery of 4 different serum samples each with 7 spiking concentrations. Ratios of observed to expected values ranged between 38.8 to 263.0% with a mean of 117.2 % and a SD of ± 57.8% (Table 5).

CV% for intra-assay variability for 4 different serum samples, of which two were spiked, ranged from 9.0 to 17.2% with a mean of 11.5% and a SD of ± 13.2% (Table 6).

CV% for inter-assay variability for 4 different serum samples, of which two were spiked, ranged from 19.1 to 22.3% with a mean of 20.7% and a SD of ± 21.9% (Table 7).

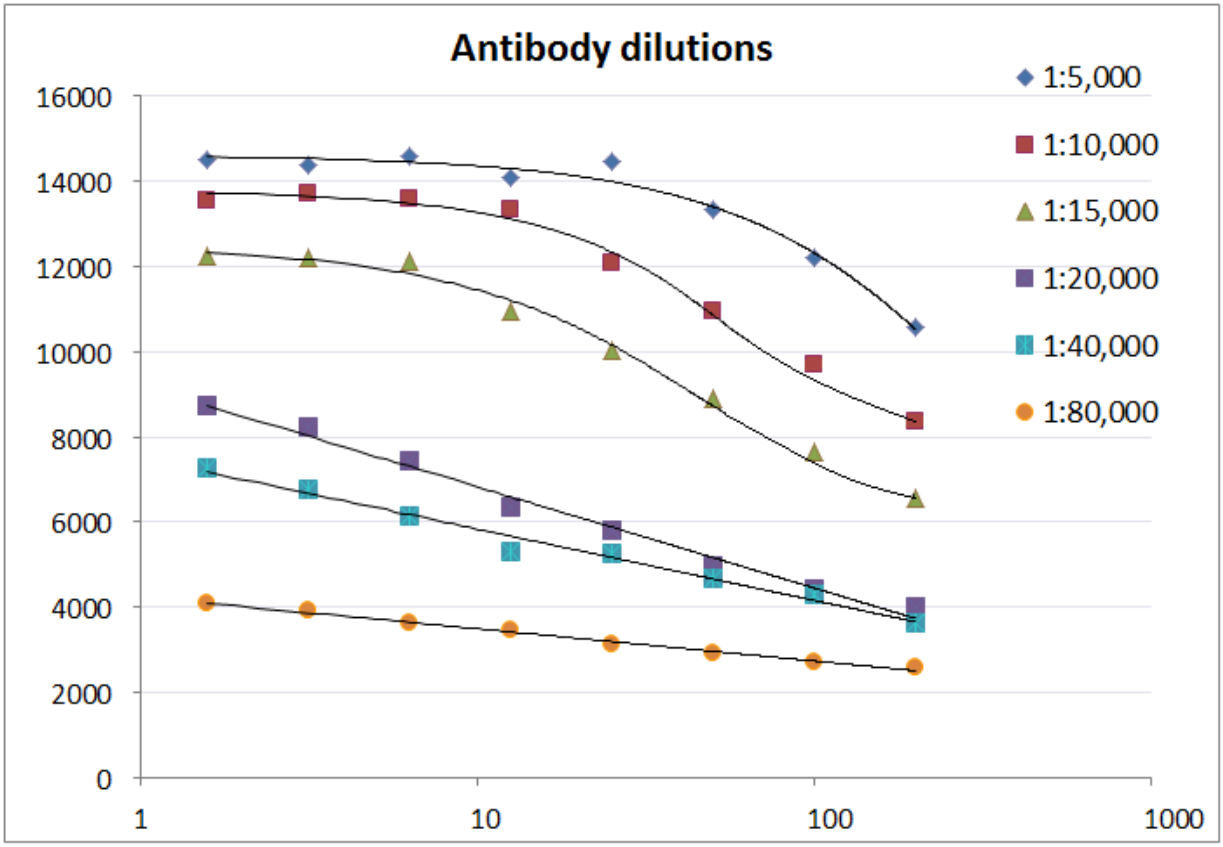

Figure 17: Assay optimization – different antibody dilutions

This graph displays standard curves with different antibody dilutions of 1:5,000, 1:10,000, 1:15,000, 1:20,000, 1:40,000, and 1:80,000. Values on the x-axis represent the canine GSTA concentrations on a logarithmic scale and values on the y-axis represent the CPM for each standard. An antibody dilution of 1:20,000 was chosen for the assay.

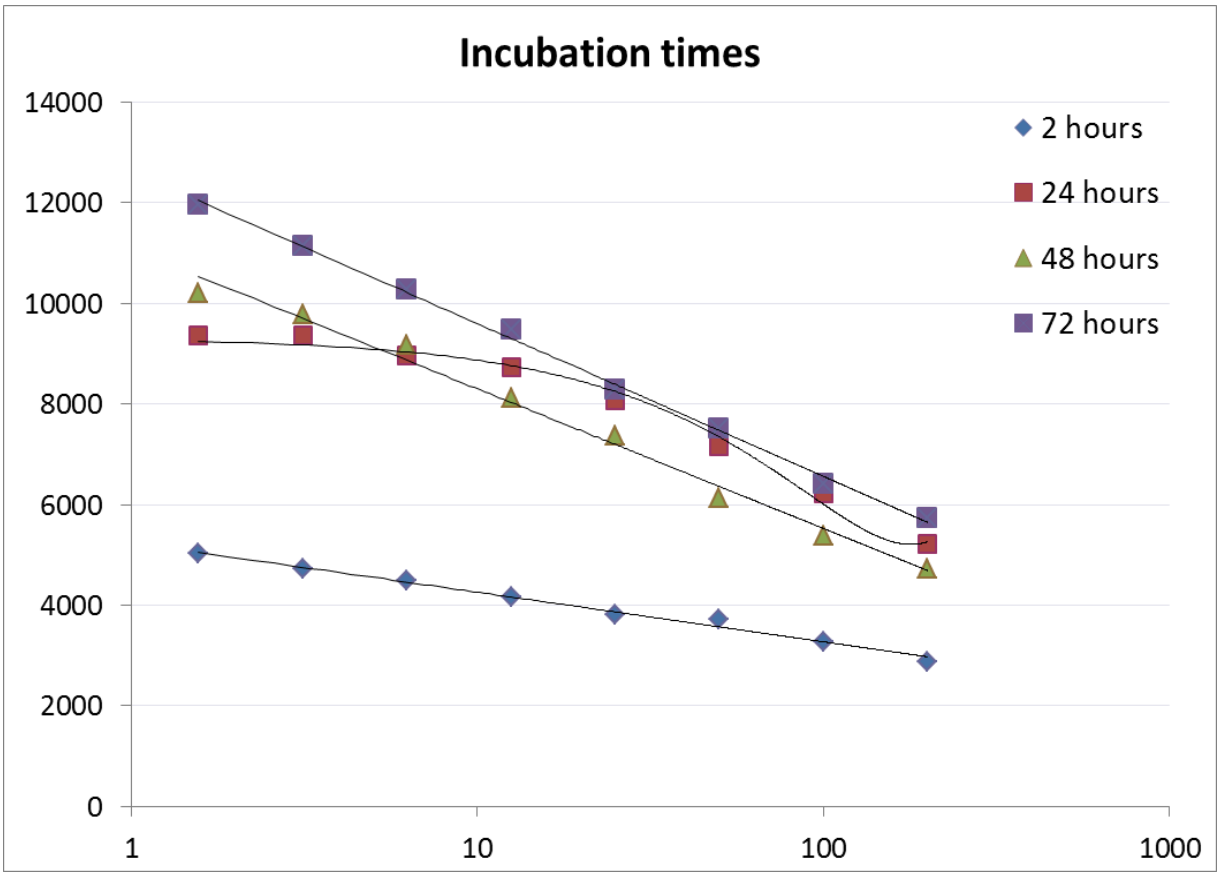

Figure 18: Assay optimization – different incubation times

This graph shows standard curves with different incubation times (i.e., 2h, 24h, 48h, and 72h), that were compared to each other to find optimal assay conditions. Values on the x-axis represent the canine GSTA concentrations on a logarithmic scale and values on the y-axis represent the CPM for each standard. Optimal assay performance was achieved when standard and unknown samples were incubated for 6 hours before addition of the tracer and the assay was then incubated for 66 h, for a total incubation time of 72 h.

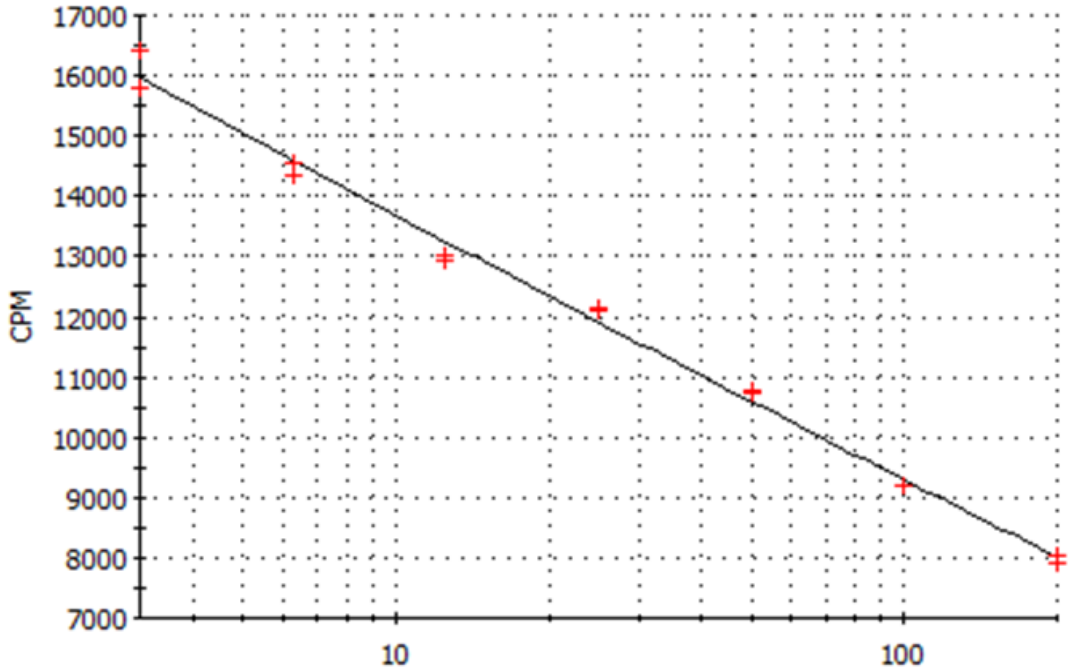

Figure 19: Standard curve for the cGSTA RIA

In this figure a typical standard curve for the cGSTA RIA is shown, with standard concentrations ranging from 3.125 to 200 µg/L. The standard curve was calculated using a 5-parameter curve fit with values on the x-axis representing the canine GSTA concentrations on a logarithmic scale. Values on the y-axis represent the CPM for each standard.

Sample	Dilution	Observed (µg/l)	Expected (µg/l)	O/E (%)
1	undiluted	40.5	N/A	N/A
	1 in 2	14.6	20.3	72.3
	1 in 4	10.1	10.1	99.3
	1 in 8	6.5	5.1	128.4
2	undiluted	34.8	N/A	N/A
	1 in 2	10.6	17.4	60.8
	1 in 4	11.0	8.7	126.1
	1 in 8	8.1	4.4	187.0
3	undiluted	22.9	N/A	N/A
	1 in 2	15.6	11.5	136.4
	1 in 4	10.5	5.7	183.2
	1 in 8	5.4	2.9	187.0
4	undiluted	24.1	N/A	N/A
	1 in 2	12.4	12.0	103.4
	1 in 4	10.0	6.0	166.8
	1 in 8	6.0	3.0	199.6

Table 4: Dilutional parallelism for the cGSTA RIA

This table shows the dilutional parallelism for 4 different serum samples run in duplicate fashion and the calculation of the observed to expected values ((O/E (%) = observed concentration/ expected concentration)*100).

Sample	Spiking conc. (µg/l)	Observed (µg/l)	Expected (µg/l)	O/E (%)
1	0	4.4	N/A	N/A
	3.125	11.3	8.1	139.4
	6.25	11.9	9.7	123.0
	12.5	15.3	12.8	119.5
	25	12.9	19.0	67.8
	50	25.4	31.5	80.7
	100	45.2	56.5	80.0
2	0	13.1	N/A	N/A
	3.125	11.3	8.1	139.4
	6.25	11.9	9.7	123.0
	12.5	15.3	12.8	119.5
	25	12.9	19.0	67.8
	50	25.4	31.5	80.7
	100	45.2	56.5	80.0
3	0	3.1	N/A	N/A
	3.125	3.4	3.1	109.7
	6.25	2.2	4.7	46.7
	12.5	3.0	7.8	38.8
	25	7.7	14.1	54.8
	50	17.5	26.6	65.8
	100	36.1	51.6	69.9
4	0	42.0	N/A	N/A
	3.125	43.6	22.6	192.9
	6.25	49.7	24.1	206.0
	12.5	44.0	27.3	161.3
	25	57.2	33.5	170.7
	50	121.0	46.0	263.0
	100	151.6	71.0	213.5

Table 5: Spiking recovery for the cGSTA RIA

This table displays the spiking recovery as determined by adding 50 µl of solutions containing 0, 3.125, 6.25, 12.5, 25, 50, or 100 µg/L cGSTA to 50 µl of 4 different serum samples and calculating the observed to expected values (O/E (%) = (observed concentration/ expected concentration)*100; N/A not applicable). The recovery ranged from 38.8 to 263.0% with a mean of 117.2%. (±57.8)

sample	mean (µg/l)	SD (µg/l)	% CV
1	12.5	1.1	**9.0%**
2	20.1	1.9	**9.7%**
3	111.8	11.5	**10.2%**
4	221.8	38.2	**17.2%**

Table 6: Intra-assay variability for the cGSTA RIA

This table shows the intra-assay variability of 4 different serum samples, which were assayed 10 times during the same run in duplicate fashion. The results were multiplied by two in order to adjust for sample dilution. The %CV for intra-assay variability ranged from 9.0 to 17.2% with a mean %CV of 11.5% (SD = standard deviation; %CV = coefficient of variation; %CV = ((SD/mean)*100).

sample	mean (µg/l)	SD (µg/l)	% CV
1	11.3	2.4	**21.5%**
2	19.0	4.2	**22.3%**
3	125.1	24.7	**19.7%**
4	294.0	56.1	**19.1%**

Table 7: Inter-assay variability for the cGSTA RIA

This table displays the inter-assay variability of 4 different serum samples, which were assayed in duplicate fashion 10 times during consecutive runs. The results were multiplied by two in order to adjust for sample dilution. The CV% for intra-assay variability ranged from 19.1 to 22.3% with a mean %CV of 20.6% (SD = standard deviation; %CV = coefficient of variation; %CV = ((SD/mean)*100).

5. Serum cGSTA concentrations in healthy dogs

Serum cGSTA concentrations were measured in 49 healthy dogs owned by staff and students of Texas A&M University. The dogs were of various breeds with ages ranging from 1 to 14 years with a mean age of 5.4 years. Twenty-three dogs were female, of which 3 were intact, and 19 dogs were male, of which 1 dog was intact. This information for the rest of the dogs was missing. Serum cGSTA concentrations of 13 dogs (26.5%) were within the determined working range (6.25 to 400 µg/L) of the assay, whereas the concentrations of 36 dogs were below the lower detection limit of 6.25 µg/L. Concentrations ranged from <6.25 to 75.1 µg/L with a median of 8.4 µg/L (Table 8).

The lower 95th percentile of serum GST alpha concentrations for theses 49 healthy dogs was used to calculate the reference interval of the assay as <14.35 µg/L (Figure 20).

Sample no.	Serum cGSTA (µg/l)		Sample no.	Serum cGSTA (µg/l)
1	<6.25		**26**	<6.25
2	<6.25		**27**	<6.25
3	**7.1**		**28**	<6.25
4	<6.25		**29**	<6.25
5	<6.25		**30**	<6.25
6	<6.25		**31**	**8.5**
7	**6.6**		**32**	**9.3**
8	**8.0**		**33**	<6.25
9	<6.25		**34**	<6.25
10	<6.25		**35**	<6.25
11	**7.8**		**36**	<6.25
12	<6.25		**37**	**8.0**
13	**14.2**		**38**	<6.25
14	<6.25		**39**	<6.25
15	<6.25		**40**	<6.25
16	**12.5**		**41**	<6.25
17	<6.25		**42**	<6.25
18	<6.25		**43**	<6.25
19	<6.25		**44**	<6.25
20	<6.25		**45**	**9.0**
21	<6.25		**46**	**75.1**
22	<6.25		**47**	<6.25
23	**14.5**		**48**	**7.3**
24	<6.25		**49**	<6.25
25	<6.25			

Table 8: Serum cGSTA concentrations in 49 healthy dogs

This table shows serum cGSTA concentrations in 49 healthy dogs. Thirty six dogs had serum concentrations below the RIA's lower detection limit of 6.25 µg/L, whereas the other 13 dogs had serum cGSTA concentrations ranging from 6.63 to 75.12 µg/L (marked in bold). The median serum concentration for the healthy group was 8.42 µg/L.

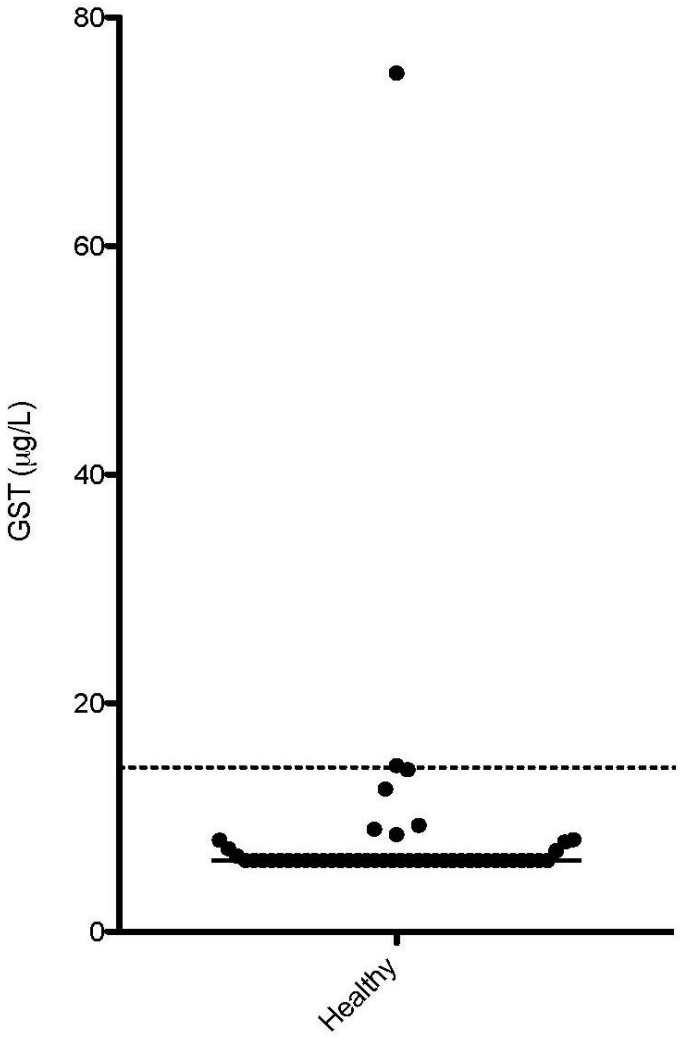

Figure 20: Serum cGSTA concentrations in 49 healthy dogs

This figure shows serum cGSTA concentrations in 49 healthy dogs, with 36 of these samples showing cGSTA concentrations below the lower limit of the working range of 6.25 µg/L. In the other 13 dogs serum cGSTA concentrations ranged from 6.63 to 75.12 µg/L. The reference interval as determined by the lower 95th percentile was <14.35 µg/L and is displayed as the dashed line. The solid line represents the median concentration of 6.25 µg/L. There was one dog that had a cGSTA concentration that was interpreted as outlier in this group. This dog could possibly have had subclinical liver disease that was not detected by other liver markers.

6. Serum cGSTA concentrations in dogs with hepatic disease

Canine GST alpha concentrations were measured by the newly developed cGSTA RIA in serum of 45 dogs with liver disease. The dogs were of various breeds with an age ranging from 1 to 17 years and a mean age of 7.8 years. Twenty-seven dogs were female, of which 4 were intact, and 17 dogs were male, of which 4 were intact. Information for age and sex were missing for one dog. The diseased group was divided into 4 subgroups. Seven dogs were diagnosed with a congenital portosystemic shunt (CPSS; group 1), 15 with chronic hepatitis (CH; group 2), 7 with hepatic neoplasia (group 3), and 16 had other types of liver disease (group 4). The cGSTA concentrations for each dog are shown in Table 9. Serum cGSTA concentrations ranged from <6.25 to >400 µg/L, with a median value of 36.4 µg/L. Thirty-nine of 45 dogs (86.7%) had measurable cGSTA concentrations. Two dogs had serum cGSTA concentrations above the upper limit of the working range of the assay and four dogs had serum cGSTA concentrations below the lower limit of the working range, which were all diagnosed with CPSS. When separating the diseased dogs into 4 groups, canine GSTA was detectable in 3 of the 7 dogs (42.9%) with CPSS (group 1), with concentrations ranging from <6.25 to 46 µg/L and with a median serum concentration of 5 µg/L. Of the 15 dogs with chronic hepatitis (group 2), all but one dog had detectable cGSTA concentrations (93.3%), with a median of 60 µg/L and a range from 13 to >400 µg/L. One dog had a serum cGSTA concentration above the upper detection limit of the assay. All 7 dogs with hepatic tumors (group 3) had serum cGSTA concentrations within the detection limit of the assay (100%) and showed a median concentration of 30 µg/L, ranging from 21 to 126 µg/L. Finally, in the group of dogs with other liver diseases (group 4), 15 of the 16 dogs (93.75%) had detectable serum cGSTA concentrations with a median of 36 µg/L and a range of 15 to >400 µg/L. One dog had a serum cGSTA concentration above the upper detection limit.

Statistical analysis showed that serum cGSTA concentrations were significantly higher in dogs with liver disease compared to healthy control dogs ($p<0.0001$). Also, there was a significant difference in serum GST alpha concentrations between dogs with PSS and dogs with chronic hepatitis as well as between dogs with PSS and dogs with other hepatobiliary diseases ($P<0,01$ for both comparisons). Also, dogs with chronic hepatitis, hepatic neoplasia, and other hepatobiliary diseases had significantly higher serum cGSTA concentrations than healthy dogs

(P<0.01). No correlation was found between serum activities of ALT and serum concentrations of cGSTA in both healthy and diseased dogs (*rho*=0.31; p=0.061) (Figure 23).

Sample no.	Chronic hepatitis (cGSTA µg/l)	Liver tumor (cGSTA µg/l)	CPSS (cGSTA µg/l)	Others (cGSTA µg/l)
1	97.7	20.6	46.0	36.1
2	70.0	30.0	12.3	36.4
3	23.0	125.9	**<6.25**	16.9
4	59.3	42.3	**<6.25**	33.2
5	60.1	27.4	**<6.25**	20.7
6	**>400**	23.7	**<6.25**	56.8
7	68.2	96.9	26.9	73.6
8	41.4			235.5
9	160.5			**>400**
10	224.2			71.0
11	81.1			152.8
12	34.2			78.8
13	58.1			18.6
14	36.0			35.3
15	13.0			15.0
16				30.8
no. of dogs	15.0	7.0	7.0	16.0
min	13.0	21.0	<6.25	15.0
median	60.0	30.0	6.25	36.0
max	>400	126.0	46.0	>400
% of total	33%	16%	16%	36%

Table 9: Serum cGSTA concentrations in 45 dogs with liver disease

This table shows serum cGSTA concentrations for 45 dogs with liver disease. The dogs were divided into 4 groups based on their final diagnosis. Below, the total number of dogs in each group, the median, and the range of cGSTA concentrations are presented under consideration of the assay's reference interval (6.25 to 400 µg/L). Three dogs had serum cGSTA concentrations above the upper limit of the reference range (marked in bold) and 4 dogs of the group of dogs with portosystemic shunts had serum cGSTA concentrations below the lower limit of the reference range.

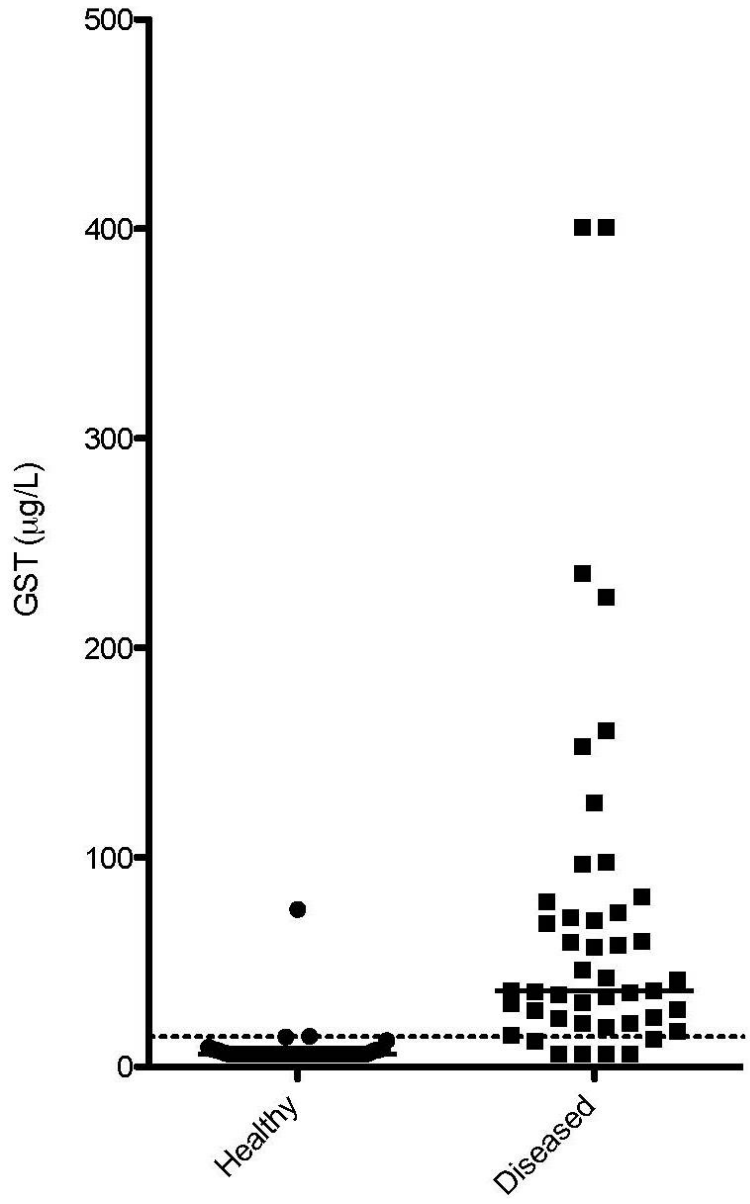

Figure 21: Comparison of serum cGSTA concentrations between healthy and diseased dogs

This figure shows serum cGSTA concentrations in 49 healthy dogs compared to the 45 dogs with hepatic disease with median cGSTA concentrations of 6.25 and 36.4 µg/L, respectively, indicated by the horizontal solid line. The statistical analysis using the Mann Whitney test for nonparametric comparison was significant ($p<0.0001$). The dashed line indicates the calculated reference interval of <14.35 µg/L. There was a significant difference in serum GST alpha concentration between the two groups $p<0.0001$.

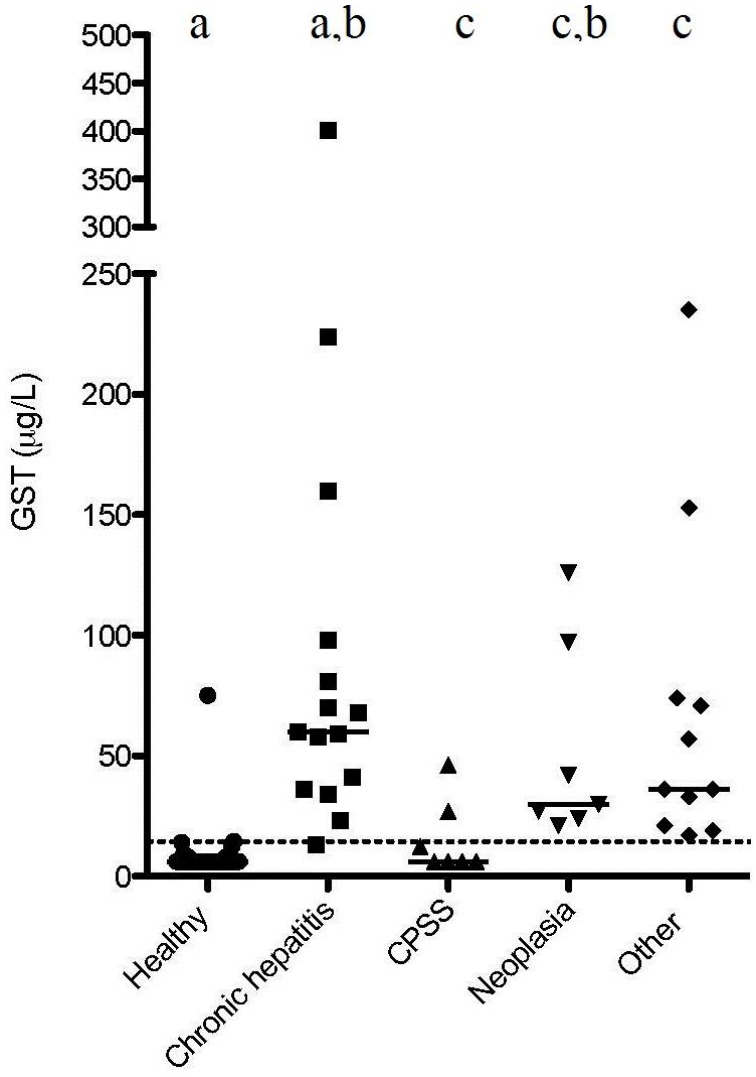

Figure 22: Comparison of serum cGSTA concentrations between healthy dogs and dogs with various types of liver disease

This figure shows the serum cGSTA concentrations in 45 healthy dogs (median cGSTA concentration: 6.25 µg/L), 15 dogs with chronic hepatitis (median cGSTA concentration: 60 µg/L), 7 dogs with CPSS (median cGSTA concentration: 5 µg/L), 7 dogs with hepatic tumors (median cGSTA concentration: 30 µg/L), and 16 dogs with other liver diseases (median cGSTA concentration: 36 µg/L). The solid lines indicate the medians and the dashed line the reference interval (<14.35 µg/L). The statistical analysis using the Kruskal-Wallis test for nonparametric comparisons between the 5 groups of dogs was statistically significant ($p<0.0001$). The results of post-testing with Dunn's test to the level of $p<0.01$ are indicated by letters. Groups with no significant difference between them have the same letter and groups where there is a significant difference have different letters.

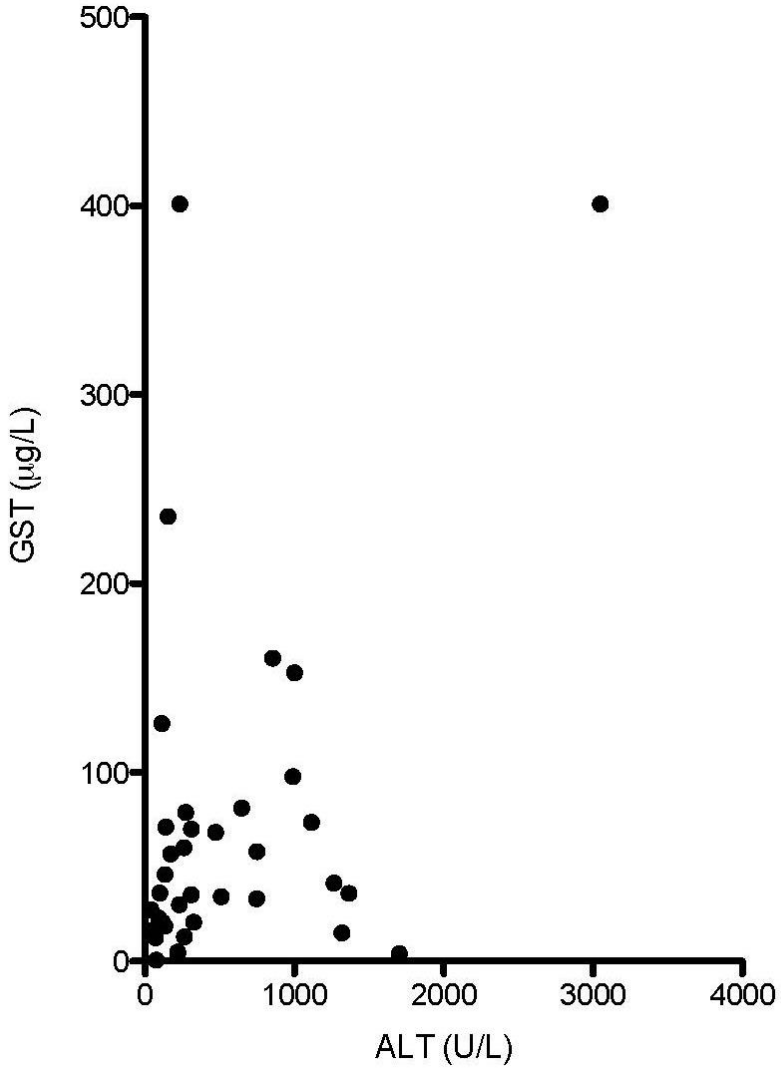

Figure 23: Correlation between ALT and GSTA in the serum of dogs

This figure displays the results of the Spearman rank correlation, showing that there is no significant correlation between the serum activities of ALT and the serum concentrations of cGSTA in both healthy and diseased dogs (*rho*=0.31; p=0.061).

V. DISCUSSION

1. Purification of canine GSTA

Canine GSTA was successfully purified from canine liver. The reproducible purification protocol described allows the isolation of cGSTA of high purity, as confirmed by SDS-PAGE (Figure 10 andFigure 11), LC/MS/MS (Figure 12), and amino acid composition analysis (Table 2).

The purification of canine GSTA has previously been reported using a glutathione affinity column (Kilty et al. 1998), as well as in a combination with HPLC chromatofocusing with a Mono P column (Igarashi 1991). However, in our laboratory using only a glutathione affinity column, did not produce pure cGSTA, but rather a mixture of different GST isoforms. Furthermore, Wiener (1986) used an extensive protocol, including a DEAE – cellulose column, $(NH_4)_2SO_4$ precipitation, a CM-cellulose column, a phenyl-sepharose CL-4B column, Bio-Gel hydroxyaptite, a GSH-agarose column and finally chromatofocusing. These protocols, as well as different protocols for the purification of porcine and human GST (Stockman 1987, Kunze 1997, Pastore et al. 1998), were evaluated for yield and purity, as well as cost-effectiveness, handling, and time. In order to achieve a cost-effective purification protocol with the resources we had available and a high purity of the end product, multiple attempts using various chromatographic columns were made. One of the protocols for the purification of human GST used a GSH-affinity column first, followed by a DEAE-Sepharose column and ion exchange chromatography with a Mono Q column (Pastore et al. 1998). The combined use of affinity chromatography and anionic exchange chromatography with a DEAE or Mono Q column, did not lead to pure canine GST alpha. Anionic exchange chromatography with a Mono Q column following GST affinity chromatography resulted in a poor purification of GST alpha with most of the GST being eluted in the flow-through. However, using the glutathione affinity chromatography as a first purification step of the crude liver homogenate, followed by cationic exchange chromatography improved the protocol significantly. This is most likely due to the high pI of canine alpha GST, causing its net charge to be positive in most buffers except highly basic buffers. Therefore, the protocol was adapted to use a Resource S column. Using the described purification protocol,

cGSTA was purified with a purity greater than 95%, as established by SDS-PAGE analysis and the Quantity One software package, as well as by LC/MS/MS analysis as discussed below.

2. Partial characterization of cGSTA

The amino acid composition analysis and LC/MS/MS showed a high degree of homology with canine GSTA2 and A3 (Table 2 and Figure 12). These were the closest sequences found to the assumed sequence of cGSTA1, as the sequence of cGSTA1 could not be found in the NCBI database. LC/MS/MS identified cGSTA2 in the sample with a high coverage of 41%. However, since the sequence of cGSTA1 is not known, it can only be assumed that cGSTA1 is also contained within the purified protein sample, as it has been shown that GSTA1 makes up over half of the alpha GSTs in the liver of humans (Mulder et al. 1999). The cytosolic GST and in particular GST alpha content in the liver of humans and dogs seems to be similar (Wiener 1986, van Ommen et al. 1990, Kilty et al. 1998). N-terminal amino acid sequencing was attempted, but was not possible since the N-terminus of GST alpha is blocked (Igarashi 1991), as has been shown for GST alpha in other species (Bogaards et al. 1992, Pastore et al. 1998, Prabhu et al. 2004). However, in fractions analyzed directly after GST affinity chromatography, the sequence of cGSTM1 ((V)-M-I/Y-F-G.L-Y-(L)-D-I-(V)) was discovered, which has been previously been shown to exist in the liver in smaller concentrations than alpha, unless there is a polymorphism causing a lack of the protein (van Ommen et al. 1990, Savolainen et al. 1996).

The apparent molecular weight of canine GST alpha was estimated by SDS-PAGE and found to be approximately 26 kDa. This was confirmed by the more accurate mass analysis by MALDI-TOF mass spectrometer, which resulted in two masses demonstrated by a higher and a smaller peak (Figure 13). The higher peak corresponded to a compound with a mass of 25,651.29 Da and was almost identical to the mass previously determined by LC/MS/MS for cGSTA2 of 25,659 Da. It is also nearly identical to the molecular mass of cGSTA3 with 25,657 Da, considering the inaccuracy/inherent variability of the mass spectrometer of 0.1%. Canine GSTA4 has a slightly higher mass of 25,727 Da. The smaller peak was determined to weigh 25,355.73 Da, which could be another isoform or represent a cleaved form of the protein.

The isoelectric point of cGSTA was found to be approximately 8.9 (Figure 14), and was therefore identical to the pI of about 8.9 for GSTA1 reported by other studies in dogs as well as in other species (Stockman 1987, Igarashi et al. 1991, Bogaards et al. 1992). Similar to SDS

PAGE, a double band was visible on the IEF gel as well. This double banding, taken together with the two mass peaks identified by MALDI-TOF mass spectrometry, conflicts with the LC/MS/MS results that identify the protein sample to be pure cGSTA. This could be explained by either post-translational modifications, a cleaved form, or different isoforms of GSTA being present in the sample.

The measurement of the specific absorbance resulted in an estimate of about 1.05 (Table 3), which resembles the specific absorbance calculated with the ExPASy–protparam program for canine GSTA2 and A3 isoforms.

3. Production of anti-cGSTA antibodies

The inoculation of the two New Zealand White rabbits with cGSTA antigen for the production of antiserum using the described protocol successfully led to the production of polyclonal antibodies in both rabbits. Polyclonal antibodies have several advantages over monoclonal antibodies: their production is less expensive and time consuming; it is also less technologically demanding and larger amounts of antibodies can be produced. In addition, polyclonal antibodies recognize multiple epitopes on an antigen. Serum will contain a heterogeneous mixture of antibodies of different, usually very high, affinity. Thus, the signal from a target protein with low expression may be amplified, as it will bind several antibodies and the antibodies will be more tolerant of minor changes of the antigen (e.g., polymorphism, denaturation) (Lipman et al. 2005). However, one of the disadvantages of polyclonal antibodies is the possible batch to batch variability.

New Zealand White rabbits were chosen as a host species for the antigen inoculation. Rabbits, sheep, and goats are the most commonly used mammals due to ease of vascular access, their robustness of the immune response, and their size, which allows smaller injections of protein with an efficient antigen production. Of these species, rabbits are used most commonly, as they are easy to handle and less expensive (Lipman et al. 2005). Furthermore, the use of polyclonal antibodies and rabbits as a carrier species has previously been very successful in our laboratory. However, rabbits also show a less consistent immune response. For this reason, and considering potential batch to batch variability, it is recommended to use at least two rabbits (Harlow et al. 1999).

Repeated subcutaneous immunizations led to an increase of the antibody titer. After two injections, a good antibody titer was achieved.

4. Development and analytical validation of a RIA for the measurement of cGSTA in dog serum

A radioimmunoassay for the measurement of cGST alpha in canine serum samples was developed and analytically validated. Before deciding to establish our own immunoassay, a commercially available GST activity assay, as well as a commercially available serum GSTA ELISA kit was tested to determine their utility for assaying GST in canine serum. Unfortunately, the activity assay did not appear to be sensitive enough for the discrimination of diseased versus healthy canine blood samples. In general, the use of enzyme activity assays does not provide a differentiation between the various GST isoenzymes, so the development of immunoassays is usually required for the specific detection of GSTs and will allow more accurate monitoring of the serum/plasma GST levels in dogs (Mulder 1996). The use of a commercially available ELISA kit for canine GSTA was evaluated, but did not appear to measure canine serum GST accurately, as it did not show sufficient linearity for the analysis of the samples, nor did it allow discrimination between samples from healthy and diseased dogs. Therefore, we developed an in-house radioimmunoassay for the measurement of canine GSTA in serum. Measurement of human GSTA by radioimmunoassay has previously been shown to provide a very accurate method for the detection of hepatocellular damage in humans (Sherman et al. 1983, Beckett et al. 1985).

The analytical validation of the RIA was performed by determination of the lower limit of detection, accuracy, linearity, precision, and reproducibility of the assay. The lower detection limit of the assay was determined to be 1.03 µg/L. The working range of the assay was determined to be 6.25 to 400 µg/L. The results of the spiking recovery did not show acceptable accuracy of the assay, as the 4 samples showed O/E between 38.8 to 263.0% (Table 5). The intra-assay variability for 4 different serum samples, of which two were spiked samples with different antigen amounts, ranged between 9.0 and 17.2% (Table 6). The inter-assay variability for the same 4 serum samples ranged between 19.1 and 22.3% (Table 7). Results for the linearity of the assay showed high variations in the observed to expected ratios (Table 4). In conclusion it can be said, that even though there is no consensus about target validation values for assay validation, this assay does not seem to have an acceptable accuracy, linearity, precision, or reproducibility. This may have been due to a matrix effect, because a relatively large amount of each patient's serum was used in the assay. However, the assay lacked sensitivity, as most of the

samples fell into the lower part of the working range or were even below the lower detection limit of the working range. Therefore further dilution of the patient serum, would have lead to undetectable measurements. Despite trying multiple assay conditions it was not possible to get this cGST alpha RIA to perform acceptably. Therefore, it will be necessary to develop another assay. The development of an ELISA is the next logical step.

5. Serum cGSTA concentrations in healthy dogs

A reference interval of <14.35 µg/L was established by the measurement of the serum cGSTA concentrations in 49 healthy dogs and calculating the lower 95th percentile of their serum GSTA concentrations (Figure 20). Serum concentrations were detectable in 13 of these animals with the remainder of the dogs having values below the lower detection limit of 6.25 µg/L (Table 8). The serum cGSTA concentrations of these 13 dogs ranged from 6.63 to 75.12 µg/L. The dog with a measured cGSTA concentration of 75.12 µg/L was interpreted as an outlier in this group and could possibly have had subclinical liver disease that was not detected by other liver markers.

The established reference interval for the cGSTA RIA is higher than what has previously been reported for humans with ranges of 0-12 ng/ml and 1.8-4.0 µg/L (Sherman et al. 1983, Beckett et al. 1985). However, this is a different species and immunoassays are not truly analytical and do not measure actual mass-concentrations of the analyte.

6. Serum cGSTA concentrations in dogs with hepatic disease

In order to assess the clinical utility of cGSTA as a novel biomarker for hepatocellular damage, serum samples from 45 dogs with hepatobiliary disease were assessed. With the exception of two dogs with a normal liver biopsy, but elevated liver enzymes, all of the diseased dogs had histopathological changes. Interestingly, the 2 dogs with normal histopathology had increased serum cGSTA concentrations. A statistically significant difference between the samples of healthy and diseased dogs was found ($p<0.0001$). Canine GSTA concentrations of 39 of the 45 dogs with hepatobiliary disease were above the determined reference interval for healthy dogs (<14.3 µg/L) (Figure 21 and Figure 22). Five of the 6 dogs with hepatobiliary disease that had serum GSTA concentrations within the reference interval were diagnosed with congenital portosystemic shunts (CPSS), which could be an indication that dogs with CPSS did not have hepatocellular injury. However, the serum ALT concentrations were increased in 3 out of the 5 dogs, which may suggest that the measurement of cGSTA may not be as sensitive for the detection of hepatocellular injury as serum ALT activity in dogs with CPSS. The other dog with hepatobiliary disease that had a serum GSTA concentration within the reference interval was diagnosed with chronic hepatitis and had a serum cGSTA concentration just barely below the upper limit of the reference interval.

Overall, these results are in line with studies in other species, such as humans, rats, and dogs showing that GST alpha may be a useful biomarker for the assessment of hepatocellular damage (Trull et al. 1994, Kilty et al. 1998, Bailey et al. 2012).

In addition, the diseased dogs were divided into 4 groups based on histopathology and other laboratory data. One group included only dogs diagnosed with CPSS (group 1). The other groups included dogs with chronic hepatitis (group 2), hepatic neoplasia (group 3), or other liver diseases (group 4). Serum cGSTA concentrations were significantly different between healthy animals and the diseased groups with exception of the group diagnosed with CPSS (Figure 22). When comparing healthy dogs to the diseased dogs and after exclusion of dogs with CPSS, a clear separation could be seen. This suggests that canine GSTA may be useful as a marker to screen for hepatic disease similarly to ALT. However, it may not be useful to distinguish between different types of liver disease and may not be useful as a marker for CPSS. Further studies would be needed to explore whether or not cGSTA is a more sensitive marker for hepatocellular/-biliary injury than ALT in the dog. This could be done by monitoring serum

cGSTA concentrations longitudinally or even by inducing hepatic injury in dogs to determine if serum cGSTA concentrations increase more rapidly after the onset of hepatocellular injury and if they decrease sooner after resolution of disease than serum ALT activities. Furthermore, different drugs could be administered to compare the performance of the two liver markers with drug induced hepatic damage.

7. Conclusion

In conclusion, canine glutathione transferase alpha was successfully purified from canine liver. Polyclonal anti-cGSTA antibodies were successfully produced in rabbits and used for the development of a radioimmunoassay for the measurement of canine GST alpha in serum. Even though the assay did not show acceptable linearity, accuracy, precision, or reproducibility, significant differences in serum cGSTA concentrations were found between healthy dogs and dogs with various types of hepatobiliary disease. This finding suggests that GST alpha warrants further study as a novel marker of hepatocellular injury in dogs. However, another assay will need to be developed before this work can take place. If future work does support the utility of GST alpha as a serum marker of canine hepatocellular injury, rigorous studies will need to be performed to compare its diagnostic performance to those of existing markers of hepatocellular injury.

VI. SUMMARY

Purification and Partial Characterization of Canine Glutathione Transferase alpha and the Development of an Immunoassay for the Measurement of Glutathione Transferase alpha concentration in Serum

Glutathione transferase alpha (GSTA) belongs to a diverse family of isoenzymes involved in the detoxification of a range of xenobiotic compounds by conjugation to glutathione. In humans, GSTA has been identified as an earlier, more specific, and more sensitive indicator of hepatocellular injury than the commonly used aminotransferases, regardless of the cause of hepatic injury. Canine GSTA (cGSTA) has also been shown to detect hepatic injury induced by warm ischemia in the dog.

The aim of this study was to develop a simple and reproducible protocol for the purification of cGSTA from canine liver, to partially characterize cGSTA, to produce anti-cGSTA antibodies in order to develop and analytically validate an RIA for the measurement of cGSTA in serum, and to compare serum cGSTA concentrations between healthy and dogs with spontaneous hepatocellular disease.

An efficient, simple, and reproducible protocol for the extraction and subsequent purification of glutathione transferase alpha from canine liver was established and some of the biochemical properties of this protein were evaluated.

Amino acid analysis as well as liquid chromatography–mass spectrometry (LC/MS/MS) analysis showed a high homology to the isoenzymes cGSTA2 and cGSTA3, respectively. The molecular weight of cGSTA was estimated by SDS-PAGE to be 25 kDa. By MALDI-TOF mass spectrometry, the mass of cGSTA was more precisely determined to be 25,651 Da. Isoelectric focusing of cGSTA revealed an isoelectric point between 9.1 and 9.3 and the specific absorbance at 280 nm was determined to be approximately 1.05.

Antibodies against cGSTA were raised in rabbits and an RIA for the measurement of cGSTA was developed and analytically validated. However, the assay did not show acceptable linearity, accuracy, precision, or reproducibility, which was assumed to be due to a lack of sensitivity of the assay leading to most clinical samples falling towards the lower limit of the assay's working range. The working range of this assay was determined to be 6.25 to 400 µg/l. In order to

determine whether there would be merit in developing a more sensitive assay for the measurement of cGSTA a preliminary reference interval of <14.35 µg/L was established. Finally, serum concentrations of cGSTA were measured in 49 healthy and 45 diseased animals and compared between the two groups of dogs to assess if cGSTA may have any utility as a biomarker for hepatocellular injury in dogs. Serum cGSTA concentrations were measurable in 39 of 45 dogs (86.7%) with hepatic disease. The median serum concentration of cGSTA was significantly higher in dogs with liver disease (6.25 – 400 µg/L, median: 36.4 µg/L; $p<0.0001$) than in healthy dogs (6.25 – 400 µg/L, median: 6.25 µg/L; $p<0.0001$). When separating the diseased dogs into 4 groups, cGSTA was detectable in 3 of the 7 dogs (42.9%) with congenital portosystemic shunts (6.25 – 46 µg/L, median: 6.25 µg/L; $p<0.0001$), with 4 dogs having serum cGSTA concentrations below the lower detection limit. It was also detectable in 14 of the 15 dogs (93.3%) with chronic hepatitis (13 – 400 µg/L, median: 60 µg/L; $p<0.0001$), except of one dog that had a serum cGSTA concentration above the upper detection limit of the assay. Serum cGSTA concentrations were furthermore measurable in all 7 dogs (100%) with hepatic tumors (21 – 126 µg/L, median: 30 µg/L; $p<0.0001$) and in 15 of the 16 dogs (93.75%) with other liver diseases (15 – 400 µg/L, median: 36 µg/L; $p<0.0001$), with one dog also having a serum cGSTA concentration above the upper detection limit. This suggests that the measurement of serum cGSTA may be able to distinguish between healthy dogs and dogs with hepatic disease, though it may not be useful to distinguish between different types of liver disease, nor as a marker for CPSS.

In conclusion, serum cGSTA appears to be a promising marker for hepatic disease and warrants further assessment as a serum marker of hepatocellular injury in dogs. However, before this work can begin a more sensitive assay for its measurement must be developed and analytically validated.

VII. ZUSAMMENFASSUNG

Reinigung und Teilchencharakterisierung von caniner Glutathion Transferase und die Entwicklung eines Immunoassays zur Messung der Konzentration der Glutathion Transferase im Serum

Glutathion Transferase alpha (GSTA) gehört zu einer groβen Familie von Isoenzymen, die bei der Entgiftung verschiedenster Fremdstoffe durch die Konjugierung mit Glutathion mitwirken. Beim Menschen wurde dieses Enzym bereits als ein schneller ansteigender, spezifischerer und sensitiverer Indikator für hepatozelluläre Schädigungen im Vergleich zu den üblichen Aminotransferasen identifiziert und das unabhängig von der Ursache der Leberschädigung. Zudem wurde gezeigt, dass canine GSTA (cGSTA) auch beim Hund eine hepatozelluläre Schädigung nach induzierter Ischämie nachweisen kann.

Ziele dieser Studie waren, ein einfaches und reproduzierbares Protokoll für die Reinigung von cGSTA aus der Leber vom Hund zu erstellen, das Protein detaillierter zu charakterisieren, Antikörper gegen cGSTA im Kaninchen zu produzieren und diese für die Herstellung und Validierung eines Immunoassays zu nutzen. Ziel war es, diesen Assay zur Messung und zum Vergleich der Konzentration von cGSTA im Serum von gesunden Hunden und Hunden mit Lebererkrankungen einzusetzen.

Es wurde daher ein effizientes, einfaches und wiederholbares Protokoll für die Extraktion sowie für die nachfolgende Reinigung von Glutathion Transferase alpha aus Hundeleber entwickelt. Nachfolgend wurden einige physiologische Eigenschaften des Proteins ermittelt. Eine Aminosäurenanalyse und Liquid-Chromatographie-Massenspektometrie/Massenspektometrie (LC/MS/MS) zeigten eine sehr hohe Übereinstimmung mit den beiden Isoenzymen cGSTA2 und cGSTA3. Das molekulare Gewicht von cGSTA wurde mittels Gelelektrophorese auf etwa 25 kDa geschätzt. Später wurde die Masse von cGSTA genauer mittels MALDI-TOF Massenspektrometrie bestimmt und betrug 25.651 Da. Die isoelektrische Fokussierung von cGSTA ergab einen isoelektrischen Punkt von ungefähr 8,9 und die spezifische Absorption bei 280 nm wurde als 1,05 ermittelt.

Antikörper gegen cGSTA wurden in Kaninchen produziert und ein RIA für die Messung von cGSTA entwickelt und analytisch validatiert. Der RIA zeigte jedoch keine gute Linearität,

Präzision, Genauigkeit oder Reproduzierbarkeit. Dies begründet sich vermutlich in der geringen Sensitivität des RIA's, was dazu führte, dass die meisten Werte der Serumproben in den unteren Messbereich des Assays fielen. Der Messbereich des Assays betrug 6,25 bis 400 µg/l. Ein vorläufiger Referenzbereich von <14,35 µg/l wurde erstellt, um zu prüfen, ob die Entwicklung eines sensitiveren Assays von Vorteil wäre. Schließlich wurde die Konzentration von cGSTA bei 49 gesunden sowie 45 leberkranken Hunden gemessen und verglichen, um zu beurteilen, ob cGSTA ein nützlicher Indikator für die Diagnose von Lebererkrankungen beim Hund sein könnte. Die cGSTA Konzentration im Serum konnte bei 39 von 45 Hunde (86,7%) mit Lebererkrankung gemessen werden. Der Mittelwert der cGSTA Konzentration im Serum war signifikant höher bei Hunden mit Lebererkrankungen (6,25 – 400 µg/l, Median: 36,4 µg/l; p<0,0001) im Vergleich zu gesunden Hunden (6,25 – 400 µg/l, Median: 6,25 µg/l; p<0,0001). Die erkrankten Hunde wurden in vier Gruppen entsprechend der Ursachen der Lebererkrankung aufgeteilt. Canine GSTA war bei 3 von 7 Hunden (42,9%) mit angeborenen portosystemischen Shunts messbar (6,25 – 46 µg/l, Median: 6,25 µg/l; p<0.0001), wobei die Mehrzahl der Hunde Serum cGSTA-Konzentrationen unterhalb der unteren Grenze des Messbereichs des Assays hatten. In der Gruppe der Hunde mit chronischer Hepatitis hatten 14 der 15 Tiere (93,3%) messbare cGSTA-Konzentrationen (13 – 400 µg/l, Median: 60 µg/l; p<0.0001), abgesehen von einem Hund mit Werten oberhalb der oberen Grenze des Messbereichs. Die Serum cGSTA-Konzentrationen waren zudem messbar bei allen 7 Hunden (100%) mit Lebertumoren (21 – 126 µg/l, Median: 30 µg/l; p<0.0001) sowie bei 15 von 16 Hunden (93,75%) mit anderweitigen Lebererkrankungen (15 – 400 µg/l, Median: 36 µg/l; p<0.0001), wobei ein Hund auch hier cGSTA-Serumkonzentrationen oberhalb des Messbereichs hatte. Dies weist darauf hin, dass die Messung von cGSTA im Serum von Hunden hilfreich bei der Differenzierung von gesunden Hunden und Hunden mit Lebererkrankung sein könnte, jedoch nicht für die Differenzierung verschiedener Ursachen der Lebererkrankung oder als Marker für kongenitale Lebershunts.
Abschließend kann festgestellt werden, dass die cGSTA Konzentrationen im Serum als Marker für hepatozelluläre Schädigung vielversprechend erscheint, jedoch sind weitere Untersuchungen notwendig, um den klinischen Nutzen von cGSTA zu prüfen. Hierzu müsste ein neuer Assay für die Messung von GSTA mit verbesserter Sensitivität entwickelt und validiert werden.

VIII. REFERENCES

Abdel M (2011): Significance of serum alpha-glutathione s-transferase assessment in hepatitis C patients with different alanine aminotransferase patterns. Gastroenterology Research.

Abei M, Tanaka N, Osuga T, Harada S (1989): Immunochemical properties and immunohistological localization of human liver glutathione S-transferase isozymes. Nihon Shokakibyo Gakkai Zasshi 86(12): 2728-2734.

Abel E L, Bammler T K, Eaton D L (2004): Biotransformation of methyl parathion by glutathione S-transferases. Toxicol Sci 79(2): 224-232.

Abel E L, Opp S M, Verlinde C L, Bammler T K, Eaton D L (2004): Characterization of atrazine biotransformation by human and murine glutathione S-transferases. Toxicol Sci 80(2): 230-238.

Ahmad H, Singhal S S, Saxena M, Awasthi Y C (1993): Characterization of two novel subunits of the alpha-class glutathione S-transferases of human liver. Biochim Biophys Acta 1161(2-3): 333-336.

Ali-Osman F, Brunner J M, Kutluk T M, Hess K (1997): Prognostic significance of glutathione S-transferase pi expression and subcellular localization in human gliomas. Clin Cancer Res 3 (12 Pt 1): 2253-2261.

Anttila S, Hirvonen A, Vainio H, Husgafvel-Pursiainen K, Hayes J D, Ketterer B (1993): Immunohistochemical localization of glutathione S-transferases in human lung. Cancer Res 53(23): 5643-5648.

Armstrong R N (1997): Structure, catalytic mechanism, and evolution of the glutathione transferases. Chem Res Toxicol 10(1): 2-18.

Atkinson H J, Babbitt P C (2009): Glutathione transferases are structural and functional outliers in the thioredoxin fold. Biochemistry 48(46): 11108-11116.

Awasthi S, Sharma R, Singhal S S, Zimniak P, Awasthi Y C (2002): RLIP76, a novel transporter catalyzing ATP-dependent efflux of xenobiotics. Drug Metab Dispos 30(12): 1300-1310.

Bailey W J, Holder D, Patel H, Devlin P, Gonzalez R J, Hamilton V, Muniappa N, Hamlin D M, Thomas C E, Sistare F D, Glaab W E (2012): A performance evaluation of three drug-induced liver injury biomarkers in the rat: alpha-glutathione S-transferase, arginase 1, and 4-hydroxyphenyl-pyruvate dioxygenase. Toxicol Sci 130(2): 229-244.

Ban N, Takahashi Y, Takayama T, Kura T, Katahira T, Sakamaki S, Niitsu Y (1996): Transfection of glutathione S-transferase (GST)-pi antisense complementary DNA increases the sensitivity of a colon cancer cell line to adriamycin, cisplatin, melphalan, and etoposide. Cancer Res 56(15): 3577-3582.

Bass N M, Kirsch R E, Tuff S A, Marks I, Saunders S J (1977): Ligandin heterogeneity: Evidence that the two non-identical subunits are the monomers of two distinct proteins. Biochimica et Biophysica Acta (BBA) - Protein Structure 492(1): 163-175.

Beckett G J, Chapman B J, Dyson E H, Hayes J D (1985): Plasma glutathione S-transferase measurements after paracetamol overdose: evidence for early hepatocellular damage. Gut 26(1): 26-31.

Beckett G J, Dyson E H, Chapman B J, Templeton A J, Hayes J D (1985): Plasma glutathione S-transferase measurements by radioimmunoassay: a sensitive index of hepatocellular damage in man. Clin Chim Acta 146(1): 11-19.

Beckett G J, Foster G R, Hussey A J, Oliveira D B, Donovan J W, Prescott L F, Proudfoot A T (1989): Plasma glutathione S-transferase and F protein are more sensitive than alanine

aminotransferase as markers of paracetamol (acetaminophen)-induced liver damage. Clin Chem 35(11): 2186-2189.

Beckett G J, Hayes P C, Hussey A J, Bouchier I A, Hayes J D (1987): Plasma glutathione S-transferase measurements in patients with alcoholic cirrhosis. Clin Chim Acta 169(1): 85-89.

Beckett G J, Hussey A J, Laing I, Howie A F, Hayes J D, Strange R C, Faulder C G, Hume R (1989): Measurements of glutathione S-transferase B1 in plasma after birth asphyxia: an early indication of hepatocellular damage. Clin Chem 35(6): 995-999.

Bengmark S, Olsson R (1974): Elimination of alkaline phosphatases from serum in dog after intravenous injection of canine phosphatases from bone and intestine. Acta Chir Scand 140(1): 1-6.

Benson A M, Talalay P, Keen J H, Jakoby W B (1977): Relationship between the soluble glutathione-dependent delta 5-3-ketosteroid isomerase and the glutathione S-transferases of the liver. Proc Natl Acad Sci U S A 74(1): 158-162.

Beuckmann C T, Fujimori K, Urade Y, Hayaishi O (2000): Identification of Mu-class glutathione transferases M2-2 and M3-3 as cytosolic prostaglandin E synthases in the human brain. Neurochemical Research 25(5): 733-738.

Blum H, Beier H, Gross H J (1987): Improved silver staining of plant proteins, RNA and DNA in polyacrylamide gels. Electrophoresis 8(2): 93-99.

Board P G (2011): The omega-class glutathione transferases: structure, function, and genetics. Drug Metab Rev 43(2): 226-235.

Board P G, Coggan M, Wilce M C, Parker M W (1995): Evidence for an essential serine residue in the active site of the Theta class glutathione transferases. Biochem J 311 (Pt 1): 247-250.

Board P G, Webb G C (1987): Isolation of a cDNA clone and localization of human glutathione S-transferase 2 genes to chromosome band 6p12. Proc Natl Acad Sci U S A 84(8): 2377-2381.

Bogaards J J, van Ommen B, van Bladeren P J (1992): Purification and characterization of eight glutathione S-transferase isoenzymes of hamster. Comparison of subunit composition of enzymes from liver, kidney, testis, pancreas and trachea. Biochem J 286 (Pt 2): 383-388.

Booth J, Boyland E, Sims P (1961): An enzyme from rat liver catalysing conjugations with glutathione. Biochem J 79(3): 516-524.

Boyer T D (1989): Special article the glutathione S-transferases: An update. Hepatology 9(3): 486-496.

Branten A J, Mulder T P, Peters W H, Assmann K J, Wetzels J F (2000): Urinary excretion of glutathione S transferases alpha and pi in patients with proteinuria: reflection of the site of tubular injury. Nephron 85(2): 120-126.

Caccuri A M, Antonini G, Nicotra M, Battistoni A, Bello M L, Board P G, Parker M W, Ricci G (1997): Catalytic mechanism and role of hydroxyl residues in the active site of theta class glutathione S-transferases: Investigation of Ser-9 and Tyr-113 in a glutatione S-transferase from the Australian sheep blowfly, Lucilia cuprina. J. Biol. Chem. 272(47): 29681-29686.

Campbell J A, Corrigall A V, Guy A, Kirsch R E (1991): Immunohistologic localization of alpha, mu, and pi class glutathione S-transferases in human tissues. Cancer 67(6): 1608-1613.

Center S A, Slater M R, Manwarren T, Prymak K (1992): Diagnostic efficacy of serum alkaline phosphatase and gamma-glutamyltransferase in dogs with histologically confirmed hepatobiliary disease: 270 cases (1980-1990). J Am Vet Med Assoc 201(8): 1258-1264.

Chapman S E, Hostutler R A (2015): A laboratory diagnostic approach to hepatobiliary disease in small animals. Clin Lab Med 35(3): 503-519.

Chen W J, Graminski G F, Armstrong R N (1988): Dissection of the catalytic mechanism of isozyme 4-4 of glutathione S-transferase with alternative substrates. Biochemistry 27(2): 647-654.

Cho S G, Lee Y H, Park H S, Ryoo K, Kang K W, Park J, Eom S J, Kim M J, Chang T S, Choi S Y, Shim J, Kim Y, Dong M S, Lee M J, Kim S G, Ichijo H, Choi E J (2001): Glutathione S-transferase mu modulates the stress-activated signals by suppressing apoptosis signal-regulating kinase 1. J Biol Chem 276(16): 12749-12755.

Clarke H, Egan D A, Heffernan M, Doyle S, Byrne C, Kilty C, Ryan M P (1997): Alpha-glutathione s-transferase (alpha-GST) release, an early indicator of carbon tetrachloride hepatotoxicity in the rat. Hum Exp Toxicol 16(3): 154-157.

Cole S P, Deeley R G (2006): Transport of glutathione and glutathione conjugates by MRP1. Trends Pharmacol Sci 27(8): 438-446.

Coles B F, Morel F, Rauch C, Huber W W, Yang M, Teitel C H, Green B, Lang N P, Kadlubar F F (2001): Effect of polymorphism in the human glutathione S-transferase A1 promoter on hepatic GSTA1 and GSTA2 expression. Pharmacogenetics 11(8): 663-669.

Combet C, Blanchet C, Geourjon C, Deleage G (2000): NPS@: network protein sequence analysis. Trends Biochem Sci 25(3): 147-150.

Cullen J M (2009): Summary of the World Small Animal Veterinary Association standardization committee guide to classification of liver disease in dogs and cats. Vet Clin North Am Small Anim Pract 39(3): 395-418.

Daemen J W, Oomen A P, Janssen M A, van de Schoot L, van Kreel B K, Heineman E, Kootstra G (1997): Glutathione S-transferase as predictor of functional outcome in transplantation of machine-preserved non-heart-beating donor kidneys. Transplantation 63(1): 89-93.

Delaney C P, O'Neill S, Manning F, Fitzpatrick J M, Gorey T F (1999): Plasma concentrations of glutathione S-transferase isoenzyme are raised in patients with intestinal ischaemia. Br J Surg 86(10): 1349-1353.

Desmots F, Rissel M, Loyer P, Turlin B, Guillouzo A (2001): Immunohistological analysis of glutathione transferase A4 distribution in several human tissues using a specific polyclonal antibody. J Histochem Cytochem 49(12): 1573-1579.

Dossin O, Rives A, Germain C (2005): Pharmacokinetics of liver transaminases in healthy dogs: Potential clinical relevance for assessment of liver damage. (abstract 152, ACVIM Annual Meeting) J Vet Intern Med.

Dufour D R, Lott J A, Nolte F S, Gretch D R, Koff R S, Seeff L B (2000): Diagnosis and monitoring of hepatic injury. I. Performance characteristics of laboratory tests. Clin Chem 46(12): 2027-2049.

Eger E I, 2nd, Koblin D D, Bowland T, Ionescu P, Laster M J, Fang Z, Gong D, Sonner J, Weiskopf R B (1997): Nephrotoxicity of sevoflurane versus desflurane anesthesia in volunteers. Anesth Analg 84(1): 160-168.

Egner P A, Kensler T W, Chen J G, Gange S J, Groopman J D, Friesen M D (2008): Quantification of sulforaphane mercapturic acid pathway conjugates in human urine by high-performance liquid chromatography and isotope-dilution tandem mass spectrometry. Chem Res Toxicol 21(10): 1991-1996.

Engle M R, Singh S P, Czernik P J, Gaddy D, Montague D C, Ceci J D, Yang Y, Awasthi S, Awasthi Y C, Zimniak P (2004): Physiological role of mGSTA4-4, a glutathione S-transferase metabolizing 4-hydroxynonenal: generation and analysis of mGsta4 null mouse. Toxicol Appl Pharmacol 194(3): 296-308.

Erhardt J, Dirr H (1995): Native dimer stabilizes the subunit tertiary structure of porcine class pi glutathione S-transferase. Eur J Biochem 230(2): 614-620.

Fleischner G, Robbins J, Arias I M (1972): Immunological studies of Y protein. A major cytoplasmic organic anion-binding protein in rat liver. J Clin Invest 51(3): 677-684.

Fuentealba C, Guest S, Haywood S, Horney B (1997): Chronic hepatitis: a retrospective study in 34 dogs. Can Vet J 38(6): 365-373.

Giannini E (2000): Utility of a-Glutathione S-Transferase Assessment in chronic hepatitis C patients with near normal ALT levels. Clin Biochem 33(4):297-301.

Gilliland F D, Li Y F, Saxon A, Diaz-Sanchez D (2004): Effect of glutathione-S-transferase M1 and P1 genotypes on xenobiotic enhancement of allergic responses: randomised, placebo-controlled crossover study. Lancet 363(9403): 119-125.

Ginn J, Sacco J, Wong Y Y, Motsinger-Reif A, Chun R, Trepanier L A (2014): Positive association between a glutathione-S-transferase polymorphism and lymphoma in dogs. Vet Comp Oncol 12(3): 227-236.

Gok M A, Pelsers M, Glatz J F, Bhatti A A, Shenton B K, Peaston R, Cornell C, Mantle D, Talbot D (2003): Comparison of perfusate activities of glutathione S-transferase, alanine aminopeptidase and fatty acid binding protein in the assessment of non-heart-beating donor kidneys. Ann Clin Biochem 40(Pt 3): 252-258.

Goto S, Iida T, Cho S, Oka M, Kohno S, Kondo T (1999): Overexpression of glutathione S-transferase pi enhances the adduct formation of cisplatin with glutathione in human cancer cells. Free Radic Res 31(6): 549-558.

Grover P L, Sims P (1964): Conjugations with glutathione. Distribution of glutathione S-aryltransferase in vertebrate species. Biochem J 90(3): 603-606.

Habig W H, Pabst M J, Fleischner G, Gatmaitan Z, Arias I M, Jakoby W B (1974): The identity of glutathione S-transferase B with ligandin, a major binding protein of liver. Proc Natl Acad Sci U S A 71(10): 3879-3882.

Harlow E D, Lane D (1999): Using antibodies: a laboratory manual. In: CSHL Press. Cold Spring Harbor, NY.

Harpur E, Ennulat D, Hoffman D, Betton G, Gautier J C, Riefke B, Bounous D, Schuster K, Beushausen S, Guffroy M, Shaw M, Lock E, Pettit S, Nephrotoxicity H C o B o (2011): Biological qualification of biomarkers of chemical-induced renal toxicity in two strains of male rat. Toxicol Sci 122(2): 235-252.

Harrison D J, Kharbanda R, Cunningham D S, McLellan L I, Hayes J D (1989): Distribution of glutathione S-transferase isoenzymes in human kidney: basis for possible markers of renal injury. J Clin Pathol 42(6): 624-628.

Hayes J D, McLellan L I (1999): Glutathione and glutathione-dependent enzymes represent a co-ordinately regulated defence against oxidative stress. Free Radic Res 31(4): 273-300.

Hayes J D, Pulford D J (1995): The glutathione S-transferase supergene family: regulation of GST and the contribution of the isoenzymes to cancer chemoprotection and drug resistance. Crit Rev Biochem Mol Biol 30(6): 445-600.

Hayes P C, Bouchier I A, Beckett G J (1991): Glutathione S-transferase in humans in health and disease. Gut 32(7): 813-818.

Hayes P C, Hussey A J, Keating J, Bouchier I A, Williams R, Beckett G J, Hayes J D (1988): Glutathione S-transferase levels in autoimmune chronic active hepatitis: a more sensitive index of hepatocellular damage than aspartate transaminase. Clin Chim Acta 172(2-3): 211-216.

Heidelbaugh J J, Bruderly M (2006): Cirrhosis and chronic liver failure: part I. Diagnosis and evaluation. Am Fam Physician 74(5): 756-762.

Hoarau P, Garello G, Gnassia-Barelli M, Romeo M, Girard J P (2002): Purification and partial characterization of seven glutathione S-transferase isoforms from the clam Ruditapes decussatus. Eur J Biochem 269(17): 4359-4366.

Hoffmann W E, Dorner J L (1977): Disappearance rates of intravenously injected canine alkaline phosphatase isoenzymes. Am J Vet Res 38(10): 1553-1556.

Hughes V F, Trull A K, Gimson A, Friend P J, Jamieson N, Duncan A, Wight D G, Prevost A T, Alexander G J (1997): Randomized trial to evaluate the clinical benefits of serum alpha-glutathione S-transferase concentration monitoring after liver transplantation. Transplantation 64(10): 1446-1452.

Hunter W M, Greenwood F C (1962): Preparation of iodine-131 labelled human growth hormone of high specific activity. Nature 194: 495-496.

Hurst R, Bao Y, Jemth P, Mannervik B, Williamson G (1998): Phospholipid hydroperoxide glutathione peroxidase activity of human glutathione transferases. Biochem J 332 (Pt 1): 97-100.

Igarashi T, Kohara A, Shikata Y, Sagami F, Sonoda J, Horie T, Satoh T (1991): The unique feature of dog liver cytosolic glutathione S-transferases. An isozyme not retained on the affinity column has the highest activity toward 1,2-dichloro-4-nitrobenzene. J Biol Chem 266(32): 21709-21717.

Ishikawa T (1992): The ATP-dependent glutathione S-conjugate export pump. Trends Biochem Sci 17(11): 463-468.

Jakobsson P J, Mancini J A, Ford-Hutchinson A W (1996): Identification and characterization of a novel human microsomal glutathione S-transferase with leukotriene C4 synthase activity and significant sequence identity to 5-lipoxygenase-activating protein and leukotriene C4 synthase. J Biol Chem 271(36): 22203-22210.

Jakobsson P J, Morgenstern R, Mancini J, Ford-Hutchinson A, Persson B (1999): Common structural features of MAPEG -- a widespread superfamily of membrane associated proteins with highly divergent functions in eicosanoid and glutathione metabolism. Protein Sci 8(3): 689-692.

Jakobsson P J, Thoren S, Morgenstern R, Samuelsson B (1999): Identification of human prostaglandin E synthase: a microsomal, glutathione-dependent, inducible enzyme, constituting a potential novel drug target. Proc Natl Acad Sci U S A 96(13): 7220-7225.

Ji X, Johnson W W, Sesay M A, Dickert L, Prasad S M, Ammon H L, Armstrong R N, Gilliland G L (1994): Structure and function of the xenobiotic substrate binding site of a glutathione S-transferase as revealed by x-ray crystallographic analysis of product complexes with the diastereomers of 9-(S-Glutathionyl)-10-hydroxy-9,10-dihydrophenanthrene. J. Biochem 33(5): 1043-1052.

Johansson A S, Mannervik B (2001): Human glutathione transferase A3-3, a highly efficient catalyst of double-bond isomerization in the biosynthetic pathway of steroid hormones. J Biol Chem 276(35): 33061-33065.

Josephy P D (2010): Genetic variations in human glutathione transferase enzymes: significance for pharmacology and toxicology. Hum Genomics Proteomics 2010: 876940.

Keen J H, Jakoby W B (1978): Glutathione transferases. Catalysis of nucleophilic reactions of glutathione. J Biol Chem 253(16): 5654-5657.

Keppler D (1999): Export pumps for glutathione S-conjugates. Free Radic Biol Med 27(9-10): 985-991.

Ketterer B, Meyer D J (1989): Gluthathione transferases: A possible role in the detoxication and repair of DNA and lipid hydroperoxides. Mutat Res 214(1): 33-40.

Khojasteh-Bakht S C, Nelson S D, Atkins W M (1999): Glutathione S-transferase catalyzes the isomerization of (R)-2-hydroxymenthofuran to mintlactones. Arch Biochem Biophys 370(1): 59-65.

Khurana S, Corbally M T, Manning F, Armenise T, Kierce B, Kilty C (2002): Glutathione S-transferase: a potential new marker of intestinal ischemia. J Pediatr Surg 37(11): 1543-1548.

Kilty C, Doyle S, Hassett B, Manning F (1998): Glutathione S-transferases as biomarkers of organ damage: applications of rodent and canine GST enzyme immunoassays. Chemico-Biological Interactions 112: 123-135.

Kim S K, Woodcroft K J, Novak R F (2003): Insulin and glucagon regulation of glutathione S-transferase expression in primary cultured rat hepatocytes. J Pharmacol Exp Ther 305(1): 353-361.

Koo D J, Zhou M, Chaudry I H, Wang P (2000): Plasma alpha-glutathione S-transferase: a sensitive indicator of hepatocellular damage during polymicrobial sepsis. Arch Surg 135(2): 198-203.

Kraft W, Ghermai A K, Winzinger H, Knoll L (1983): [Comparison of serum AST, ALT, AP and GGT activities in the diagnosis of liver diseases in dogs]. Berl Munch Tierarztl Wochenschr 96(12): 421-431.

Kunze T (1997): Purification and characterization of class alpha and Mu glutathione S-transferases from porcine liver. Comp Biochem Physiol B Biochem Mol Biol 116(4): 397-406.

Laborde E (2010): Glutathione transferases as mediators of signaling pathways involved in cell proliferation and cell death. Cell Death Differ 17(9): 1373-1380.

Ladner J E, Parsons J F, Rife C L, Gilliland G L, Armstrong R N (2004): Parallel evolutionary pathways for glutathione transferases: structure and mechanism of the mitochondrial class kappa enzyme rGSTK1-1. J. Biochem 43(2): 352-361.

Leaver M J, George S G (1998): A piscine glutathione S-transferase which efficiently conjugates the end-products of lipid peroxidation. Mar Environ Res 46(1-5): 71-74.

Lien S, Larsson A K, Mannervik B (2002): The polymorphic human glutathione transferase T1-1, the most efficient glutathione transferase in the denitrosation and inactivation of the anticancer drug 1,3-bis(2-chloroethyl)-1-nitrosourea. Biochem Pharmacol 63(2): 191-197.

Lipman N S, Jackson L R, Trudel L J, Weis-Garcia F (2005): Monoclonal versus polyclonal antibodies: distinguishing characteristics, applications, and information resources. ILAR J 46(3): 258-268.

Litwack G, Ketterer B, Arias I M (1971): Ligandin: a hepatic protein which binds steroids, bilirubin, carcinogens and a number of exogenous organic anions. Nature 24;234(5330):466-7.

Liu S, Zhang P, Ji X, Johnson W W, Gilliland G L, Armstrong R N (1992): Contribution of tyrosine 6 to the catalytic mechanism of isoenzyme 3-3 of glutathione S-transferase. J Biol Chem 267(7): 4296-4299.

Lum G, Gambino S R (1972): Serum gamma-glutamyl transpeptidase activity as an indicator of disease of liver, pancreas, or bone. Clin Chem 18(4): 358-362.

Mannervik B, Alin P, Guthenberg C, Jensson H, Tahir M K, Warholm M, Jörnvall H (1985): Identification of three classes of cytosolic glutathione transferase common to several mammalian species: correlation between structural data and enzymatic properties. Proc. Natl. Acad. Sci. USA 82(21): 7202-7206.

Mannervik B, Awasthi Y C, Board P G, Hayes J D, Di Ilio C, Ketterer B, Listowsky I, Morgenstern R, Muramatsu M, Pearson W R, et al. (1992): Nomenclature for human glutathione transferases. Biochem J 282 (Pt 1): 305-306.

Mannervik B, Board P G, Hayes J D, Listowsky I, Pearson W R (2005): Nomenclature for mammalian soluble glutathione transferases. S Helmut and P Lester methods in enzymology. Academic Press. Vol 401: 1-8.

Mannervik B, Danielson U H (1988): Glutathione transferases--structure and catalytic activity. CRC Crit Rev Biochem 23(3): 283-337.

Mannervik B, Jensson H (1982): Binary combinations of four protein subunits with different catalytic specificities explain the relationship between six basic glutathione S-transferases in rat liver cytosol. J Biol Chem 257(17): 9909-9912.

Mannes G A, Stellaard F, Paumgartner G (1982): Increased serum bile acids in cirrhosis with normal transaminases. Digestion 25(4): 217-221.

Marchler-Bauer A, Derbyshire M K, Gonzales N R, Lu S, Chitsaz F, Geer L Y, Geer R C, He J, Gwadz M, Hurwitz D I, Lanczycki C J, Lu F, Marchler G H, Song J S, Thanki N, Wang Z, Yamashita R A, Zhang D, Zheng C, Bryant S H (2015): CDD: NCBI's conserved domain database. Nucleic Acids Res 43(Database issue): D222-226.

Marnett L J, Riggins J N, West J D (2003): Endogenous generation of reactive oxidants and electrophiles and their reactions with DNA and protein. J Clin Invest 111(5): 583-593.

McMonagle M P, Halpenny M, McCarthy A, Mortell A, Manning F, Kilty C, Mannion D, Wood A E, Corbally M T (2006): Alpha glutathione S-transferase: a potential marker of ischemia-reperfusion injury of the intestine after cardiac surgery? J Pediatr Surg 41(9): 1526-1531.

Morel F, Rauch C, Coles B, Le Ferrec E, Guillouzo A (2002): The human glutathione transferase alpha locus: genomic organization of the gene cluster and functional characterization of the genetic polymorphism in the hGSTA1 promoter. Pharmacogenetics 12(4): 277-286.

Morel F, Schulz W A, Sies H (1994): Gene structure and regulation of expression of human glutathione S-transferases alpha. Biol Chem Hoppe Seyler 375(10): 641-649.

Moyo R, Chimponda T, Mukanganyama S (2014): Inhibition of hematopoietic prostaglandin D2 synthase (H-PGDS) by an alkaloid extract from Combretum molle. BMC Complement Altern Med 14: 221.

Mukhtar H, Bresnick E (1976): Effects of phenobarbital and 3-methylcholanthrene administration on glutathione-S-epoxide transferase activity in rat liver. Biochem Pharmacol 25(9): 1081-1084.

Mulder T P, Peters W H, Court D A, Jansen J B (1996): Sandwich ELISA for glutathione S-transferase Alpha 1-1: plasma concentrations in controls and in patients with gastrointestinal disorders. Clin Chem 42(3): 416-419.

Mulder T P, Court D A, Peters W H (1999): Variability of glutathione S-transferase alpha in human liver and plasma. Clin Chem 45(3): 355-359.

Ning B, Wang C, Morel F, Nowell S, Ratnasinghe D L, Carter W, Kadlubar F F, Coles B (2004): Human glutathione S-transferase A2 polymorphisms: variant expression, distribution in prostate cancer cases/controls and a novel form. Pharmacogenetics 14(1): 35-44.

Oakley A (2011): Glutathione transferases: a structural perspective. Drug Metab Rev 43(2): 138-151.

Palmer C N, Young V, Ho M, Doney A, Belch J J (2003): Association of common variation in glutathione S-transferase genes with premature development of cardiovascular disease in patients with systemic sclerosis. Arthritis Rheum 48(3): 854-855.

Pastore A, Lo Bello M, Aureli G, Federici G, Ricci G, Di Ilio C, Petruzzelli R (1998): Purification and characterization of a novel alpha-class glutathione transferase from human liver. Int J Biochem Cell Biol 30(11): 1235-1243.

Pohanka M (2013): Role of oxidative stress in infectious diseases. A review. Folia Microbiol (Praha) 58(6): 503-513.

Poldervaart J H, Favier R P, Penning L C, van den Ingh T S, Rothuizen J (2009): Primary hepatitis in dogs: a retrospective review (2002-2006). J Vet Intern Med 23(1): 72-80.

Pongstaporn W, Pakakasama S, Sanguansin S, Hongeng S, Petmitr S (2009): Polymorphism of glutathione S-transferase Omega gene: association with risk of childhood acute lymphoblastic leukemia. J Cancer Res Clin Oncol 135(5): 673-678.

Prabhu K S, Reddy P V, Jones E C, Liken A D, Reddy C C (2004): Characterization of a class alpha glutathione-S-transferase with glutathione peroxidase activity in human liver microsomes. Arch Biochem Biophys 424(1): 72-80.

Price C, Alberti K (1979): Biochemical assessment of liver function. Liver and biliary disease—pathophysiology, diagnosis, management. London. WB Saunders: 381-416.

Ramakers B P, de Goeij M, van der Hoeven J G, Peters W H, Pickkers P (2009): Inflammation-induced hepatotoxicity in humans. Shock 31(2): 151-156.

Raza H, Ahmed I, John A (2004): Tissue specific expression and immunohistochemical localization of glutathione S-transferase in streptozotocin induced diabetic rats: modulation by Momordica charantia (karela) extract. Life Sci 74(12): 1503-1511.

Reinemer P, Dirr H, Ladenstein R, Schäffer J, Gallay O, Huber R (1991): The three-dimensional structure of class pi glutathione S-transferase in complex with glutathione sulfonate at 2.3 A resolution. The EMBO journal 10(8): 1997.

Reinemer P, Dirr H W, Ladenstein R, Huber R, Lo Bello M, Federici G, Parker M W (1992): Three-dimensional structure of class π glutathione S-transferase from human placenta in complex with S-hexylglutathione at 2.8 Å resolution. J Mol Biol 227(1): 214-226.

Ruscoe J E, Rosario L A, Wang T, Gate L, Arifoglu P, Wolf C R, Henderson C J, Ronai Z, Tew K D (2001): Pharmacologic or genetic manipulation of glutathione S-transferase P1-1 (GSTpi) influences cell proliferation pathways. J Pharmacol Exp Ther 298(1): 339-345.

Ruscoe J E, Rosario L A, Wang T L, Gate L, Arifoglu P, Wolf C R, Henderson C J, Ronai Z, Tew K D (2001): Pharmacologic or genetic manipulation of glutathione S-transferase P1-1 (GST pi) influences cell proliferation pathways. J Pharmacol Exp Ther 298(1): 339-345.

Ryberg D (1997): Genotypes of glutathione transferase M1 and P1 and their significance for lung DNA adduct levels and cancer risk. Carcinogenesis 18(7): 1285-1289.

Savolainen V T, Pjarinen J, Perola M, Penttila A, Karhunen P J (1996): Glutathione-S-transferase GST M1 "null" genotype and the risk of alcoholic liver disease. Alcohol Clin Exp Res 20(8): 1340-1345.

Sheehan D, Meade G, Foley V M, Dowd C A (2001): Structure, function and evolution of glutathione transferases: implications for classification of non-mammalian members of an ancient enzyme superfamily. Biochem J 360(Pt 1): 1-16.

Sherman M, Bass N M, Campbell J A, Kirsch R E (1983): Radioimmunoassay of human ligandin. Hepatology 3(2): 162-169.

Shull R M, Hornbuckle W (1979): Diagnostic use of serum gamma-glutamyltransferase in canine liver disease. Am J Vet Res 40(9): 1321-1324.

Sidlova K, Skalicka V, Kotaska K, Pechova M, Chada M, Bartosova J, Hribal Z, Nevoral J, Vavrova V, Prusa R (2003): Serum alpha-glutathione S-transferase as a sensitive marker of hepatocellular damage in patients with cystic fibrosis. Physiol Res 52(3): 361-365.

Singh S P, Zimniak L, Zimniak P (2010): The human hGSTA5 gene encodes an enzymatically active protein. Biochim Biophys Acta 1800(1): 16-22.

Sinning I, Kleywegt G J, Cowan S W, Reinemer P, Dirr H W, Huber R, Gilliland G L, Armstrong R N, Ji X, Board P G, et al. (1993): Structure determination and refinement of human alpha class glutathione transferase A1-1, and a comparison with the Mu and Pi class enzymes. J Mol Biol 232(1): 192-212.

Smith G J, Ohl V S, Litwack G (1977): Ligandin, the glutathione S-transferases, and chemically induced hepatocarcinogenesis: a review. Cancer Res 37(1): 8-14.

Solter P F, Hoffmann W E, Chambers M D, Schaeffer D J, Kuhlenschmidt M S (1994): Hepatic total 3 alpha-hydroxy bile acids concentration and enzyme activities in prednisone-treated dogs. Am J Vet Res 55(8): 1086-1092.

Stevens J M, Hornby J A, Armstrong R N, Dirr H W (1998): Class sigma glutathione transferase unfolds via a dimeric and a monomeric intermediate: impact of subunit interface on conformational stability in the superfamily. Biochem J 37(44): 15534-15541.

Stockman P K, McLellan L I, Hayes J D (1987): Characterization of the basic GST b1 & B2 subunits from human liver. Biochem J 15;244(1):55-61.

Stoehlmacher J, Park D J, Zhang W, Groshen S, Tsao-Wei D D, Yu M C, Lenz H J (2002): Association between glutathione S-transferase P1, T1, and M1 genetic polymorphism and survival of patients with metastatic colorectal cancer. J Natl Cancer Inst 94(12): 936-942.

Sundberg A G, Appelkvist E L, Backman L, Dallner G (1994): Urinary pi-class glutathione transferase as an indicator of tubular damage in the human kidney. Nephron 67(3): 308-316.

Sundberg A G, Nilsson R, Appelkvist E L, Dallner G (1993): Immunohistochemical localization of alpha and pi class glutathione transferases in normal human tissues. Pharmacol Toxicol 72(4-5): 321-331.

Tars K, Olin B, Mannervik B (2010): Structural basis for featuring of steroid isomerase activity in alpha class glutathione transferases. J Mol Biol 397(1): 332-340.

Teichert J, Sohr R, Hennig L, Baumann F, Schoppmeyer K, Patzak U, Preiss R (2009): Identification and quantitation of the N-acetyl-L-cysteine S-conjugates of bendamustine and its sulfoxides in human bile after administration of bendamustine hydrochloride. Drug Metab Dispos 37(2): 292-301.

Tetlow N, Board P G (2004): Functional polymorphism of human glutathione transferase A2. Pharmacogenetics 14(2): 111-116.

Trull A K (2001): The clinical validation of novel strategies for monitoring transplant recipients. Clin Biochem 34(1): 3-7.

Trull A K, Facey S P, Rees G W, Wight D G, Noble-Jamieson G, Joughin C, Friend P J, Alexander G J (1994): Serum alpha-glutathione S-transferase--a sensitive marker of hepatocellular damage associated with acute liver allograft rejection. Transplantation 58(12): 1345-1351.

Valentine B A, Blue J T, Shelley S M, Cooper B J (1990): Increased serum alanine aminotransferase activity associated with muscle necrosis in the dog. J Vet Intern Med 4(3): 140-143.

van Lieshout E M, Roelofs H M, Dekker S, Mulder C J, Wobbes T, Jansen J B, Peters W H (1999): Polymorphic expression of the glutathione S-transferase P1 gene and its susceptibility to Barrett's esophagus and esophageal carcinoma. Cancer Res 59(3): 586-589.

van Ommen B, Bogaards J J, Peters W H, Blaauboer B, van Bladeren P J (1990): Quantification of human hepatic glutathione S-transferases. Biochem J 269(3): 609-613.

van Wagensveld B A, Scheepers J J, van Gulik T M, Frederiks W M, Bleeker W K, Obertop H, Gouma D J (1997): Alpha glutathione S-transferase as novel parameter for hepatocellular damage in the isolated perfused rat liver. Transplant Proc 29(8): 3449-3451.

Vandenberghe Y, Foriers A, Rogiers V, Vercruysse A (1990): Changes in expression and “de novo” synthesis of glutathione S-transferase subunits in cultured adult rat hepatocytes. Biochem Pharmacol 39(4): 685-690.

Vargo M A, Colman R F (2001): Affinity labeling of rat glutathione S-transferase isozyme 1-1 by 17beta -iodoacetoxy-estradiol-3-sulfate. J Biol Chem 276(3): 2031-2036.

Vargo M A, Colman R F (2004): Heterodimers of wild-type and subunit interface mutant enzymes of glutathione S-transferase A1-1: interactive or independent active sites? Protein Sci 13(6): 1586-1593.

Wang G, Zhang L, Li Q (2006): Genetic polymorphisms of GSTT1, GSTM1, and NQO1 genes and diabetes mellitus risk in Chinese population. Biochem Biophys Res Commun 341(2): 310-313.

Watanabe T, Ohashi Y, Kosaka T, Arakawa S, Shibaya Y, Yamoto T, Manabe S, Takasaki W (2006): Expression of the theta class GST isozyme, YdfYdf, in low GST dogs. Arch Toxicol 80(5): 250-257.

Watanabe T, Sugiura T, Manabe S, Takasaki W, Ohashi Y (2004): Low glutathione S-transferase dogs. Arch Toxicol 78(4): 218-225.

Wiener H (1986): Heterogeneity of dog-liver glutatione S-transferases - Evidence for a unique temperature dependence of the catalytic process. Eur J Biochem 2;157(2):351-63.

Wilce M C, Board P G, Feil S C, Parker M W (1995): Crystal structure of a theta-class glutathione transferase. EMBO J 14(10): 2133-2143.

Xu H M, Chen Y, Xu J, Zhou Q (2012): Drug-induced liver injury in hospitalized patients with notably elevated alanine aminotransferase. World J Gastroenterol 18(41): 5972-5978.

Yanbaeva D G, Wouters E F, Dentener M A, Spruit M A, Reynaert N L (2009): Association of glutathione-S-transferase omega haplotypes with susceptibility to chronic obstructive pulmonary disease. Free Radic Res 43(8): 738-743.

Yang Y, Sharma R, Zimniak P, Awasthi Y C (2002): Role of alpha class glutathione S-transferases as antioxidant enzymes in rodent tissues. Toxicol Appl Pharmacol 182(2): 105-115.

Zhong S, Howie A F, Ketterer B, Taylor J, Hayes J D, Beckett G J, Wathen C G, Wolf C R, Spurr N K (1991): Glutathione S-transferase mu locus: use of genotyping and phenotyping assays to assess association with lung cancer susceptibility. Carcinogenesis 12(9): 1533-1537.

Zinkl J G, Bush R M, Cornelius C E, Freedland R A (1971): Comparative studies on plasma and tissue sorbitol, glutamic, lactic and hydroxybutyric dehydrogenase and transaminase activities in the dog. Res Vet Sci 12(3): 211-214.

IX. APPENDIX

1. Legend of Figures

2. Legend for Tables

X. PUBLICATIONS

This work is unpublished.

XI. ACKNOWLEDGEMENTS

First of all I would like to thank my parents, Maja and Martin Mischel, for their unconditional and unending love and support. Even though it has separated us by a great distance, they have always supported my dreams with love and calm and unerring advice. I am eternally grateful to them for all that they have done for me.

I would also like to thank Prof. Barbara Kohn for providing me with this unique and exciting opportunity as well as Prof. Jörg Steiner for his sponsorship and mentorship throughout this project. My unflappable supervisor Prof. Jonathan Lidbury deserves a special thank you for his invaluable guidance and unwavering support. He always made himself available to help with any and all questions or problems and made the whole process an enjoyable one. Prof. Jan Suchodolski, who was always available with helpful advice and an open mind, also deserves my deepest gratitude. Finally, Prof. Larry Dangott deserves all the *Kuchen* for his friendly advice, professional guidance, and mass spectrometry action.

I also had a great time working with the GI lab team at Texas A&M University. Thanks for all the “chit chat” and fun times. I would especially like to thank Blake Guard and Julia Honneffer for reviewing my thesis.

Last but not least, thank you to all of the great friends that I have made in College Station for all the good times and support throughout my stay here, including my lab parents and the coolest landlords ever, Lori and Doug Kessler.

XII. SELBSTSTÄNDIGKEITSERKLÄRUNG

Hiermit bestätige ich, dass ich die vorliegende Arbeit selbständig angefertigt habe. Ich versichere, dass ich ausschließlich die angegebenen Quellen und Hilfen Anspruch genommen habe.

College Station, den 1.4.2016 Madeline Mischel